Ann. Rev. Earth Planet. Sci. 1986. 14: 493–571

CHEMICAL GEODYNAMICS

Alan Zindler

Lamont-Doherty Geological Observatory and Department of Geological Sciences, Columbia University, Palisades, New York 10964

Stan Hart

Center for Geoalchemy, Department of Earth, Atmospheric, and Planetary Sciences, Masachusetts Institute of Technology, Cambridge, Massachusetts 02139

1. INTRODUCTION

Chemical geodynamics, developed by Allegre (1982) as an integrated study of the chemical and physical structure and evolution of the solid Earth, is a field of inquiry that has evolved from a marriage of mantle geochemistry and geophysics. By its very nature, geophysics can only characterize the present state of the Earth; geochemistry, on the other hand, supplies the necessary historical or time-averaging power but is inherently weak in terms of providing three-dimensional information. The two approaches are thus necessary and complementary to each other, and our prognosis is that this relatively young marriage will surely flourish in the years to come.

The evidence for a chemically heterogeneous mantle is, today, unequivocal. However, the nature, development, and scale of this heterogeneity in the mantle remains problematic. In this synthesis, we discuss the various lines of observation and argument that have been used to approach this problem and to work toward the development of quantitative geodynamic models. We first present the geochemical evidence, which is organized in terms of three principal "boundary conditions": (*a*) scale lengths inferred for mantle heterogeneities, (*b*) correlation and interrelationships of various mantle isotopic tracers (Sr, Nd, Pb, and He), and (*c*) initial chemical composition of the Earth. We then consider the interplay between geophysics and geochemistry and attempt to present an unbiased assessment of the current state of the art.

0084–6597/86/0515–0493$02.00

2. MANTLE CHEMICAL HETEROGENEITY: A MATTER OF SCALE

The Role of Chemical Diffusion

Estimates for the scale length over which demonstrable isotopic heterogeneities exist range from mineralogical (cm) scale to scale lengths comparable to mantle dimensions (> 1000 km). The short end of this range can be evaluated by use of existing data on diffusion of cations in relevant mantle phases. For the purposes of this discussion, it is not necessary to review all available diffusion data in detail. We note only that cation diffusion in olivine, diopside, and basalt melt is observed to follow a compensation law (Hart 1980, Sneeringer et al 1984), and this allows several brief generalizations to be made. Compensation (the existence of a well-defined relationship between the preexponential factor and the activation energy in the Arrhenius-type description of diffusion) implies a temperature at which individual element Arrhenius lines intersect. For olivine, diopside, and basalt melt, the crossover temperatures are 1360, 1300, and 1370°C and the diffusion coefficients are $\sim 4 \times 10^{-11}$, 3×10^{-14}, and 2×10^{-7} cm^2 s^{-1}, respectively.

By virtue of the compensated nature of diffusion in olivine, diopside, and basalt melt, we need not separately consider the differences in diffusion rate as a function of species, pressure, or diffusion direction (Hart 1980); at the temperature of particular interest to isotopic homogenization between mantle phases (1300–1400°C), diffusion in each of these phases may be characterized by a single diffusion coefficient. Hofmann & Hart (1978) used 10^{-13} cm^2 s^{-1} for solid phases and 10^{-7} cm^2 s^{-1} for melt phases; the more comprehensive set of diffusion data now available supports the choice of these values, and thus the following conclusions of Hofmann & Hart (1978) remain valid:

1. In the presence of a melt phase, mantle minerals will achieve isotopic equilibrium on time scales of 10^5 yr (at 1350°C).
2. Maintenance of isotopic disequilibrium between minerals for a period of 1 b.y. requires a melt-free system where the host phases are not in contact (i.e. are separated by low-solubility barrier phases such as olivine) and where the temperature does not exceed 1100–1200°C.
3. In a mantle containing 5% basaltic partial melt at 1370°C, and for trace elements with bulk crystal/liquid partition coefficients < 0.1, the maximum scale length ($\sim \sqrt{Dt}$) over which these elements can be diffusively transported is $\sim 500\sqrt{t}$ (in meters), where t is in billions of years (Hofmann & Magaritz 1977). Thus, over the age of the Earth,

diffusion will not eradicate isotopic heterogeneities that are developed on larger than a kilometer scale, even in the presence of a melt.

This latter calculation can be used to constrain the minimum dimension of a heterogeneity that can survive a melting event in a mantle segment with a *homogeneous* solidus temperature. For a mantle diapir rising with an ascent velocity of 5 cm yr^{-1}, it will take $\sim$ 0.3 m.y. to generate 5% partial melt (for 180 cal g^{-1} heat of fusion, and 2°C km^{-1} difference between the melting curve and adiabat). If isotopic heterogeneities existed in this diapir prior to the onset of melting, they will be diffusively erased over scale lengths of some 10 m, even if we assume no convective mixing of the melt. Since most basaltic eruptions almost certainly integrate much larger volumes of mantle than this, we conclude that the minimum size of mantle heterogeneities that can be visualized by studying basalts is set by the volumes and dynamics of melt segregation and transport rather than by diffusion considerations, at least for a source with a homogeneous solidus temperature.

In contrast, we can consider a diapir with relatively fertile zones that have lower solidus temperatures than the surrounding depleted matrix. At the onset of melting, the melt will be restricted to the fertile zones, and it is conceivable that very small-scale heterogeneities may be sampled. Thus, when heterogeneities are observed in basalts, we cannot be sure whether they document kilometer- or meter-scale heterogeneity in the source mantle.

Ultramafic Rocks

Scale lengths of mantle isotopic heterogeneities may be investigated by direct observations of mantle-derived rocks. Two types of material are accessible for this kind of study: (*a*) ultramafic xenoliths erupted in alkaline volcanic rocks and kimberlites; and (*b*) tectonically exposed ultramafic rocks, such as alpine ultramafics and high-temperature peridotites. Xenolith material, by virtue of its small size (< 30 cm), is useful for studying only very small scale lengths. In contrast, high-temperature peridotites may have outcrop scale lengths of up to 35 km (e.g. Ronda massif, Spain).

Numerous early studies reported isotopic disequilibrium between minerals in anhydrous ultramafic xenoliths (e.g. Stueber & Ikramuddin 1974, Dasch & Green 1975); it now appears that much of this observed heterogeneity was a result of alteration and analytical artifacts (Jagoutz et al 1980, Zindler & Jagoutz 1986, Richardson et al 1985).

Ultramafic xenoliths that contain hydrous (metasomatic?) phases often display Sr and Nd isotopic disequilibria between minerals such as

phlogopite, amphibole, and clinopyroxene (Menzies & Murthy 1980b, Kramers et al 1983, Richardson et al 1985). However, it is not yet clear whether these metasomatic phases are long-term residents of mantle environments or whether they simply represent young events in some way related to the early stages of the volcanic event in which the xenoliths were erupted. As discussed by Zindler & Jagoutz (1986), intermineral isotopic disequilibria do not appear to be a common long-lived feature of the upper mantle, although internodule isotopic variations are extreme (Figure 1).

In contrast, larger-scale isotopic variations have been clearly documented in orogenic lherzolite massifs. In a pioneering study, Polve & Allegre (1980) analyzed diopside separates from various parts of the Lherz, Lanzo, and Beni Bousera massifs and observed ranges in $^{87}Sr/^{86}Sr$ of 0.7020–0.7032, 0.7020–0.7030, and 0.7020–0.7033, respectively. Results of a sys-

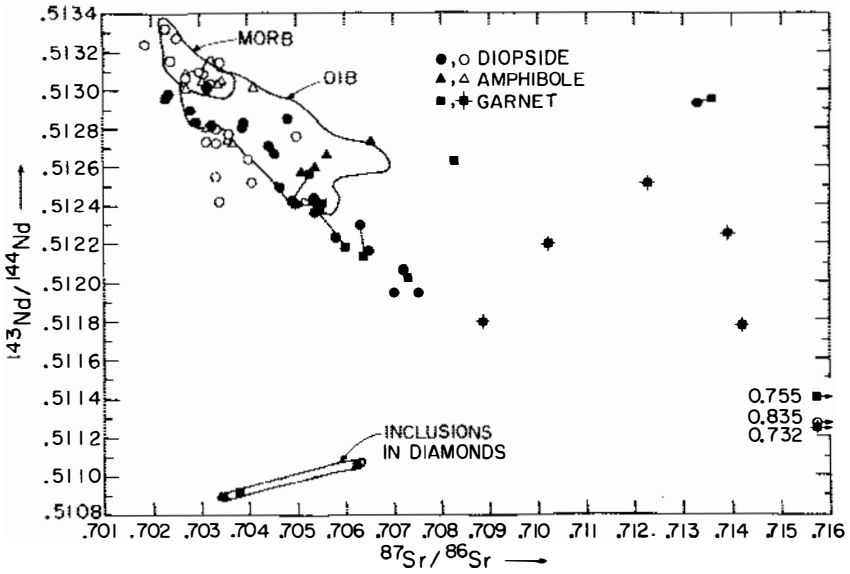

Figure 1 Nd-Sr isotope correlation plot, showing analyses of various minerals from mantle xenoliths and megacrysts. Localities are divided either as African kimberlites (solid symbols) or other localities, usually with alkali basalt hosts (open symbols). The xenolith data of Richardson et al (1985) have first been age corrected back to 90 Myr using mineral Sm/Nd, then corrected ahead to present using average bulk rock Sm/Nd ~ 0.10; solid lines connect coexisting garnet-cpx pairs. Other African kimberlite data are plotted as present-day values, as insufficient data are available to make age corrections (though these will shift points only very slightly on this plot—generally < 0.00006 in $^{143}Nd/^{144}Nd$). Data references are as follows: Basu & Tatsumoto (1979, 1980), Cohen et al (1984), Jagoutz et al (1980), Kramers et al (1981, 1983), Menzies & Murthy (1980a,b), Menzies & Wass (1983), Richardson et al (1984, 1985), Stosch et al (1980), Zindler & Jagoutz (1986).

tematic scale-length study of the Ronda massif (Reisberg & Zindler 1985, 1986; see Figure 2), using Sr and Nd isotopes in peridotite clinopyroxene separates, show significant isotopic variation on scale lengths of 10–20 m (0.7031–0.7034 for Sr and 0.51255–0.51285 for Nd) in agreement with the work of Polve & Allegre (1980). Reisberg & Zindler (1985, 1986) have further shown that mean $^{143}Nd/^{144}Nd$ ratios for 5–10 km^2 terrains (as documented by Cr-diopside separates from river sediments) vary from 0.51325 to 0.51300 for terrains separated by less than 10 km. The total range in $^{143}Nd/^{144}Nd$ measured at Ronda over a scale length of $\sim$30 km is on the order of 95% of the total variation observed in oceanic basalts (Figure 3). Results from St. Paul's Rocks (in the equatorial mid-Atlantic) and Zabargad Island [in the Red Sea (Figures 2, 3)] also provide qualitative support for the above conclusions (Roden et al 1984, Brueckner et al 1986).

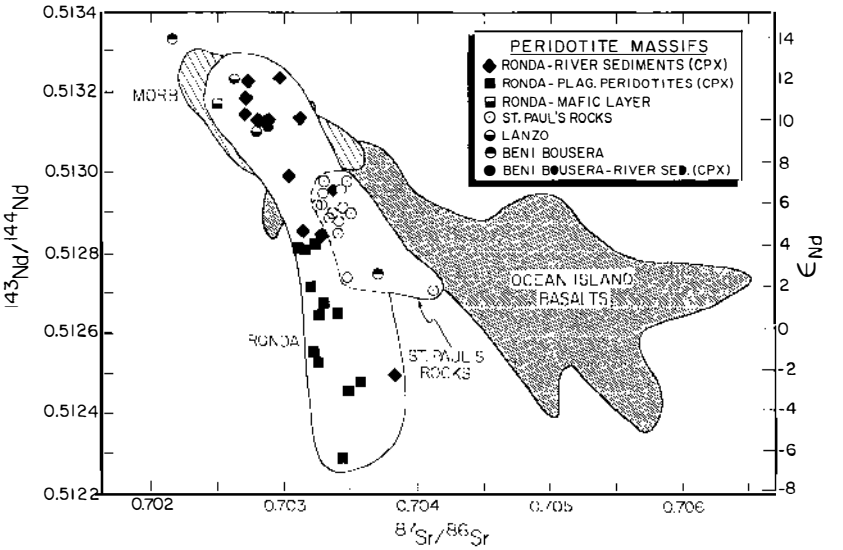

Figure 2 $^{87}Sr/^{86}Sr$ vs $^{143}Nd/^{144}Nd$ variation diagram for peridotite massifs. While all localities, with the exception of St. Paul's Rocks, contain some samples that fall within the depleted MORB (mid-oceanic ridge basalts) field ($^{143}Nd/^{144}Nd > 0.5132$), extreme heterogeneity occurs within these massifs. The enriched portions of the Ronda, Beni Bousera, and Zabargad massifs tend to be EM I type (see discussion in Section 3), a result that tends to support an intramantle metasomatic origin for this component (Menzies 1983). Scale lengths for the observed isotopic heterogeneities are discussed in the text and are shown in Figure 3. Data sources are as follows: Ronda (Reisberg & Zindler 1986, Zindler et al 1983); St. Paul's Rocks (Roden et al 1984); Zabargad (Brueckner et al 1986); Lanzo and Beni Bousera (Richard & Allegre 1980).

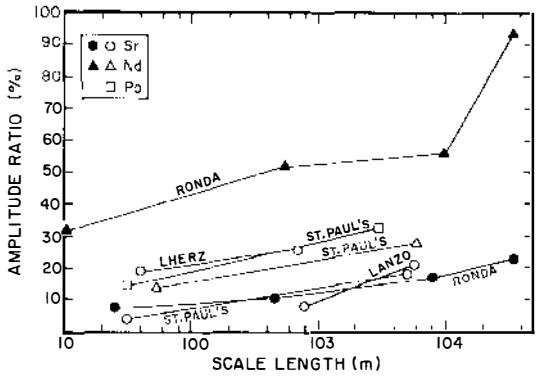

Figure 3 Isotopic heterogeneity versus scale length for ultramafic rocks from three orogenic massifs (Lherz, Ronda, and Lanzo) and one oceanic massif (St. Paul's Rocks). Isotopic variability is expressed as a percentage of the total isotopic range observed in all oceanic basalts (MORB and OIB; see discussion later in text). Two end points plotted represent the scale length of the maximum observed variation in each massif (*right*) and the largest variation observed at the smallest scale length (*left*). St. Paul's samples are whole rocks; Lherz, Ronda, and Lanzo samples are diopsides. Data are from Polve & Allegre (1980), Roden et al (1984), and Reisberg & Zindler (1985, 1986).

Basalts

Inferring domain sizes of mantle heterogeneities based on observations of erupted basalts is a very complex issue, though this avenue is the principal source of the proof that mantle geochemical heterogeneities do in fact exist. The basic problem is one of trying to elucidate three-dimensional domain sizes from "planform" observations. First, we do not truly know the degree of partial melting represented by any given basaltic melt, and estimates vary widely, from values $< 1\%$ to values as high as 20–30%. Second, we have very poor control on the depth of origin of basaltic magmas. The problem is worse, however, than simply establishing a depth of segregation, as source materials may represent diapirs that have ascended from deep within the mantle (e.g. the "plume" model of Morgan 1971 or Schilling 1973). Furthermore, if the uprising plumes or diapirs undergo any solid-state mixing during their ascent, the final basaltic melt product may represent some confused average of large vertical sections of mantle. Thus, it is obvious that basalts from two volcanoes on Hawaii, for example, separated by 10 km of horizontal distance, need not be giving us interpretable information regarding isotopic mantle variations on 10-km scale lengths.

Despite these problems, we believe that useful constraints may be defined by working at the extreme ends of the scale-length spectrum. For example, significant isotopic heterogeneity has been observed between samples of

MORB from a single dredge haul (leRoex et al 1983) and within the eruptives of a single small seamount (10-km base diameter, 42-km^3 volume) (Zindler et al 1984). In the seamount case, it seems unlikely that this variability can be ascribed to several major mantle plumes coming from disparate depths. Zindler et al (1984) used these data to argue for a mantle that is heterogeneous on a kilometer or smaller scale but homogeneous on a 20–100 km scale.

At the other extreme (large scale lengths), there appear to be large areas of the Earth that, in planform, show coherent and characteristic isotopic signatures (Dupre & Allegre 1983). One of these, termed the Dupal anomaly (Hart 1984b), is more or less continuously present worldwide between the equator and 60°S latitude. Figure 4 shows a planform of this anomaly, which is contoured using several different isotopic criteria. It is difficult to conceive of the isotopic delineation of such a megascale anomaly by melting of mantle that is anything but heterogeneous on a large (> 1000 km) scale. These results, taken together with the aforementioned seamount data, enable us to conclude that mantle heterogeneities must exist *at least* on both small and very large scales.

In light of these results, we consider it useful to establish a measure of the amplitude of isotopic variability and then to relate this measure to the planform scale length. As an amplitude measure, we take the extreme values of $^{87}Sr/^{86}Sr$, $^{143}Nd/^{144}Nd$, and $^{206}Pb/^{204}Pb$ measured on any oceanic basalt [both ocean island basalt (OIB) and midocean ridge basalt (MORB); see Figure 14]. The isotopic "variability" (amplitude ratio, or *AR*) of a given basalt suite (island, volcano, section of ridge, etc) is then expressed as a percentage of this total possible variation. Amplitude ratios for selected basalt suites are shown as a function of sampling scale length in Figure 5. Also shown for comparison is the field of "first-order" observations derived from ultramafic massifs (taken from Figure 3). It is apparent from this plot that the maximum attainable amplitude ratio increases with scale length, whereas relatively small amplitude ratios can be observed at all scale lengths.

The important feature of this plot is the *upper* bound of the wedge-shaped field, which convincingly shows that large amplitude ratios occur only for large scale lengths. Note that the data from orogenic massifs suggest an upper bound that is shifted toward considerably smaller scale lengths. This difference indicates that the magmatic processes involved in basalt production are capable of considerable averaging on a 10-km scale.

This analysis suggests several important implications with respect to the nature of mantle heterogeneities. While heterogeneities of relatively small isotopic amplitude may exist on small scales (meters to kilometers), as documented by the seamount studies, it does not appear possible to explain

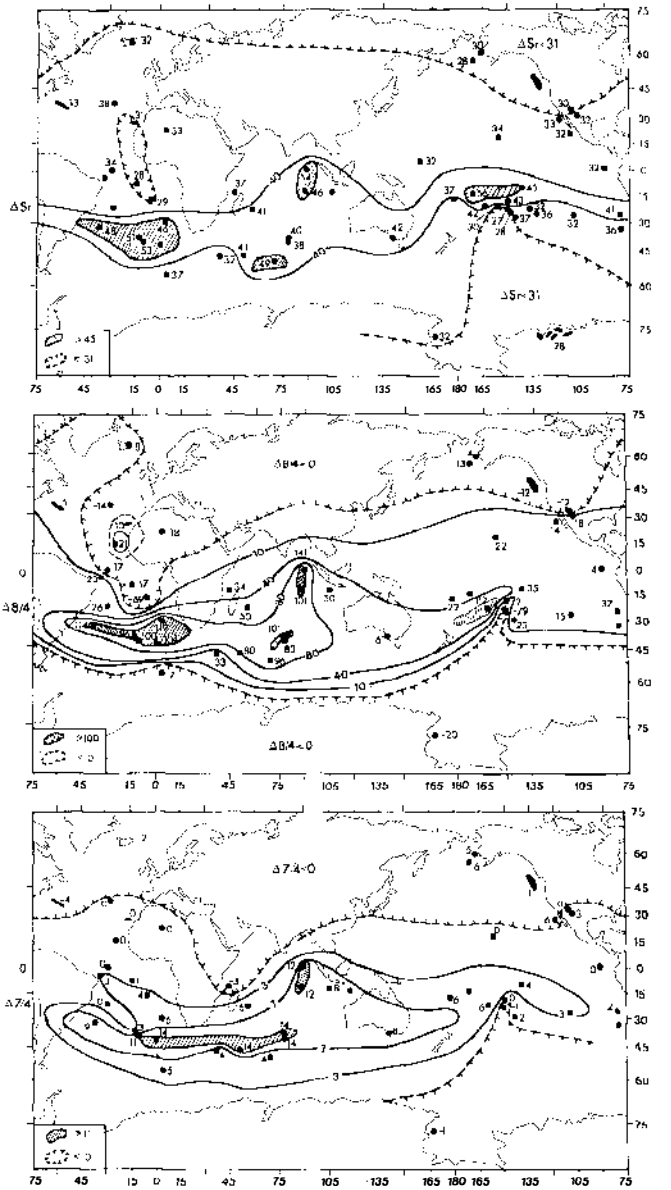

Figure 4 World maps showing the distribution of three isotopic criteria used to outline the very large-scale anomalous region that encircles the globe between the equator and 60°S. This region is termed the Dupal anomaly (Hart 1984b). The three anomaly criteria are ΔSr (upper figure: absolute $^{87}Sr/^{86}Sr$ value, third & fourth significant figures only; that is, ΔSr for 0.70350 = 35), Δ8/4 [middle figure: vertical deviation in $^{208}Pb/^{204}Pb$ from a Northern Hemisphere reference line (NHRL on Figures 9*A,C*)], and Δ7/4 (lower figure: vertical deviation in $^{207}Pb/^{204}Pb$ relative to the NHRL in Figures 9*B,D*).

the whole observed range of oceanic mantle heterogeneity with small-scale (< 10 km) heterogeneities alone. To accomplish this with the preferential melting model proposed by Sleep (1984) would require that melting processes in certain broad regions of the oceanic mantle can selectively tap only the more enriched portions of small heterogeneities, whereas in other regions the melting process is unable to be so selective, thereby averaging in a larger fraction of more depleted matrix. Since it is difficult to envision a mechanism for such large-scale modulation of the melting process, one could argue that the small-scale heterogeneities (blobs) are themselves variable in composition, with large volumes of the mantle typified by blobs

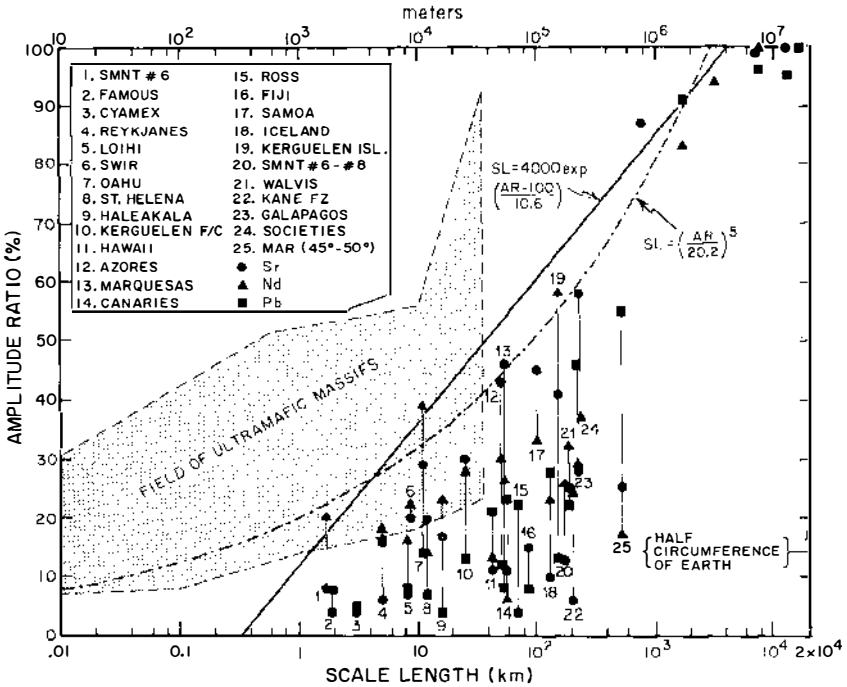

Figure 5 Amplitude ratio (AR) versus scale length (SL) for various volcanoes, islands, island groups, and ridge segments. Vertical lines connect the AR values observed for Sr, Nd, and Pb at each locality. Points for Sr, Nd, and Pb plotted at 100% AR are the normalizing values, given for Nd by Kane–Walvis (SL = 7780 km), for Sr by Kane–Societies (SL = 12,400 km), and for Pb by Mid-Indian Ocean ridge–Tubuai (16,700 km). Other points plotted in upper-right quadrant are for other various island pairs that provide large AR for minimal scale lengths (Nd: Walvis–Mid-Atlantic Ridge, 94%, 3030 km; Sr: Tahaa–Juan de Fuca, 99%, 7100 km; Tahaa–Tubuai, 87%, 770 km; Pb: Walvis–Tubuai, 95%, 13,500 km; St. Helena–Mid-Indian Ocean ridge, 96%, 7600 km; Walvis–St. Helena, 91%, 1700 km). Arbitrary exponential and power-law curves are shown as possible upper-bound fits to the data. Also shown is the outline of the field for ultramafic massifs, taken from Figure 3. Data references may be found in Zindler et al (1982), Hart (1984b), and White (1985).

that are more enriched than those in other regions. For example, in this model, all of the mantle underlying the Dupal anomaly region (Figure 4) would contain blobs of a more enriched character than the blobs in mantle lying outside the Dupal region. In essence, this model implies that the isotopic *contrast* between blobs and their depleted mantle matrix is systematically larger in Dupal mantle regions than elsewhere. The upper bound in Figure 5 would then be providing a measure of the degree of isotopic contrast between small-scale blobs and their matrix.

Alternative interpretations derived from the data of Figures 4 and 5 are equally possible. The simplest of these would view the oceanic mantle as isotopically heterogeneous not only on small scales, but also on the largest scales possible (thousands of kilometers), with the extent of heterogeneity increasing with scale length. In the context of a plume model, this could be accomplished by allowing the lower mantle to carry the enriched isotopic signatures, with sub-Dupal lower mantle being substantially more "enriched" than other regions, and then allowing this material to mix with (be "polluted" by) the depleted and homogeneous upper mantle (Dupre & Allegre 1983). The isotopic contrast would then be between the upper and lower mantles, with Dupal regions showing the largest contrast because of the more enriched nature of the lower-mantle component. Yet another view (Anderson 1985) suggests that basaltic magmas generated in the transition region could rise into, and become contaminated by, a variably enriched shallow mantle. The enhanced enrichment of Dupal-type shallow mantle may document extensive Pangeatic subduction of altered oceanic crust and sediment into the sub-Dupal mantle (Anderson 1982a). In this model, the isotopic contrast is between the upper and lower parts of the *upper* mantle, with Dupal uppermost mantle being more enriched than ambient upper mantle.

These various interpretations (models) for the systematics depicted in Figures 4 and 5 lead to very different views of convective processes in the mantle. The first model would be consistent with whole-mantle convection, the second would require a two-layered mantle, with limited exchange between the layers over geologic time and relatively inefficient convective mixing of the lower mantle, and the third requires a three-layer mantle with a depleted transition region overlain by a relatively stagnant, enriched upper layer.

3. ISOTOPIC CHARACTERIZATION OF GEOCHEMICALLY DISTINCT MANTLE COMPONENTS

In recent years, isotope geochemists have devoted considerable attention to investigating the relationships between various isotope systems in oceanic

basalts and their implications for mantle chemical structure. There are now seven decay schemes for which a significant body of analytical data exist for oceanic basalts: ^{87}Rb-^{87}Sr, ^{147}Sm-^{143}Nd, ^{238}U-^{206}Pb, ^{235}U-^{207}Pb, ^{232}Th-^{208}Pb, ^{176}Lu-^{176}Hf, and ($^{238}U + ^{235}U + ^{232}Th$)-$^{4}He$. Over the past decade, our understanding has evolved from thinking in terms of linear correlations and two-component mixing for two-isotope systems (e.g. the Sr-Nd isotope correlation; DePaolo & Wasserburg 1976a, O'Nions et al 1977, Allegre et al 1979), to thinking in terms of at least three components, which may define an approximate planar or two-dimensional mixing array in three-, four-, or five-dimensional space (e.g. $^{87}Sr/^{86}Sr$, $^{143}Nd/^{144}Nd$, $^{206}Pb/^{204}Pb$, $^{207}Pb/^{204}Pb$, $^{208}Pb/^{204}Pb$; Zindler et al 1982). Allegre & Turcotte (1985) and White (1985) have recently proposed that there are five types of sources from which all oceanic basalts may be produced by variable mixing relationships.

The present status of oceanic isotopic data is summarized in a series of two-dimensional variation diagrams (Figures 6–12). Hafnium isotopic data are not represented here because, in general, the overall high degree of correlation between Hf and Nd isotope ratios permits accurate inference of the behavior of $^{176}Hf/^{177}Hf$ based on $^{143}Nd/^{144}Nd$ (e.g. Patchett & Tatsumoto 1980). Brief consideration of the data arrays in Figures 6–12 clearly demonstrates the inadequacy of simple two-component mixing models to explain isotopic variations in oceanic basalts [as originally pointed out by Sun & Hanson (1975) based on Sr-Pb systematics]. Even the Sr-Nd variation diagram (Figure 6), until recently thought to represent a linear array (the "mantle array" of, for example, DePaolo & Wasserburg 1977), requires a substantially more complex interpretation. This is an important, first-order conclusion based on all currently available data and is not subject to interpretation. Thus, we must consider that any model for the evolution of the mantle-crust system that presumes only two geochemically distinct components within the mantle is necessarily inaccurate.

Until recently many geochemists felt that the apparent differences in the relative positions of various localities in the Sr-Nd and Pb-Pb variation diagrams (Figures 6, 9) documented a decoupling of the U-Th-Pb system from Rb-Sr and Sm-Nd. Zindler et al (1982) proposed that there was a coherence in these variations that became apparent when they were viewed as different two-dimensional projections of an approximately planar three-dimensional surface. Delineation of this three-dimensional mantle plane is shown in Figure 13, where every data point represents the averaged isotopic values for an island or ridge system. It should be noted that this plane is defined by averaged data, and that many localities show intraisland isotopic variations that do not lie in the plane (e.g. Stille et al 1983, Staudigel et al 1984). There are also several localities for which data have recently been reported that, even when averaged, do not lie on the plane [e.g.

Koolau series, Oahu (Stille et al 1983); Walvis Ridge (Richardson et al 1982); Samoa (White & Hofmann 1982, White 1985)]. While for many localities, the mantle plane remains a useful representation, an accumulating body of evidence suggests that it too is an oversimplification.

The interrelationships displayed by the various isotope ratios in Figures 6–12 delineate a number of important constraints regarding the definition of isotopically distinct mantle components:

1. The "depleted" isotopic character of N-type MORB (high $^{143}Nd/^{144}Nd$, low $^{87}Sr/^{86}Sr$ and $^{206}Pb/^{204}Pb$) requires the existence of a depleted end-member MORB-mantle component (DMM) that is clearly identifiable along ridge segments well removed from hotspot volcanic activity.

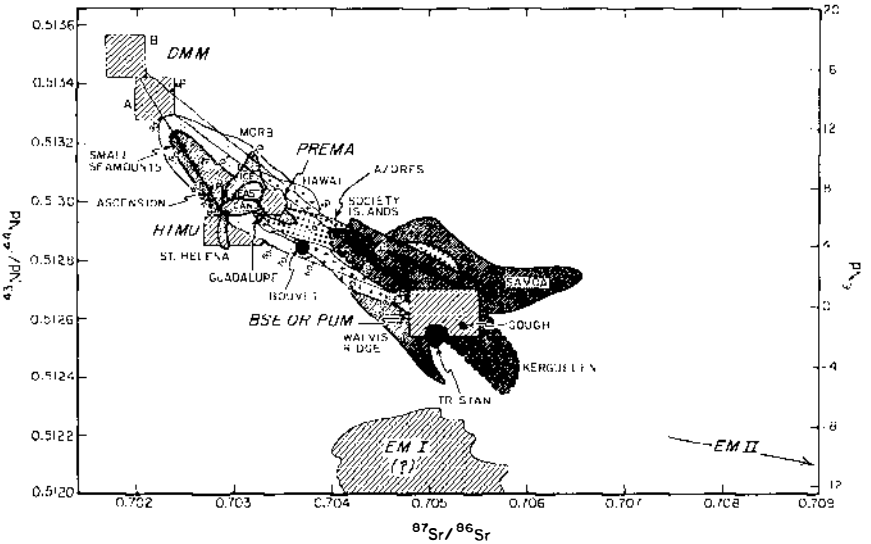

Figure 6 $^{143}Nd/^{144}Nd$ vs $^{87}Sr/^{86}Sr$ variation diagram for oceanic basalt suites. [Data sources may be found in Zindler et al (1982), Hart (1984b), and White (1985).] Proposed mantle components are shown as cross-hatched boxes and blobs labeled DMM (A and B), HIMU, PREMA, BSE or PUM, EM I, and EM II (see discussion in text). Mixing lines between DMM (A and B), HIMU, and BSE or PUM, with tick marks indicating percentages of one end member, are constructed using the following source compositions for Sr and Nd, respectively (in ppm): DMM (1)—6, 0.33; DMM (2)—12, 0.65; HIMU—120, 6.5; BSE—18.4, 1.0. The HIMU composition assumes a magmatic origin for this component; had we assumed it to be a high-μ peridotite (where $\mu = {}^{238}U/^{204}Pb$), with lower concentrations of Sr and Nd but a similar Sr/Nd ratio, the shapes of the mixing curves would not change, only the positions of the tick marks (see discussion in text). The two values given for DMM delimit the possible concentration range for this component and result in two sets of tick marks on each mixing line that goes to DMM A or DMM B. Note that none of the mixing lines are highly curved because of the similarity in Sr/Nd ratios in all components.

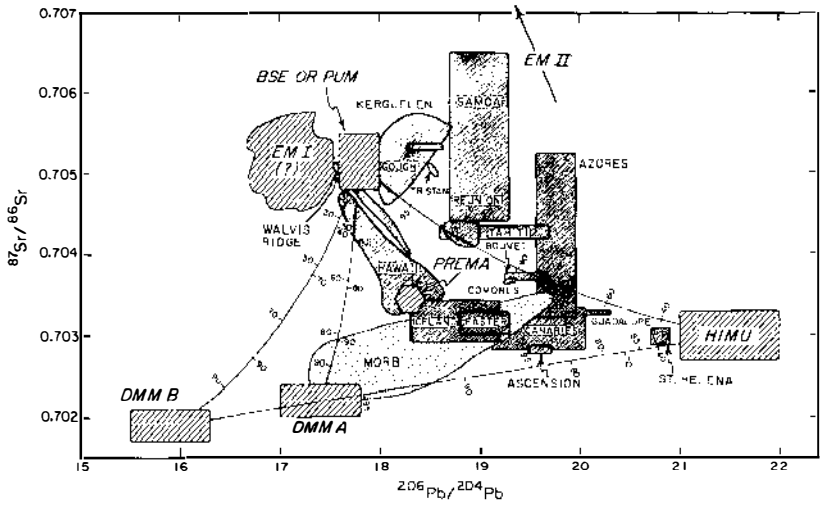

Figure 7 $^{87}Sr/^{86}Sr$ vs $^{206}Pb/^{204}Pb$ variation diagram for oceanic basalt suites. Data sources, components, and mixing lines are as in Figure 6. Pb concentrations are as follows (in ppm): DMM (1)—0.02; DMM (2)—0.04; HIMU—0.4; BSE—0.135. Islands lying outside the DMM-HIMU-BSE mixing triangle document the existence of EM II and are geographically situated within the Dupal anomaly. The Koolau series of Oahu (Stille et al 1983) and the Walvis Ridge (Richardson et al 1982) document the existence of EM I.

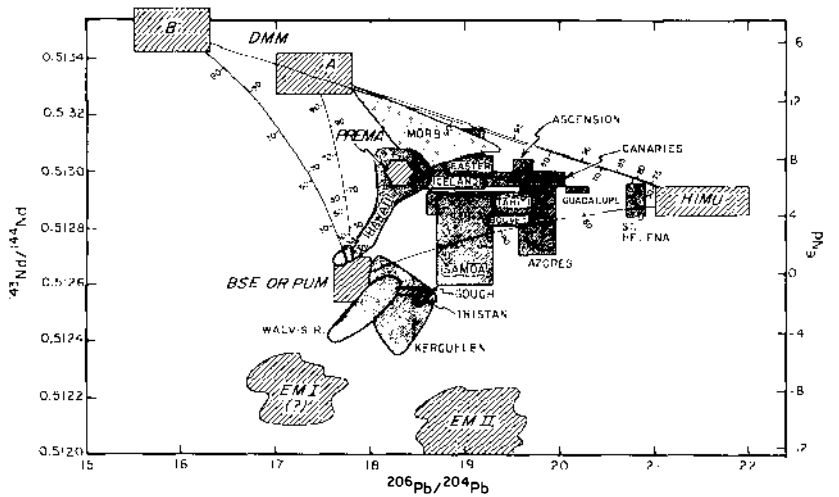

Figure 8 $^{143}Nd/^{144}Nd$ vs $^{206}Pb/^{204}Pb$ variation diagram for oceanic basalt suites. Data sources, components, mixing lines, and other considerations are as in Figures 6 and 7.

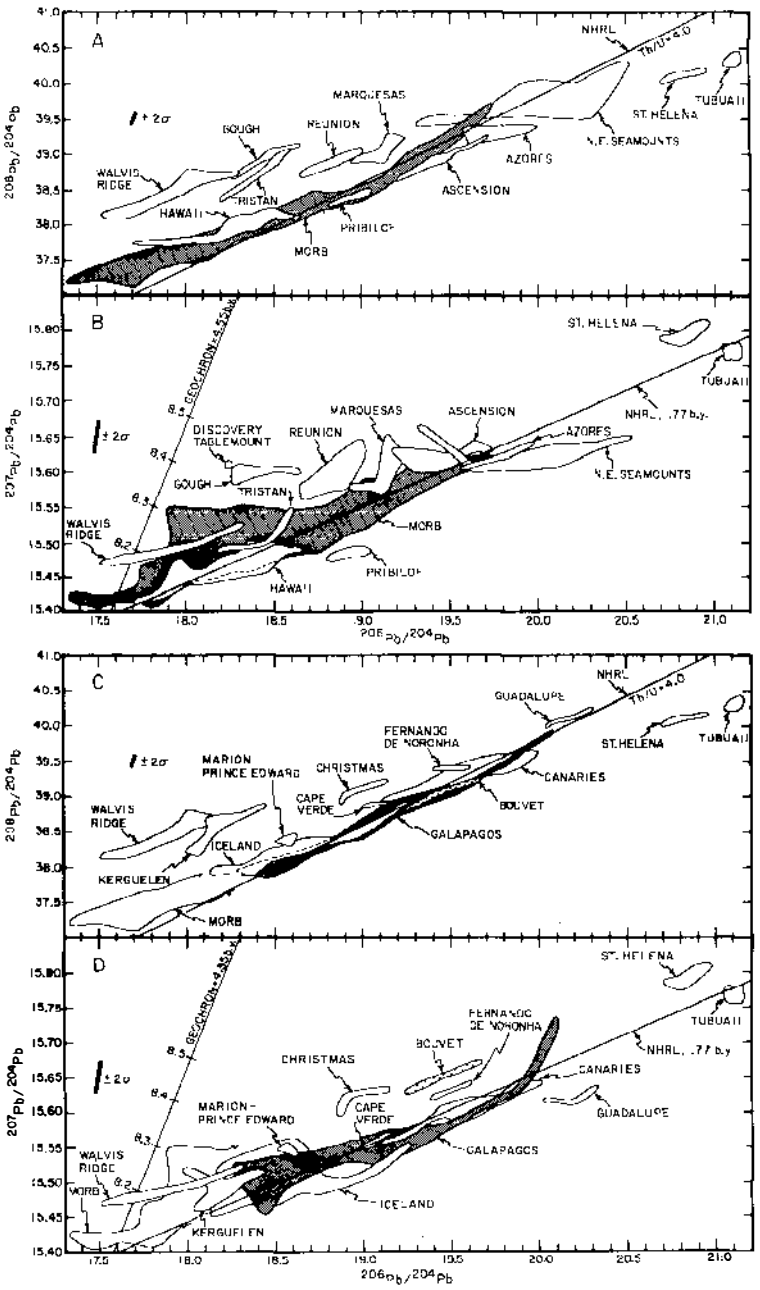

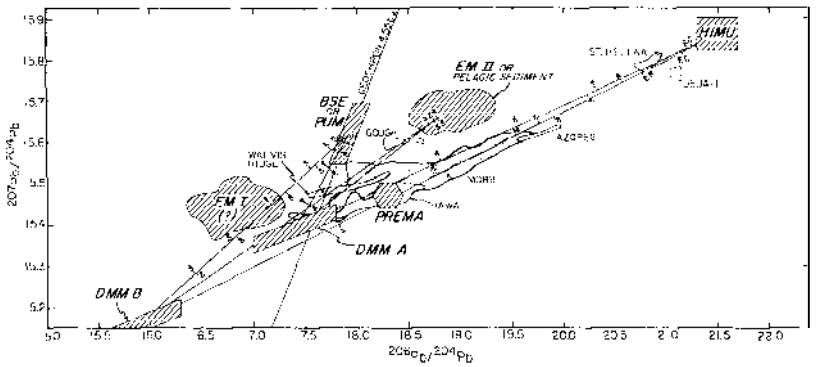

Figure 9 (*opposite and above*) (*A–D*) $^{208}Pb/^{204}Pb$–$^{207}Pb/^{204}Pb$–$^{206}Pb/^{204}Pb$ isotope variation diagrams for a variety of oceanic basalts. Two panels are shown for each plot in the interest of clarity. A 4.55-b.y. geochron is shown, with single-stage μ-values (tick marks), along with the Northern Hemisphere reference line (NHRL) of Hart (1984b). This NHRL, when interpreted as a secondary isochron, has a slope of 1.77 b.y. and a second-stage Th/U (wt. ratio) of 4.0. Islands lying significantly above the NHRL are part of the Dupal anomaly belt. Data sources may be found in Hart (1984b). Typical 2σ analytical precision is also shown ($\pm 0.05\%$ amu^{-1}). (*above*) In this panel, DMM (A and B), HIMU, BSE, EM I, and EM II component compositions are indicated on a $^{207}Pb/^{204}Pb$ vs $^{206}Pb/^{204}Pb$ diagram, with MORB and selected island fields from panels *B* and *D* shown for reference. Parameters and considerations for mixing lines are as in Figures 6 and 7.

2. The very high $^{206}Pb/^{204}Pb$ ratios observed at St. Helena and Tubuaii (Figure 9), coupled with the low $^{87}Sr/^{86}Sr$ and intermediate $^{143}Nd/^{144}Nd$ ratios at these sites, suggest a mantle component that is markedly enriched in U and Th relative to Pb (HIMU) without an associated increase in Rb/Sr.
3. Trends for Walvis Ridge, Kerguelen, and Samoa in Figure 6, which extend beyond presumed bulk silicate Earth (BSE) values for $^{143}Nd/^{144}Nd$ and/or $^{87}Sr/^{86}Sr$, require the existence of at least two "enriched" mantle components (EM I and EM II).
4. The high $^{3}He/^{4}He$ ratios that are found at Iceland and Hawaii demand the involvement of relatively undegassed mantle, or a mantle segment that was enriched in volatiles during the Archean (see Figure 16). Although this component is often described as "primitive" or undifferentiated mantle, the Sr, Nd, and Pb characteristics of Iceland and Hawaii (Figures 10–12) are not consistent with such an interpretation.
5. The high frequency of Nd and Sr isotopic compositions at about 0.5130 and 0.7033, respectively (Figures 6, 14, 15), suggests that the existence of a mantle component with this isotopic character (at least when scale lengths for melting volumes are considered) is more likely than constant

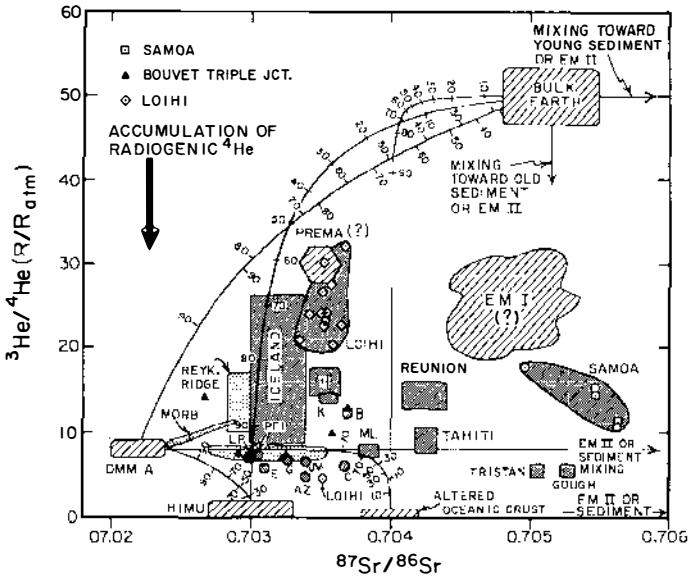

Figure 10 ^{3}He/^{4}He vs ^{87}Sr/^{86}Sr variation diagram of oceanic basalt suites. DMM, HIMU, BSE (labeled Bulk Earth), PREMA, EM I and EM II components are shown as crosshatched fields. Mixing lines and considerations are as in Figure 6; Helium concentrations for the various components are as follows (std cm^3 g^{-1}) DMM (1)—6.5×10^{-6}; DMM (2)—1.3×10^{-5}; HIMU—2.7×10^{-5}; EM II (for "young" sediment or EM II case)—5.3×10^{-6}. Sr concentrations are given in Figure 6 caption. Mixing lines are also shown to an altered crust component presumed to have a He concentration of 1.5×10^{-6} std cm^3 g^{-1}. In general, we have assumed fairly low He concentrations in those components presumed to have low ^{3}He/^{4}He ratios. However, this assumption may be highly variable, since it is strongly dependent on the age of these components because of the rapid growth of ^{4}He in materials with high U/^{4}He ratios. This situation is qualitatively depicted by contrasting mixing trajectories shown for "young" and "old" EM II or sediment mixing. Because of the potential for pre- or posteruptive accumulation of radiogenic ^{4}He (as indicated by the black arrow), ^{3}He/^{4}He ratios measured at ocean islands (particularly those in the waning stages of their volcanic cycles) must be considered as minimum values for mantle sources. The large number of components, together with the potential for radiogenic ^{4}He accumulation, precludes the unique definition of mixing scenarios for individual localities. Localities given by abbreviation are as follows: LP—La Palma, Canary Islands; PEI—Prince Edward Island; E—Easter Island; G—Galapagos; AZ—Azores; JM—Jan Mayen; B—Bouvet; C—Comores; H—Hualalai, Hawaii; K—Kilauea, Hawaii; ML—Mauna Loa, Hawaii. Data sources for ^{3}He/^{4}He shown in this diagram (as well as for Figures 11 and 12) are as follows: Poreda et al (1980), Rison (1981), Kurz & Jenkins (1981), Rison & Craig (1982), Craig & Rison (1982), Kurz (1982), Kurz et al (1982, 1983, 1985), Allegre et al (1983a), Condomines et al (1983).

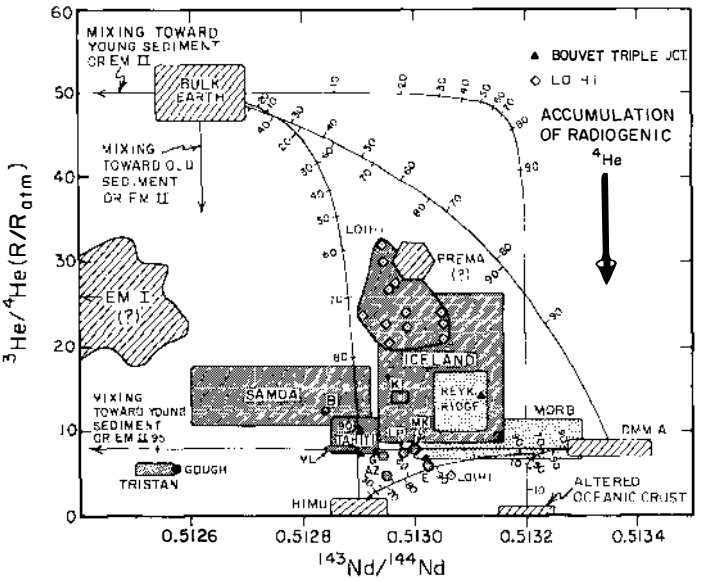

Figure 11 $^{3}He/^{4}He$ vs $^{143}Nd/^{144}Nd$ variation diagram for oceanic basalt suites. Components, considerations, mixing lines, locality abbreviations, and data sources are as in Figure 10 (except that MK stands for Mauna Kea). He and Nd concentrations for mixing lines are given in captions to Figures 10 and 6, respectively.

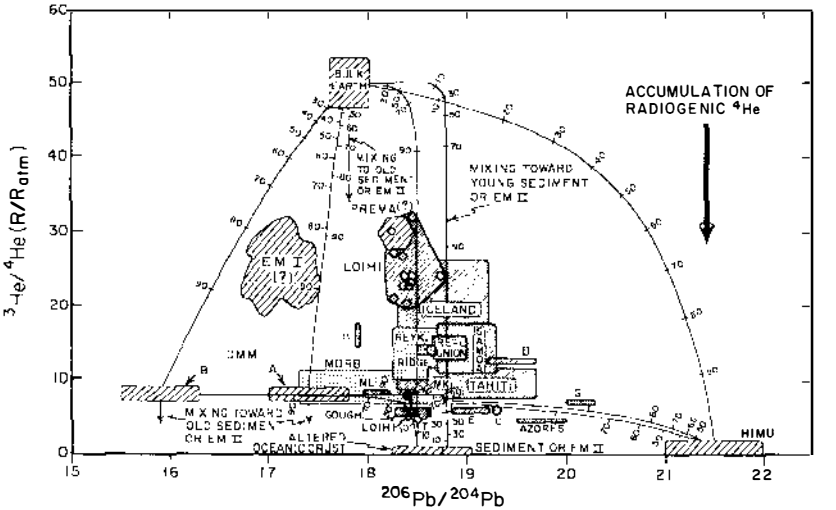

Figure 12 $^{3}He/^{4}He$ vs $^{206}Pb/^{204}Pb$ variation diagram for oceanic basalt suites. Components, considerations, mixing lines, locality abbreviations, and data sources are as in Figure 10 (except that T stands for Tristan). He and Pb concentrations for mixing lines are given in captions to Figures 10 and 7, respectively.

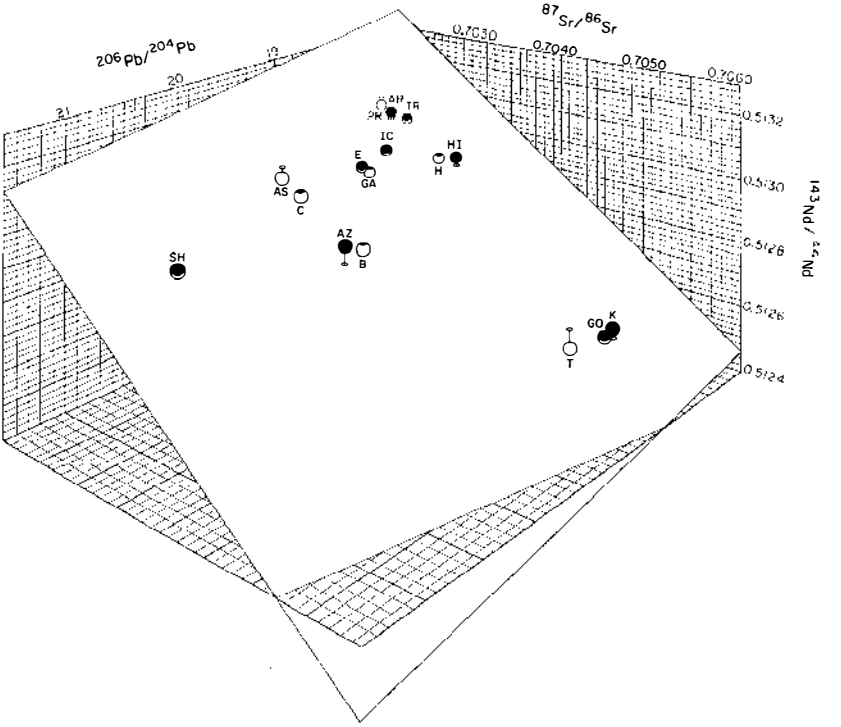

Figure 13 Three-dimensional plot of average $^{206}Pb/^{204}Pb$, $^{143}Nd/^{144}Nd$, and $^{87}Sr/^{86}Sr$ for basalts from oceanic ridges and islands. The best-fit plane is shown. Closed and open symbols, whose size approximates the uncertainty of a single analysis, lie above and below the "mantle plane," respectively. Lines connecting data points to the plane are parallel to the $^{143}Nd/^{144}Nd$ axis and indicate those points that do not intersect the plane. Localities are as follows: AR—Mid-Atlantic Ridge; PR—East Pacific Rise; IR—Indian Ocean ridges; C—Canary Islands; AZ—Azores; AS—Ascension; SH—St. Helena; GO—Gough; T—Tristan da Cunha; B—Bouvet; E—Easter Island; HI—Hawaiian Islands; H—Island of Hawaii; GA—Galapagos; K—Kerguelen; IC—Iceland. Data sources are given in Zindler et al (1982).

mixing proportions between spatially distant components that are far removed from these isotopic values. We refer to this component as PREMA (*pre*valent *ma*ntle).

Mantle He Signals: Potential Problems

Because of its dominantly primordial origins, ^{3}He offers tremendous potential as a tracer for geochemically distinct mantle components and reservoirs. However, the interpretation of mantle $^{3}He/^{4}He$ signals may not be as straightforward as is often presumed, and thus it merits our further consideration here.

$^3He/^4He$ variations in oceanic basalts are displayed in histogram fashion in Figure 14 (along with Sr, Nd, and Pb isotope ratios for reference). In contrast to Sr, Nd, and Pb, MORB $^3He/^4He$ values occupy a relatively small portion of the OIB array (1–32 Ra; Ra denotes the atmospheric value of $^3He/^4He$) and lie totally within this array, rather than defining one end of it (as is the case for the other isotope ratios). Basalts from Loihi Seamount, a young submarine volcano located on the southeast flank of Kilauea on the

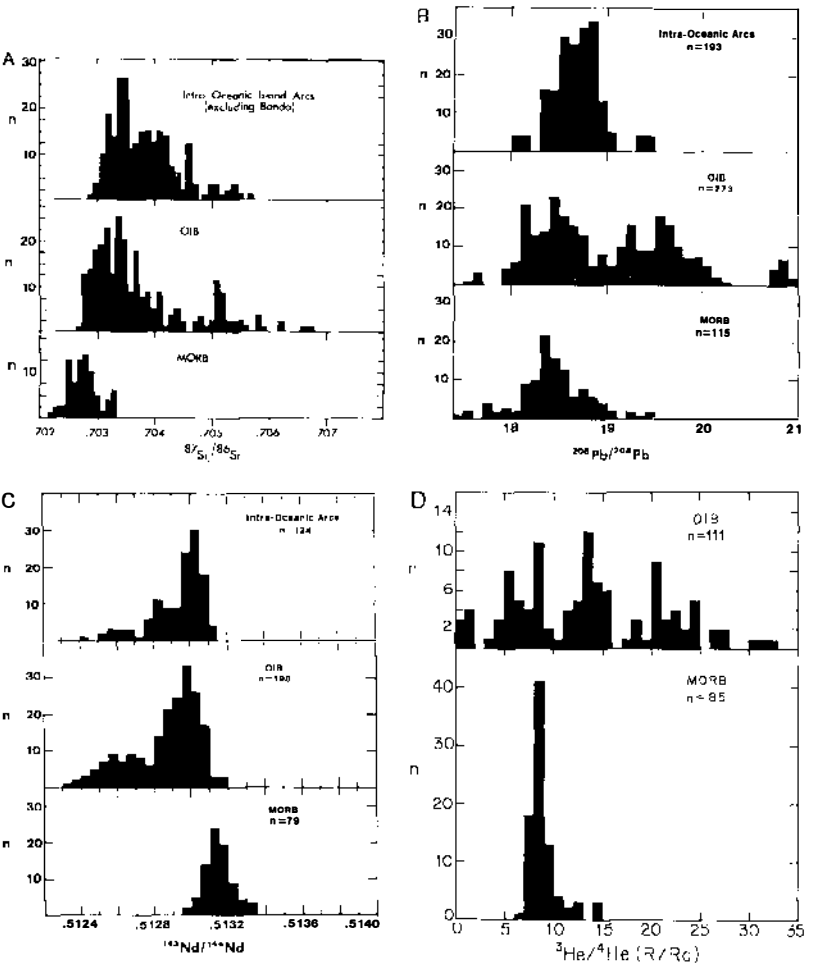

Figure 14 Histograms of $^{87}Sr/^{86}Sr$, $^{143}Nd/^{144}Nd$, $^{206}Pb/^{204}Pb$, and $^3He/^4He$ in MORB, oceanic island basalts, and intraoceanic arcs (adapted from Morris & Hart 1983). Data sources for the He data in (*D*) are those given in Figure 10 caption plus Ozima & Zashu (1983).

Island of Hawaii, span nearly the entire known range of oceanic $^3He/^4He$ values (4–32 Ra; Kurz et al 1983) while displaying only minor variations in $^{87}Sr/^{86}Sr$ (from 0.70335 to 0.70370; Staudigel et al 1984). Some of the lowest, or least primitive, $^3He/^4He$ ratios found on oceanic islands come from Tristan da Cunha and Gough (~ 5 Ra; Kurz et al 1982); these areas are known for their Sr and Nd isotope ratios, which approximately coincide with many estimates for the bulk silicate earth (BSE). Recently, Graham et al (1984, 1986) have measured $^3He/^4He$ ratios of ~1 Ra in alkali basalts from several small seamounts adjacent to the East Pacific Rise at about 12°N.

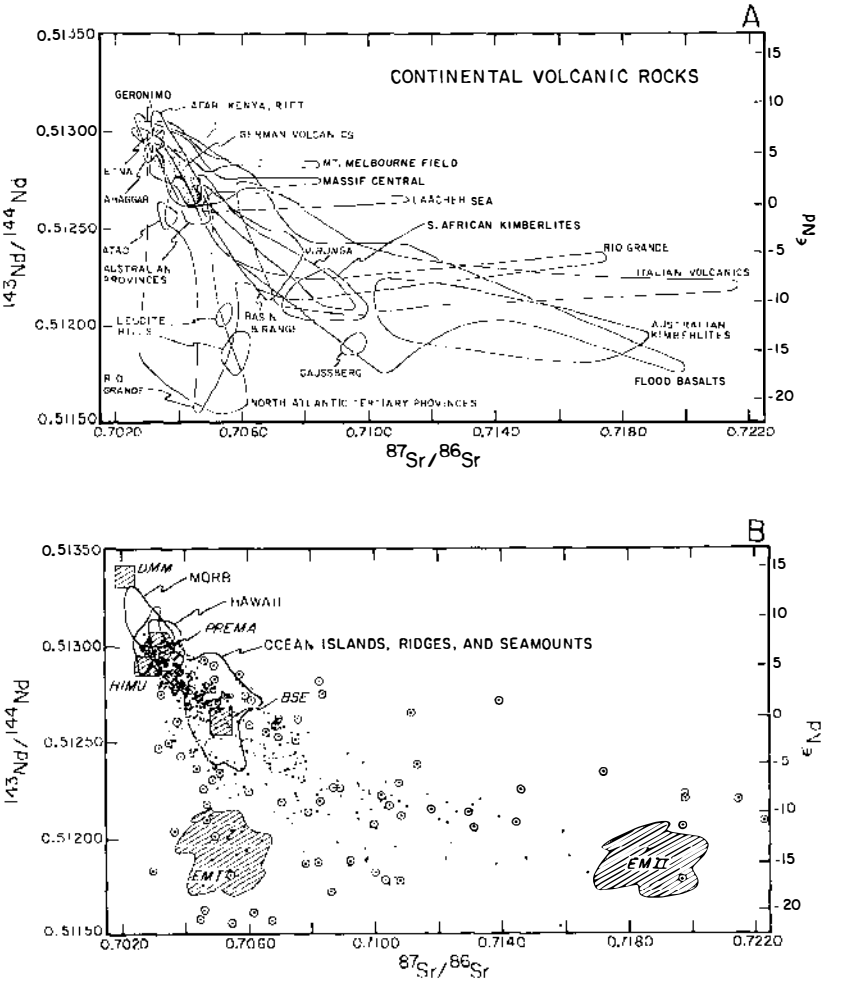

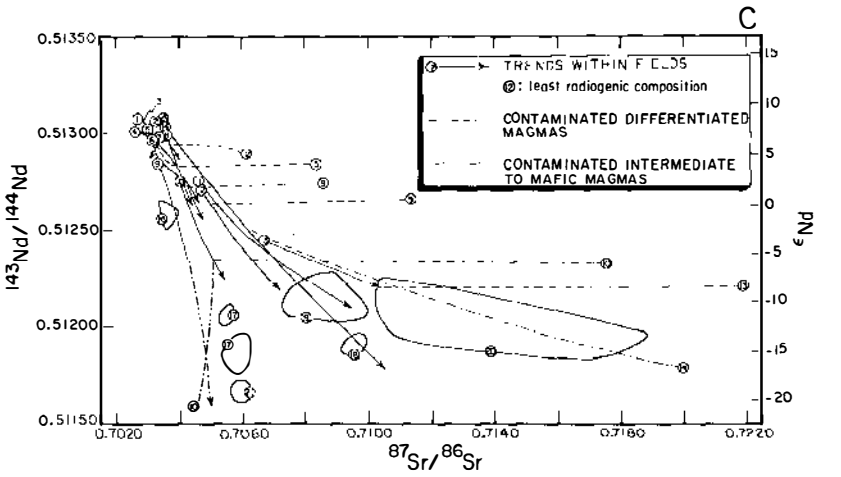

Figure 15 Comparison of more than 500 individual Sr and Nd isotope ratios for continental volcanic rocks taken from Worner et al (1986). Data sources can be found in Worner et al (1986). Panel *A* shows fields for individual provinces (except that all flood basalts are grouped into a single field). Note that fields converge toward PREMA in the upper left-hand corner of the diagram. Individual "branches" of the combined arrays diverge toward EM I–type compositions at low $^{87}Sr/^{86}Sr$, and EM II–type compositions at high $^{87}Sr/^{86}Sr$. These mixing trends are similar to those observed in oceanic basalts, except that the continental basalts extend to much more extreme values.

Panel *B* shows individual data points, with fields for MORB, Hawaii, and ocean islands (OIB) shown for reference. The paucity of data between the two lower branches of the array ($^{87}Sr/^{86}Sr \sim 0.7065$, $^{143}Nd/^{144}Nd < 0.5124$) suggests that EM I– and EM II–type mixing processes are mutually exclusive. Worner et al (1986) propose [in accord with prior suggestions by Menzies (1983) and Hawkesworth et al (1984)] that these enriched components exist within the subcontinental source mantle, since selective assimilation of only upper or lower crustal materials, without mixing between them, seems unlikely (although, without question, many of these rocks have been contaminated by crustal components; such data points are circled where specifically discussed in the original publication).

Panel *C* shows depleted and enriched end members for individual fields. Numbers correspond to the following localities: (1) North Atlantic Tertiary provinces; (2) Afar and Kenya Rift; (3) Geronimo volcanic field; (4) Australian provinces; (5) Mt. Melbourne, Antarctica; (6) Etna; (7) Ahaggar; (8) Massif Central; (9) Central European provinces; (10) Rio Grande Rift; (11) Virunga volcanic field; (12) Basin and Range, western United States; (13) Italian provinces; (14) continental flood basalts; (15) Oslo Rift; (16) Ataq; (17) Leucite Hills; (18) Gaussberg; (19) South African kimberlites; (20) Marie Byrd Land; (21) Smokey Butte. Depleted end-member compositions for ten of the fields fall precisely at PREMA. This, together with the fact that none of the more than 500 analyses fall within the N-type or depleted end of the MORB field (Panel *B*), suggests PREMA rather than DMM as a depleted mixing end member (Carlson 1984, Worner et al 1986). Horizontal arrays extending to high values of $^{87}Sr/^{86}Sr$ are interpreted by Worner et al (1986) as documenting assimilation of high-Sr crust by differentiated magmas with very low Sr contents (due to extensive plagioclase fractionation).

Collectively, these and other observations have led to the widely held view (e.g. Anderson 1985) that the U-Th-He system has been "decoupled" from the U-Th-Pb, Sm-Nd, Rb-Sr, and Lu-Hf systems (i.e. that the U-Th-He system, by virtue of the gaseous daughter product, has been subject to perturbations that have not affected the other systems). It is the nature, location, and timing of these perturbations that are of interest to us if we are to accurately interpret the He isotope signal in oceanic basalts.

The petrogenesis of mantle magmas typically results in an increase of U/Pb, Rb/Sr, Nd/Sm, and probably U/Pb (see Watson et al 1986) ratios in derived basalts relative to presumed mantle sources. These increases, however, are modest and rarely, if ever, approach an order of magnitude (e.g. Zindler et al 1979). In contrast, U/He ratios in OIB magmas are higher than estimated mantle source values by up to six orders of magnitude (if we assume single-stage source evolution; see Figure 16). The high degree of incompatibility expected for both U and He in candidate mantle phases makes it appear highly unlikely that such fractionations can occur during magma generation (see Zindler & Hart 1986). Several authors (e.g. O'Nions & Oxburgh 1983, Allegre et al 1986) have suggested or implied that rapid

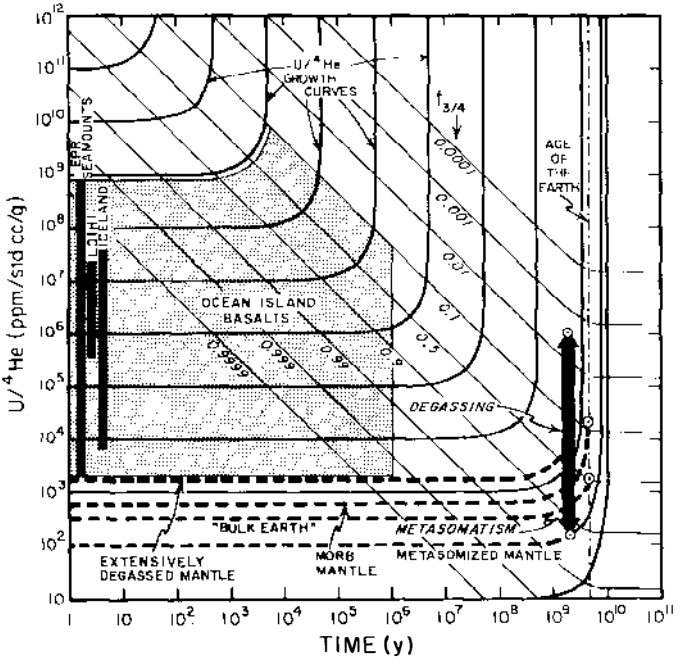

Figure 16 $U/^4He$ [ppm/(std cm^3/g)] vs time (in years). Diagram is designed to aid in the assessment of the evolution of $^3He/^4He$ ratios in systems with a given $U/^4He$ ratio. Heavy solid lines, labeled "$U/^4He$ growth curves," document closed-system changes in $U/^4He$ due to growth of radiogenic ^4He from U and Th decay. Contours are shown for values of $f_{3/4}$ ranging from 0.9999 to 0.0001 [thin solid lines with slopes of ~ -1; $f_{3/4} = (^3He/^4He)_p/(^3He/^4He)_t$, where $(^3He/^4He)_p$ is the present-day He isotope ratio in a system that has been closed since time t]. The $^{232}Th/^{238}U$ ratio is taken as 3.0; use of values of 3.5 or 4.0 would shift the $f_{3/4}$ contours slightly to the left without qualitatively changing the appearance or the implications of the diagram.

The inner two heavy dashed lines toward the base of the diagram indicate closed-system evolution paths for the MORB source reservoir and BSE over the past 4.4×10^9 and 4.55×10^9 yr, respectively (following R. Hart et al 1985). U concentrations are from Table 3, and initial $^3He/^4He$ ratios are taken as 100 Ra, although use of 200 Ra would not significantly shift the positions of the paths because of the log-log scale. Present-day $^3He/^4He$ ratios in the MORB source and BSE reservoirs are assumed to be 8 and 50 Ra, respectively; again, use of 30 Ra or 80 Ra for BSE would not significantly change the diagram. The resulting present-day $U/^4He$ ratios in the MORB source and BSE reservoirs are ~ 630 and ~ 310, respectively. Note that these values are substantially lower than $U/^4He$ ratios measured in basalts from Iceland (Condomines et al 1983, Kurz et al 1985), Loihi (Kurz et al 1983), and several small seamounts adjacent to the East Pacific Rise at $\sim 12°N$ (Graham et al 1984, 1986), a result which suggests large amounts of pre- or posteruptive degassing.

The outer two heavy dashed lines show hypothetical closed-system evolution paths for extensively degassed and metasomatized mantle segments over the past 2×10^9 yr. These mantle segments are presumed to have evolved from the MORB reservoir at this time. The metasomatized reservoir, considered a possible analog for EM I, has incorporated a He-rich, U-poor fluid component that has resulted in a factor of 10 reduction in its $U/^4He$ ratio. This has the effect of "freezing-in" its 2-b.y. $^3He/^4He$ ratio, as indicated by the downward traverse across $f_{3/4}$ contours from ~ 0.70 to ~ 0.93. The extensively degassed reservoir is considered to be a possible analog for HIMU, originating as either a metasomatic residuum or a degassed magma. This increase in $U/^4He$ shifts the material above the $f_{3/4} = 0.01$ contour, leading to a present-day $^3He/^4He$ ratio less than the atmospheric value. Note that even this extensively degassed mantle material will have a relatively low $U/^4He$ ratio today owing to the 2-b.y. aging period.

Heavy solid bars at the left side of the diagram show ranges for ocean island and seamount basalts from sources mentioned above. (Note that these bars are for reference only, and that their positions have no time significance.) The shaded field labeled "ocean island basalts" is drawn to include these bars and is arbitrarily terminated at 10^6 yr and $f_{3/4} = 0.1$ (i.e. factor of ten closed-system reduction in $^3He/^4He$). This field documents the potential for $^3He/^4He$ reduction in real systems on time scales that may be appropriate for high-level magma evolution. "Worst-case" scenarios involve the preeruptive loss of He from a magma [via continuous diffusive loss (CDL) or exhalative loss (EL) models], which results in an increase in $U/^4He$ from ambient mantle values (heavy dashed lines) into the shaded field. Subsequent "aging" of the magma results in $^3He/^4He$ reductions, as indicated by the $f_{3/4}$ contours. For example, a mantle melt that is degassed 2×10^5 yr ago to a $U/^4He$ ratio of $\sim 2 \times 10^7$ will have suffered about a 50% reduction of its original mantle $^3He/^4He$ ratio by the present day; this magma will then have a present-day $U/^4He$ ratio of 10^7. As another example, a magma that degasses 5×10^4 yr ago to a $U/^4He$ ratio of $\sim 10^9$ will suffer a 90% reduction in $^3He/^4He$ by today, at which time it will have a $U/^4He$ ratio of $\sim 10^8$. The observed disparity between mantle and basalt $U/^4He$ ratios clearly documents the potential for $^3He/^4He$ reduction during high-level magma evolution.

solid-state diffusion of He relative to U may explain large U/He variations; this, however, now seems unlikely based on measured diffusion rates for He in olivine (Hart 1984a). We conclude, therefore, that U/He ratios document magma degassing, which may occur prior to or during eruption. The important question in the present context is whether or not significant amounts of ^{4}He can accumulate subsequent to this degassing and prior to sampling and analysis (see also the comprehensive discussion in Kurz & Jenkins 1981).

By and large, ^{3}He/^{4}He ratios are determined on "zero-age" rocks or in fluid (or melt) inclusions in phenocrysts, so that in-situ production of ^{4}He is not presumed to be significant. Even in rocks that are not "zero age," the extent of the problem can be assessed by measuring U, Th, and He concentrations and correcting ^{3}He/^{4}He ratios for in-situ accumulation of ^{4}He. However, ^{3}He/^{4}He ratios measured in volcanic rocks are typically equated with mantle source values, and thus it is implicity assumed that ^{4}He accumulation during mantle or crustal magma storage is not important. We suggest that in the face of abundant evidence for preeruptive degassing of magmas, this may be a dangerous presumption.

The change in ^{3}He/^{4}He with time in a given system can be assessed by defining a factor $f_{3/4}$ that represents the fractional change in ^{3}He/^{4}He with time:

$$f_{3/4} = (^3\text{He}/^4\text{He})_f/(^3\text{He}/^4\text{He})_o = 1-[2.178 \times 10^{-13}(\text{U}/^4\text{He})t],$$

where U is in ppm total U, ^{4}He is in std cm^3 g^{-1}, t is in years, and the subscripts f and o refer to final and initial values respectively.

There will be essentially no change in the ^{3}He/^{4}He ratio of a system (that is, $f_{3/4} \geq 0.95$ when the product $(\text{U}/^4\text{He})t \leq 2.3 \times 10^{11}$). U/^{4}He ratios (in many cases estimated from K contents using a K/U value of 1.27×10^4 from Jochum et al 1983) in the range 5×10^5 to $> 10^8$ are not uncommon in basalts from ocean islands and seamounts (Graham et al 1984, 1986, Condomines et al 1983, Kurz et al 1983, 1985), and "zero age" ($f_{3/4} \geq 0.95$) in such cases may stipulate times since degassing of < 2000 to 500,000 yr. These relationships are shown in Figure 16, where U/^{4}He [ppm/(std cm^3/g)] is plotted versus time and contoured for values of $f_{3/4}$ ranging from 0.9999 to 0.0001. Thus, for a given present-day U/^{4}He ratio at the left side of the diagram, changes in ^{3}He/^{4}He back in time can be traced. For example, a rock with U/^{4}He $= 10^7$ and ^{3}He/^{4}He $= 5$ Ra today would have had a ^{3}He/^{4}He ratio of 30 Ra 383,000 yr ago (had it or the predecessor magma existed as a closed system over that time interval). Based on U/^{4}He ratios shown in Figure 16 for Hawaii, Iceland, and several small seamounts near the East Pacific Rise, it is clear that accumulation of radiogenic ^{4}He during

magma transit and storage may result in perturbation of indigenous mantle He isotope signatures.

Extensive preeruptive degassing of magmas will likely result in correlation of $U/^4He$ ratios with factors that document increasing magma differentiation. The relationships in Figure 17 document a tendency for cogenetic suites to display an inverse correlation of $U/^4He$ with Mg#. A number of factors, however, preclude a strictly quantitative analysis of this kind of diagram (Zindler & Hart 1986), although the convincing, and in some cases, striking negative correlations that are observed support the contention that preeruptive degassing may be an important phenomenon.

MODELING OF HE LOSS VIA DEGASSING We have modeled the effects of preeruptive He loss on $^3He/^4He$ ratios using two end-member models: (*a*)

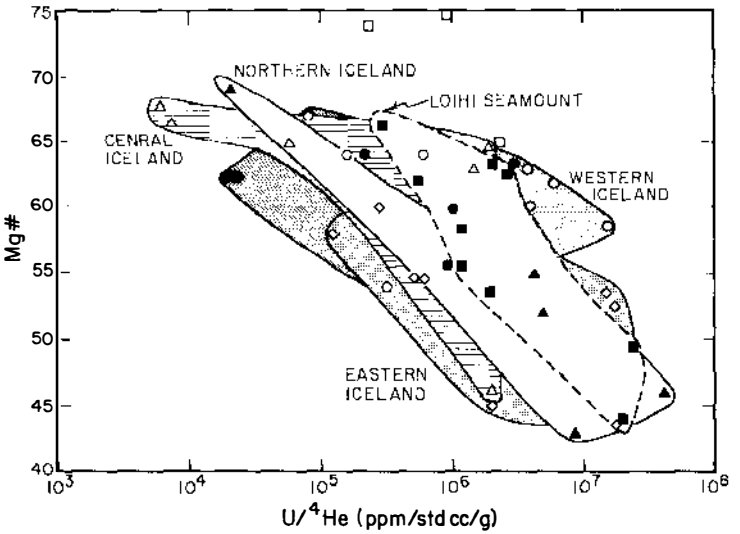

Figure 17 Mg# vs $U/^4He$ [ppm/(std cm^3/g)] variation diagram for samples from Iceland (Condomines et al 1983, Kurz et al 1985) and Loihi (Kurz et al 1983). Mg # (atomic) calculated with $Fe_2O_3/FeO = 0.2$. In many cases, U had to be estimated from K contents by taking advantage of the relative constancy of K/U in basalts (Jochum et al 1983). Data for Iceland are broken down into northern (closed triangles), central (open triangles), eastern (diamonds), and western (open and closed circles) regions (see Kurz et al 1985). The Kurz et al data were obtained by crushing only, and so they may tend to underestimate He contents. Loihi data include closed and open squares, but the open squares are not included in the Loihi field because they have clearly accumulated olivine and therefore have anomalously high Mg#s. Note that all fields, to greater and lesser degrees, display negative correlations between the two plotted parameters. We interpret this as strong evidence that degassing of magmas, resulting in increased $U/^4He$, proceeds in conjunction with crystal fractionation, which causes reduction of the Mg#.

continuous diffusive loss from a magma chamber (CDL model), and (*b*) exhalative loss via partitioning into an evolved CO_2 gas phase (EL model). The general behavior of the CDL model (described in detail in Zindler & Hart 1986) is illustrated in Figure 18, which shows the rapid loss of initial ^3He and ^4He, the buildup of radiogenic $^4He^*$, and a crossover of $^4He_0$ and $^4He^*$ at time $t \sim 2.3$ m.y. The total ^4He ($^4He_0 + {}^4He^*$) becomes constant for

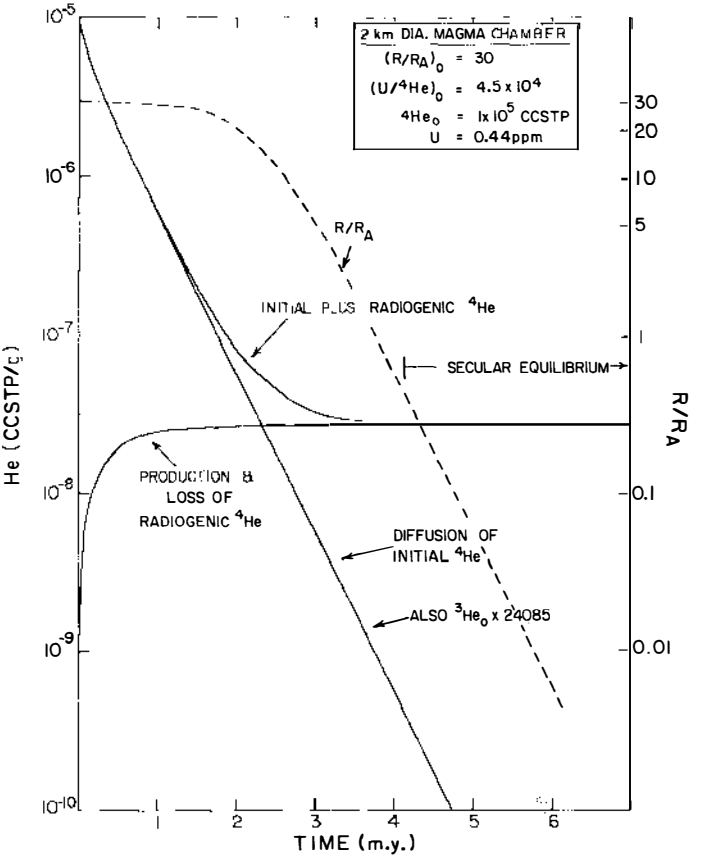

Figure 18 Variation of He concentrations and $^3He/^4He$ ratio (log scales) as a function of time for the CDL model. Model parameters are given on the figure; a He diffusion coefficient of 7.5×10^{-5} cm^2 s^{-1} was used (see text). Curves show the diffusion loss of initial ^3He and ^4He (approximately log-linear), the in-situ production and concurrent diffusional loss of radiogenic ^4He, and the sum of initial plus radiogenic ^4He. This latter quantity approaches steady state (secular equilibrium) for times > 4 m.y. Also shown (dashed curve) is the evolution of $^3He/^4He$ ratios (right-side axis) as a function of time. For the chosen parameters, the $^3He/^4He$ ratio decreases very rapidly for times > 2 m.y. Governing equations are derived in Zindler & Hart (1986).

$t > 4$ m.y., which represents a state of secular equilibrium between $^4He^*$ loss and $^4He^*$ production. The decrease of $^3He/^4He$ with time (also shown in Figure 18) is related to the fact that ^4He loss is being balanced by ^4He production, whereas ^3He is simply lost. For the particular parameters chosen for Figure 18, the $^3He/^4He$ ratio drops by 10% in $\sim$ 1.5 m.y., and by 50% in $\sim$ 2.3 m.y.

Ultimately, however, the evolutionary history of magma chambers depends on thermal budget considerations. By noting that thermal diffusivities are $\sim$ 100 times higher than He diffusivities (at 1200°C), we see that it may be difficult to keep a magma chamber molten long enough for He diffusion to cause significant reduction in $^3He/^4He$. For example, a 2-km static magma chamber will cool below its solidus in $\sim$ 20,000 yr [for ΔH (fusion) = 150 cal g^{-1}, thermal diffusivity = 0.006 cm^2 s^{-1}, and ΔT (magma–wall rock) = 150°C]. The only conceivable way of avoiding such a short lifetime is to intrude, or refill, a magma chamber that has been in prior existence long enough to substantially preheat the environment so that ΔT between wall rock and magma approaches zero.

Figure 19 gives solidification times (in millions of years) as a function of ΔT for spherical magma chambers of various diameters (0.5–10 km) that have been refilled for the last time [see Zindler & Hart (1986) for details]. Curves represent the time required by the CDL model to decrease $^3He/^4He$ by 10% as a function of various initial $U/^4He$ ratios (10^3–3×10^6). Clearly, the effect on $^3He/^4He$ is a sensitive function of the initial $U/^4He$ ratio. For magmas that start at mantle values ($\lesssim 10^3$), changes in $^3He/^4He$ will likely not exceed 10%, even with a magma chamber life of several million years and $\Delta T = 10$°C. However, for magmas with high initial $U/^4He$ values (perhaps resulting from degassing at depth, as discussed below), changes in $^3He/^4He$ due to evolution in such a system may be dramatic.

The EL model assumes that He is lost from a magma by partitioning into, and subsequent loss of, a CO_2-rich fluid or gas phase once CO_2 solubility is exceeded at a given pressure. Experimental work has shown that basaltic magmas may dissolve large quantities of CO_2 at depth (3–7 wt%; Mysen et al 1975). In contrast, the average CO_2 content in Mid-Atlantic Ridge basalts is on the order of 0.13 wt% (Delaney et al 1978), a value that is in accord with saturation limits predicted for MORB (at pressures of $\sim$ 250–400 bars) by Khitarov & Kadik (1973). Greenland et al (1985) have recently constructed a mass-balance model for several volatile species in Kilauea magmas. They estimate that the magmas arrive at the summit magma chamber (2–5 km depth) laden with 0.32 wt% of both CO_2 and H_2O. More than 90% of this CO_2 is lost by preeruptive degassing, $\sim$ 6% is lost during eruption, and less than $\sim$ 3% is retained in the magma. (In contrast, H_2O

solubility is not exceeded within the magma chamber, and most of the H_2O is outgassed at eruption.)

These observations suggest that preeruptive degassing of CO_2 from magmas is not only important, but that it dominates the CO_2 flux from the mantle to the atmosphere, with eruptive degassing accounting for a relatively minor component of this flux. During the exsolution of a CO_2-rich gas phase from a magma, He is expected to behave as an infinitely dilute trace element and partition according to Henry's law between the silicate melt and gas or fluid phases. We have modeled this process using the partitioning data of Kurz & Jenkins (1981) together with temperature corrections discussed by Kurz (1982).

In order to predict the change in $U/^4He$ in a system that has outgassed CO_2 prior to eruption, we need to know the amount of CO_2 that has been

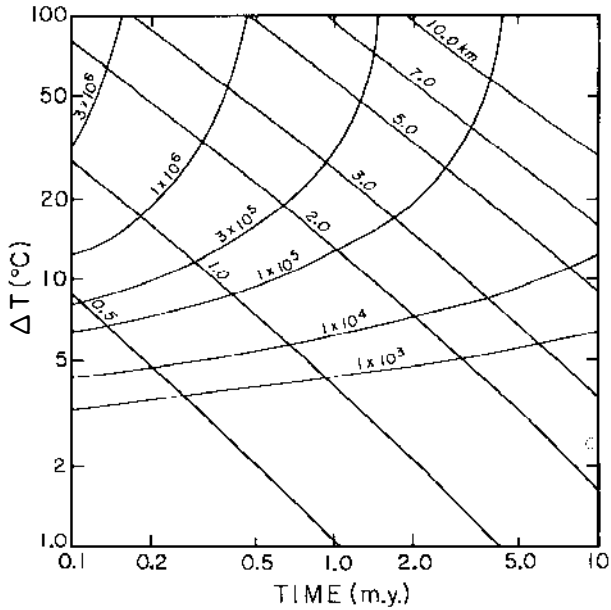

Figure 19 Solidification time (in millions of years) versus temperature contrast [ΔT(°C)] between a refilled spherical magma chamber and uniform wall-rock temperature subsequent to refilling for the last time. Magma chambers of various diameters (in km) are shown as solid diagonal lines. Curves represent the time required by the CDL model to decrease the $^3He/^4He$ ratio by 10% as a function of various initial $U/^4He$ ratios [ppm (std cm^3 g^{-1})] ranging from 10^3–3×10^6, of magma chamber diameters, and of values of ΔT. Cooling models calculated for conductivity of 2.5×10^{-3} cal s^{-1} cm^{-1} deg^{-1}, specific heat of 0.36 cal g^{-1} °C^{-1} (basalt at 1200°C), and density of 2.9 g cm^{-3} (Birch et al 1942); latent heat taken as 110 cal g^{-1} (Yoder 1976). The nonconvecting fixed melting-point formulation of Flemings (1974) was used for the thermal model; the fact that basalt has a melting interval of $\sim$ 100°C was accounted for to first order by using an "effective" latent heat of 146 cal g^{-1}.

lost and the depth of outgassing. Figure 20 shows the relationship between the change in the U/^{4}He ratio ($f_{U/He}$) and F(the wt% of CO_2 that has been outgassed) for values of D ranging from 1.35×10^{-3} to 6.77×10^{-3} corresponding to pressures of 300–1500 bars. [D is the liquid/gas partition coefficient (moles He per gram of liquid/moles He per gram of CO_2) and derives directly from K, the Henry's law constant for He solubility (Kurz & Jenkins 1981).] The curves are calculated using a Rayleigh model that presumes that gas bubbles are rapidly removed from the system as they are formed, so that the total gas is not maintained in equilibrium with the residual liquid system.

Unfortunately, the CO_2 budget of the mantle is ill constrained, so that primary magma CO_2 contents are difficult to estimate. We can, nevertheless, compare increases in U/^{4}He in magmas relative to the mantle (see Figure 16) with predicted CO_2 losses (Figure 20) and measured CO_2

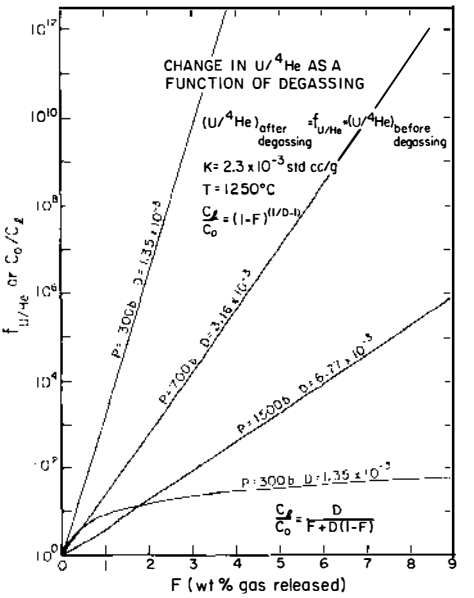

Figure 20 Changes in U/^{4}He are shown as a function of F, the wt% of CO_2 gas released from a magma. Here $f_{U/He}$ is the ratio of U/^{4}He in the magma after degassing to that before degassing. Curves for 300, 700, and 1500 b (bars) are shown for a Rayleigh degassing model [$C_l/C_0 = (1-F)^{(1/D)-1}$]; a 300-b curve for an equilibrium degassing model is also shown for reference {$C_l/C_0 = D/[F + D(1-F)]$}. In these equations, the subscript "l" refers to the final magma and "0" refers to the magma prior to degassing. The Rayleigh model essentially assumes that as CO_2 exsolves from the magma, it is rapidly removed from the system (that is, it either escapes or is segregated at the top of a body of magma). Variation of D with pressure is discussed in Zindler & Hart (1986). Note that, for a given F or wt% CO_2 released, He is lost much more efficiently at lower pressures.

solubilities in magmas. MORBs, for example, have $U/^4He$ ratios on the order of 6×10^3, or about a factor of 10 higher than a model mantle source ($f_{U/He} = 10$). If we assume that this outgassing occurs in the upper kilometer of the oceanic crust ($P \sim 300$–700 bars), we would predict the loss of something between 0.30 and 0.75 wt% CO_2, compared with a value of 0.13 wt% CO_2 retained in the erupted lava (Delaney et al 1978). Such amounts of CO_2 are likely to exceed solubility limits in basalt at pressures less than 1 kbar, and it is likely, therefore, that He loss from MORBs occurs via more extensive CO_2 outgassing at greater depths, or that MORBs arrive at shallow levels supersaturated with CO_2.

To produce large values of $f_{U/He}$ by outgassing CO_2, OIB magmas must arrive at relatively shallow levels supersaturated with CO_2. Because of this requirement, the time scales permitted for radiogenic ^4He accumulation will be on the order of magma residence times in high-level magma chambers. Such time scales may range from very short times in high-throughput environments such as midoceanic ridges, to several million years for large magma chambers in stagnating systems, such as might occur during the waning stages of volcanism at an ocean island.

The potential for producing changes in $^3He/^4He$ in the context of the EL model is still significantly greater than for the CDL model because the He loss may occur over much shorter time spans and is not strongly coupled to heat loss. That is, in the CDL model, He diffusion from the magma chamber occurs as the magma cools, and effective evolution times at high values of U/He will be limited. In the EL model, however, significant outgassing of a high-level magma may occur with very little associated cooling, allowing more time for evolution of the high U/He system. For example, with the CDL model, a magma chamber diameter of 1 km, and a magma with $(U/^4He)_0 = 5 \times 10^3$ and $(U/^4He)_f = 4.2 \times 10^6$, reduction of $^3He/^4He$ over 7×10^6 yr is on the order of 6.7% (with an initial $^3He/^4He$ value of 30 Ra). This is a minimum value for the CDL model, however, because outgassing of CO_2, even at depth, will substantially increase the potential for change in $^3He/^4He$ by diffusive loss of He from a magma chamber. By comparison, magma that attains a $U/^4He$ ratio of 4.2×10^6 by degassing will suffer more than 50% reduction of $^3He/^4He$ over 7×10^5 yr, or a 6.7% reduction in less than 10^5 yr (see Figure 16).

The arguments presented here are necessarily qualitative because of the lack of constraints on magma residence times, CO_2 budgets, and depths for degassing. We cannot, therefore, make specific statements regarding changes in $^3He/^4He$ ratios measured at individual localities. We can, however, draw several general conclusions, which may be used as guidelines for the interpretation of $^3He/^4He$ data until such time as a more quanti-

tative treatment is feasible:

1. Low $U/^4He$ ratios in MORBs preclude any significant preeruptive reduction of $^3He/^4He$ ratios.
2. Low $U/^4He$ ratios in some OIBs ($U/^4He < 10^5$) are subject to a maximum of a few percent reduction of $^3He/^4He$ over time scales ranging up to 10^6 yr.
3. OIBs with $U/^4He$ between 10^6 and $\sim 5 \times 10^8$ may be subject to significant reduction of $^3He/^4He$ ($\geq 10\%$), with preeruptive aging over time periods ranging from 5.6×10^5 to 1.0×10^3 yr.
4. Where $U/^4He$ ratios of magmas are not available because $^3He/^4He$ ratios have been measured in fluid inclusions in phenocrysts, the potential for preeruptive $^3He/^4He$ reduction may be considered to increase with decreasing magma throughput in the system and with the degree of differentiation of the host magma.
5. Where $^3He/^4He$ values may have suffered preeruptive reduction, measured ratios should be considered as minimum values for the mantle source.

The Proverbial Bulk Silicate Earth (BSE)

The question of whether or not there exists today some primitive, undifferentiated segment of the Earth's mantle is central to the development of a viable and comprehensive model for the geochemical evolution of the Earth. The concept of such a primitive mantle segment has become quite common in the modern literature, although the terminology used to describe it has been varied. Essentially, the idea is that during accretion, core formation, and associated degassing, the silicate Earth achieves a fairly homogeneous state as a result of high heat flow and rapid convection. Those elements that do not enter the core or the atmosphere will then be represented in their initial, or primordial, abundance ratios in the silicate portion of the Earth. The elusive, primitive mantle segment (BSE) is then one that is supposed to have survived from this time as a closed system.

Documentation of the existence of such material today has been sought via two separate lines of reasoning: (*a*) that some oceanic and continental basalts are observed to have Nd isotope ratios similar to chondrites and to the presumed BSE (e.g. DePaolo & Wasserburg 1976a,b, O'Nions et al 1977, Wasserburg & DePaolo 1979, Jacobsen & Wasserburg 1979, DePaolo 1981); and (*b*) that some oceanic and continental basalts have $^3He/^4He$ ratios that are significantly higher than the atmospheric value (e.g. Lupton & Craig 1975, Kurz et al 1982, 1983). Although tacitly accepted throughout much of the literature, these two lines of reasoning do not

represent unique interpretations of the available data, nor, in fact, are they altogether consistent with each other [since the highest observed $^3He/^4He$ ratios do not represent samples or locales with chondritic $^{143}Nd/^{144}Nd$, or single-stage Pb that lies on the geochron (see Figures 11, 12)].

As fate would have it, the first series of high-precision measurements of $^{143}Nd/^{144}Nd$ in young basalts ranged from $\varepsilon_{Nd} \sim 13$ [where $\varepsilon_{Nd} = 10^4 (^{143}Nd/^{144}Nd_{measured} - {}^{143}Nd/^{144}Nd_{chondrites})(^{143}Nd/^{144}Nd_{chondrites})^{-1}$, and $^{143}Nd/^{144}Nd_{chondrites} = 0.51262$] in MORBs to $\varepsilon_{Nd} \sim 0 \pm 2$ for continental flood basalts and the island of Tristan da Cunha (Richard et al 1976, DePaolo & Wasserburg 1976a,b, O'Nions et al 1977). The observed correlation of $^{143}Nd/^{144}Nd$ with $^{87}Sr/^{86}Sr$ gave rise to the "mantle array" (early version of Figure 6) and was presumed to permit estimation of an average $^{87}Sr/^{86}Sr$ value for BSE (0.7045–0.7050). Implicit in this line of reasoning, and explicit in many of the models that followed (e.g. Jacobsen & Wasserburg 1979, DePaolo 1980, O'Nions et al 1979, Allegre et al 1980), was the idea first discussed by Schilling (1973) that isotopic variations in mantle-derived basalts result from mixing between depleted and undepleted (or primitive) mantle reservoirs. The data, however, which were taken to justify the notion of primitive undifferentiated mantle, would always have been equally well or better explained by mixing between a MORB source component and an enriched component with $\varepsilon_{Nd} < 0$ (Anderson 1982b). As more data have been acquired, the need for enriched mantle material has become more evident, and consequently compelling arguments for an undifferentiated mantle reservoir have been diminished.

Even when we explain away chondritic $^{143}Nd/^{144}Nd$ ratios as mixing phenomena, we must deal with the source for ^3He in the mantle. Despite the problems concerning production of ^4He, the range of $^3He/^4He$ ratios measured in mantle-derived basalts (Figure 14) clearly demonstrates that there are at least more and less "primitive", if not primordial, materials in the suboceanic mantle. However, as noted earlier, when we take $^3He/^4He$ ratios at face value, there is little evidence to suggest that high $^3He/^4He$ ratios occur in rocks that have ε_{Nd} values close to zero (see Figure 11). Furthermore, high $^3He/^4He$ ratios need not indicate the existence of primitive mantle; they could just as well document intramantle metasomatism of a previously depleted mantle segment, which resulted in a relative stabilization of high $^3He/^4He$ ratios at some time in the past (Figure 16; Rison & Craig 1982, Anderson 1985).

Based on the above discussion, we deem it reasonable to at least examine the consequences of a mantle that no longer contains any primitive undifferentiated components. Such a scenario could evolve in two different ways. First, enriched and depleted segments could evolve via continuous differentiation of a homogeneous mantle that had a chondritic Sm/Nd

value subsequent to accretion. Second, borrowing from Armstrong (1981), we might consider that separation of the core did not result in homogenization of the silicate portion of the Earth. Certainly, with separation of the core and atmosphere, extensive differentiation of the silicate Earth may occur in conjunction with a substantial upward flux of incompatible elements. This likely resulted in at least the transient production of a granitic or alkali basaltic crust. Whether or not the silicate portion of the Earth was ever homogenized subsequent to this time depends on how effective early mantle convection was with regard to destruction of these earliest differentiates. If they survived to be reworked and cratonized during the Archean, then even mantle that has existed as a closed system for the past 4.4 b.y. may have a depleted Nd isotopic signature due to the separation of these early differentiates with low Sm/Nd ratios.

Even if "primordial" mantle material has survived unfractionated since accretion or core formation, we contend that no geochemical observation to date demands this survival. However, neither do the data demand that no such "primordial" component survives. Accordingly, we shall consider both possibilities in our subsequent evaluation of geochemical mantle models.

The Source of Midocean Ridge Basalts (MORBs)

The observation that MORBs that are well removed from any hotspot volcanism display unique "depleted" isotopic characteristics that are not observed elsewhere in oceanic or continental volcanic domains (see Figures 6–12, 15) documents the existence of a depleted mantle segment, which constitutes an important volumetric fraction of the MORB source reservoir. We refer to this depleted segment as end-member-depleted MORB mantle (DMM) and suggest that MORBs with more "enriched" isotopic signatures result from the inclusion of relatively enriched components in a DMM matrix.

Recent modeling of midocean ridge isotopic variations (Cohen & O'Nions 1982a, leRoex et al 1983, Allegre et al 1984) and studies of seamounts situated near the East Pacific Rise (Batiza & Vanko 1984, Zindler et al 1984, Graham et al 1984, 1986) all support this view of the MORB source mantle. In fact, this is one of the more notable successes of recent geochemical work on the mantle, and we embrace it without reservation in our subsequent discussion of mantle chemical dynamics.

The question of whether the MORB source mantle is heterogeneous on a large or global scale (100–10,000 km) is a bit more difficult to approach. The scale of melting and the rate of magma production at a given ridge segment will likely affect the chemical influence of the dispersed enriched components if their solidi are lower than that of DMM (Zindler et al 1984, Sleep

1984). The chemical influence of the dispersed components will also be diminished by processing through large magma chambers, which may be present at faster spreading ridges (Allegre et al 1984). Within this context, we might expect that some large-scale geochemical variations between MORBs may result from variable styles of magma processing at ridges with variable rates of magma throughput.

Recent work by Dupre & Allegre (1983) on MORBs from the Indian Ocean has shown that these rocks, even when far removed from hotspots, tend to be isotopically distinct from MORBs of other latitudes and oceans (Hart 1984b). For present purposes, the critical question with regard to these data is whether they document distinct differences in the isotopic character of the DMM component, the enriched components, or both, or whether they simply represent an increased abundance of enriched components. While none of these explanations can be categorically excluded, the latter is consistent with the large amounts of subduction known to have characterized the Southern Hemisphere during the Phanerozoic (Anderson 1982a) and the hypothesized origins for enriched mantle components (EMs), which are discussed subsequently.

With regard to the location of the MORB reservoir, we know that MORB source material is present beneath all active ridges. Essentially, all other volcanic materials (e.g. ocean islands, continental basalts, intra-oceanic arcs, etc) known to have feeder systems that extend to deeper mantle levels than at least the melt segregation region under midocean ridges ($\geq$ 100 km) tend to have OIB-type isotopic signatures that are distinct from N-type MORB or DMM (Figures 14, 15). Taken at face value, this may mean that the MORB source mantle is restricted to the uppermost hundred or several hundred kilometers of the upper mantle. Such a suggestion is perhaps reasonable if DMM comprises relatively low-density depleted peridotite. In the context of the present discussion, we note that the only rocks at the surface of the Earth, other than normal MORBs, that are known to have DMM isotopic signatures are a subset of ultramafic xenoliths and orogenic lherzolites (Figures 1, 2). This suggests that DMM is peridotitic, as opposed to eclogitic or "piclogitic" (the latter having been suggested by Anderson 1983, Anderson & Bass 1985), and documents the existence of at least some DMM in the uppermost mantle beneath continents, particularly the relatively young mobile zones in which the xenolith localities and orogenic peridotites occur (e.g. the Rio Grande Rift, the Rhine Graben, East Africa, and Alpine zones of the western Mediterranean).

Recent work with rare gases has shown that DMM is characterized by (*a*) $^{3}He/^{4}He$ ratios of 8.0 ± 1.0 Ra (e.g., Kurz et al 1982; Figure 14); (*b*) $^{40}Ar/^{36}Ar$ ratios that are probably in excess of 25,000 (Allegre et al 1983a, Sarda et al 1985); and (*c*) occasionally observed excesses of ^{129}Xe, formed

by the ancient decay of now-extinct ^{129}I (Staudacher & Allegre 1982, Allegre et al 1983a). The xenon and argon data, taken together, strongly support a catastrophic degassing of proto-DMM during the first $\sim 10^8$ yr of Earth history (Staudacher & Allegre 1982, R. Hart et al 1986, Sarda et al 1985). $^3He/^4He$ ratios of 8 Ra, although substantially lower than "planetary" or solar values of ~ 100 to 200 Ra (Jeffrey & Anders 1970, Craig & Lupton 1978), are still markedly enriched in primordial ^3He compared with the atmosphere, and these values suggest that the early degassing was more efficient for Ar and Xe than for He (e.g. R. Hart et al 1985, Sarda et al 1985); this is consistent with the enhanced solubility of the lighter noble gases in silicate melts (e.g. Ozima & Podosek 1983).

When the He isotope data for MORBs are compared with the data for other isotopic systems displayed in Figures 10–12 and 14, it is apparent that MORB $^3He/^4He$ ratios cover a relatively small fraction of the total oceanic basalt range, and that in contrast to all the other systems, MORBs fall *within* the oceanic range rather than defining one end of it. The latter observation may relate to the rapid accumulation of radiogenic ^4He in degassed and/or recycled materials and the influence of such processes and/or materials at some ocean islands. The relatively rapid diffusion of He in the presence of a small amount of melt ($D = 7 \times 10^{-5}$ cm^2 s^{-1} at 1200°C, extrapolated from Kurz & Jenkins 1981) may contribute to the smoothing of $^3He/^4He$ variations in the MORB reservoir during magmatic processing, if heterogeneities are on the order of 1 km or less.

A Prevalent Mantle Composition (PREMA)

Isotopic compositions of ocean islands and enriched MORBs, which are intermediate between DMM, BSE, HIMU, and EM components in Figures 6–9, have traditionally been interpreted as mixtures of these or other end-member components. Following the reasoning of Morris & Hart (1983) and Carlson (1984), we suggest the existence of a distinct mantle component with this isotopic character ("PREMA" for *pre*valent *ma*ntle). The position of this component is shown in Figures 6–12 and 15 and is seen to coincide with (*a*) fields for many ocean islands, including Iceland and Hawaii; (*b*) the most depleted representatives of many continental basalt suites (Figure 15); and (*c*) fields for many intraoceanic island arcs (see Figure 14). The coincidence of this component with Iceland and Hawaii, and with their respective high $^3He/^4He$ ratios (Figures 10–12), suggests that at least some portion of PREMA is relatively gas rich.

If PREMA represents a mixture of DMM, HIMU, and EM (with or without BSE) on a scale of 100 m or less, then the process of sampling during melting may necessarily result in a fairly restricted range of compositions, as we have already discussed for the MORB mantle. Such a

result could not be easily distinguished from a mantle segment with PREMA characteristics that is homogeneous down to a meter or centimeter scale. On the other hand, if distinct components that compose PREMA are separated by large distances in the mantle (> 100 km) or reside within separate convective regimes, then the PREMA composition must result from a very reproducible mixing process that acts over large distances. We believe that the ramifications of both of these scenarios should be considered, and that the current geochemical data base is consistent with either of them.

The origin of a PREMA component may be envisioned in several different ways. First, as discussed earlier in Section 2, we might imagine that significant differentiation of the silicate portion of the Earth occurred contemporaneously with core segregation (e.g. Anderson 1979, Armstrong 1981). If something on the order of 50% of the present-day continental crust (or the trace-element equivalent) were segregated at this time, then PREMA today might represent the most primitive remaining mantle, having essentially survived unscathed since the earliest days of Earth history. In this context, the high $^3He/^4He$ ratios at Iceland and Hawaii would not be surprising. A variation of this scenario might suggest that, over the first part of Earth history (~ 1–2×10^9 yr), the entire mantle mixed convectively, which resulted in a PREMA-type depletion of the whole mantle. Subsequent splitting into upper and lower mantle convective regimes would then preserve PREMA in the lower mantle today, while the upper mantle would continue to be depleted by crust extraction, evolving toward DMM.

Alternatively, PREMA may evolve via the quasi-continuous separation of a crustal component from the mantle over time. We can hypothesize that the creation of new continental crust at volcanic arcs results in the complementary production of enriched and depleted mantle segments (EM, HIMU, and DMM). The EM, HIMU, and DMM components may then remix into the convecting mantle with time constants of 1–2×10^9 yr, so that at any given time, the mantle contains "quasi-steady-state" amounts of these materials. The ambient remixed mantle material will then represent PREMA. It would then follow that (*a*) PREMA is the chemical complement of the continental crust, (*b*) PREMA is approximately the mean composition of the mantle, and (*c*) that DMM + EM I + EM II + HIMU = PREMA.

These scenarios allow significant latitude for the location of PREMA in the mantle today, providing that it does represent a distinct component. If PREMA is close to the average mantle composition and is complementary to the continental crust, then it may occupy much of the mantle and be overlain by a relatively thin layer dominated by low-density DMM (see

Figure 26). Alternatively, PREMA may reside totally within the lower mantle, with the upper mantle comprising a mixture of DMM, EMs, and HIMU. Volcanic rocks from arcs, continents, and islands with PREMA signatures are generally thought to be derived from depths in excess of 100 km, so that either of the above scenarios would be feasible.

A High U/Pb Mantle Component (HIMU)

Isotopic evidence for the existence of the HIMU component derives largely from consideration of the Pb isotope systematics displayed in Figure 9, where oceanic basalts appear to mix from the depleted MORB zone near the geochron out toward the islands of St. Helena and Tubuaii. The extreme enrichments of ^{206}Pb and ^{208}Pb observed at these islands suggest an enrichment in U + Th relative to Pb on the order of 1.5–2.0 $\times$ 10^9 yr ago (Tatsumoto 1978). These enrichments are not paralleled by an increase in Rb/Sr, and thus the islands are characterized by relatively low $^{87}Sr/^{86}Sr$ values ($\sim$ 0.7029). This unradiogenic Sr, which characterizes HIMU, suggests the possibility that HIMU has evolved from DMM some time in the past.

Chase (1981) and Hofmann & White (1982) suggested that HIMU might evolve from subduction of ancient altered oceanic crust, which is significantly enriched in U by interaction with seawater. At face value, it would appear difficult to provide U enrichments by seawater alteration without introducing a high $^{87}Sr/^{86}Sr$ signature. However, if the oceanic crust underwent alteration a few billion years ago, when the seawater Sr isotope curve was much closer to the mantle Sr evolution curve, a significant seawater Sr imprint might have been avoidable. It may be, however, that the fractionation of U from Th in the alteration cycle is sufficient to preclude the model.

Zindler et al (1982) proposed that HIMU might result from the subduction of ancient oceanic crust from which the alteration component had been removed by subduction-related processes. This proposal was made largely to avoid the problem of Th/U fractionations during alteration. The viability of this model hinges on the likelihood of a primary magmatic increase in U/Pb and Th/Pb during the generation of MORB melts. Relatively low μ values in hand-picked MORB glasses ($\sim$ 9.4), however, now seem to suggest that significant enrichments of U relative to Pb do not occur during MORB magmatism. However, further processing of MORB through subduction zones may effect such enrichments, as evidenced by low-μ values in island-arc volcanics (e.g. Tatsumoto 1978).

Vollmer (1977), Vidal & Dosso (1978), and Allegre and co-workers (e.g. Allegre et al 1980, Allegre 1982) have proposed that HIMU may result from extraction of Pb from some portion of the mantle to the core over a

significant portion of Earth history ($\sim 15\%$ of the core formed since 4.4×10^9 yr ago). A lack of constraints not only on the time scales for core formation, but also on the nature of the light elements in the core (S, Si, O), as well as the hypothesized chalcophilic tendencies for Pb at current lower-mantle pressures and temperatures, makes it difficult to evaluate this mechanism. For present purposes, we must allow that it remains a possibility.

Another mechanism that must be considered as a plausible means by which to produce HIMU is the mobilization of Pb (and Rb?) in a metasomatic fluid and its subsequent removal from some mantle segment. The behavior of Pb in the continental crust suggests its affinity for volatile-rich ore-bearing fluids and provides qualitative support for this hypothesis, although there is no available data with which to evaluate such behavior in the mantle. Mantle metasomatism might thus result in the production of a residual degassed HIMU component and a complementary gas-rich low-μ component.

Regardless of the mechanism by which HIMU is created, its ubiquitous presence in the interactive mantle is clearly documented by the mixing trends in Figure 9. We thus propose that HIMU is present as a dispersed component within the mantle.

Enriched Mantle Components (EMs)

The isotopic character of islands that lie outside the DMM, HIMU, and BSE mixing domains (outlined in Figures 7 and 8) necessitates the existence of EM components, whether or not we think a BSE component actually exists (Anderson 1982b, Cohen & O'Nions 1982b, Richardson et al 1982). Proposed modes of origin for EM components now include (*a*) injection into the mantle via subduction of continentally derived sediment or crust (Cohen & O'Nions 1982b), altered oceanic crust (Hofmann & White 1982), ocean island crust, or seamounts; (*b*) delamination of subcontinental lithosphere (McKenzie & O'Nions 1983); and (*c*) mantle metasomatism (e.g. Menzies & Murthy 1980a, Menzies 1983). It is significant that all of these mechanisms can operate in convergent margin tectonic settings.

EM components are characterized by low $^{143}Nd/^{144}Nd$, variable $^{87}Sr/^{86}Sr$, and high $^{207}Pb/^{206}Pb$ and $^{208}Pb/^{204}Pb$ (at a given value of $^{206}Pb/^{204}Pb$). We refer to the low and high $^{87}Sr/^{86}Sr$ EMs as EM I and EM II, respectively. Comparison of Figures 6 and 15 reveals that the tendency for the continental data array to "fan out" at low $^{143}Nd/^{144}Nd$ is mimicked, to a lesser degree, by the oceanic data array (Worner et al 1986). This behavior in the continental suites has been attributed both to the existence of enriched subcontinental mantle components and to the contamination of some mantle-derived magmas by upper and lower continental crustal materials, lying at high and low values of $^{87}Sr/^{86}Sr$, respectively (e.g. Carter

et al 1978, Hawkesworth et al 1983, 1984, Worner et al 1986). The similarity between the continental and oceanic arrays suggests similar styles of enrichment for the subcontinental and suboceanic mantle (although enrichment of the continental mantle is clearly more extreme), as well as the possible involvement of the continental crust in the production of EMs.

A review of the isotopic character of ultramafic nodules shows that many of those that contain hydrous phases plot below the oceanic array (Figure 1). If these materials represent metasomatized DMM, then the effect has been to decrease Sm/Nd substantially while increasing Rb/Sr only moderately (Menzies 1983, Zindler & Jagoutz 1986). These nodules, as well as some portions of ultramafic massifs (Reisberg & Zindler 1985, 1986, Brueckner et al 1986; Figure 2), are displaced from the oceanic array toward measured compositions for lower continental crustal materials (e.g. Hamilton et al 1979, Stosch & Lugmair 1984). Although little is known of the Pb isotopic character of ultramafic nodules, the range observed for $^{206/204}$Pb in massifs encompasses the whole range of oceanic Pbs (Hamelin & Allegre 1985a). We suggested earlier that metasomatized materials might have low U/Pb ratios and, with time, unradiogenic Pb (similar to that thought to characterize the lower continental crust). It is thus difficult to distinguish between recycled lower continental crust and metasomatized mantle as candidates for the EM I component.

EM II, characterized by high $^{87}Sr/^{86}Sr$ and low $^{143}Nd/^{144}Nd$, has a strong similarity with upper continental crust or continentally derived sediment (e.g. Hawkesworth & Vollmer 1979, Carlson 1984, Worner et al 1986). Subducted continental material has been strongly implicated in several island-arc volcanic suites [e.g. Banda arc (Morris 1984), Martinique (Davidson 1983), Lesser Antilles (White & Patchett 1984)], and the isotopic signatures of these "contaminated" arcs bear a strong kinship with the EM II clan of OIB. (In contrast, there are no EM I–type arcs.) There are, as well, some ultramafic nodules, predominantly from South African kimberlites, that display this EM II isotopic signature (Figure 1). Menzies (1983) has proposed that the high $^{87}Sr/^{86}Sr$, or high Rb/Sr (EM II–type) character of these nodules is imprinted by incorporation of a hydrous metasomatizing agent, whereas EM I–type signatures are produced by CO_2-rich fluids. Experimentally determined solubilities for CO_2 and H_2O in mantle melts (e.g. Khitarov & Kadik 1973) document the very high solubility of H_2O, relative to CO_2, and make it likely that mantle-derived metasomatic fluids are dominated by CO_2. EM II–type metasomatism may thus require a source of crustal water (perhaps in a subduction environment) and derive its isotopic character indirectly from the continental crust.

As noted earlier, the oceanic islands exhibiting strong EM II signatures are almost exclusively restricted to the Southern Hemisphere and serve to

delineate the Dupal anomaly. Enhanced rates of Pangeatic subduction into the Dupal mantle (Anderson 1982a) may account for this observed localization. Based on the high Δ7/4 (Hart 1984b) character of the EM components, they must have been isolated from other mantle components (DMM, PREMA, etc) for a long period of time (> 3 b.y.). Isolation in the continental crust or subcontinental lithosphere is one obvious solution, although long-term isolation within the mantle is not precluded by our present understanding of mantle dynamics.

Anderson (1982c, 1983, 1985) has proposed that the MORB reservoir is overlain by an "enriched" layer of material situated in the uppermost mantle. While this tends to contravene conventional geochemical wisdom, which places enrichments deeper with the mantle, it does not violate constraints that derive solely from analysis of the present geochemical data base. The question of a shallow versus deep enriched zone in the mantle essentially depends on one's view of the mechanism by which the enrichment is created. For example, if we accept that enrichments are related in some way to subduction, then rapid extraction and stabilization of the enriched components from the downgoing slab in the uppermost mantle will result in a shallow enriched zone, while entrainment of enriched components to great depth along with the bulk of the subducting slab will result in relative enrichment at depth.

Isotope Systematics in Oceanic Basalts: The Role of Mixing

Implicit in our discussion of component characterization is our contention that oceanic basalt isotope systematics reflect mixing. This interpretation is supported by studies that document mixing at individual localities (e.g. Langmuir et al 1978, Zindler et 1979), as well as the various lines of reasoning that suggest relatively small-scale heterogeneities within magma source regions. Early interpretations of basalt isotope systematics suggested two- or three-component mixing to explain the various arrays. Here, we identify a *minimum* of four distinct components (DMM, HIMU, EM I, EM II), and it is thus not possible to delineate unique "component recipes" for individual ocean islands or ridge segments. It is, however, useful to qualitatively discuss constraints on mixing that derive from simultaneous consideration of the two-dimensional variation diagrams (Figures 6–12).

Our estimated component isotopic compositions are schematically depicted in Figures 6–9. Mixing lines between DMM, HIMU, and BSE are shown for reference. (Element concentrations used for mixing calculations are given in the figure captions.) Essentially, these mixing lines lie on the mantle plane (Figure 13; Zindler et al 1982), and (as discussed earlier) those localities that lie outside the DMM-HIMU-BSE mixing

domain (Kerguelen, Walvis Ridge, Tristan, Gough, Samoa, Azores, Reunion, Tahiti) demand the existence of the EM components. Having invoked the EM components, we no longer require BSE as a mixing end member, and all observed compositions can result from mixing between DMM, HIMU, EM I, and EM II. If this mixing hypothesis is accurate, then the relative positions of individual localities, with respect to the components, should remain constant from one diagram to the next. Comparison of Figures 6–9 provides general support for this hypothesis.

The estimated composition of PREMA is also shown in Figures 6–9. In general, it is intermediate between DMM and HIMU but is displaced slightly toward EM II. Insofar as PREMA does represent a distinct mantle component and not simply a highly reproducible mixture, then PREMA may represent the depleted end-member OIB component, obviating the need for DMM in the OIB source reservoir (Morris & Hart 1983). This is readily apparent from the position of PREMA in Figures 7 and 8, even though mixing lines to PREMA are not shown (i.e. they are not expected to be highly curved). In this context, only the isotopic composition of N-type MORB documents the existence of DMM.

Direct extrapolation of the mixing relationships discussed above to the He variation diagrams (Figures 10–12) is not straightforward, partly because of the degassing considerations discussed earlier. Intramantle decoupling of He and lithophile trace elements (e.g. during fluid-phase metasomatism) may also contribute to this difficulty. We have, nevertheless, estimated $^3He/^4He$ ratios in the various components to facilitate direct comparison of Figures 10–12 with Figures 6–9.

While the $^3He/^4He$ ratio in DMM is tightly constrained by the narrow range of $^3He/^4He$ observed in MORBs (see Figure 14), values for other components are ill constrained. The BSE $^3He/^4He$ ratio is taken to be 50 Ra, although a choice of 30 or 100 Ra would not significantly alter the relationships in Figures 10–12. If we assume a BSE U value of 20.8 ppb (Table 1) and a BSE $U/^4He$ ratio of ~ 310 (Figure 16), the BSE He concentration (for single-stage evolution) will be on the order of 7×10^{-5} std $cm^3\ g^{-1}$. A similar analysis for DMM, with $U/^4He$ taken to be ~ 600 (Figure 16) and U to be 8.4 ppb (Table 3), yields a He concentration of $\sim 1.4 \times 10^{-5}$ std $cm^3\ g^{-1}$. Using the 9.6 enrichment factor for MORB over the MORB source (Table 3), we predict He concentrations on the order of 1.3×10^{-4} for MORBs. This is about a factor of four higher than the highest He concentration measured in a MORB glass (Kurz & Jenkins 1981) and thus implies $\sim 80\%$ He loss from even the most He-rich MORB (equivalent to ~ 0.2 wt% CO_2 degassing; see Figure 20). These considerations suggest that BSE will be relatively gas rich compared with

DMM, and that mixing lines between them in Figures 10–12 will be convex upward.

Given that $^3He/^4He$ ratios at ocean islands can only safely be interpreted as minimum values, we cannot use interisland relationships in Figures 10–12 to document component $^3He/^4He$ ratios. For the case of HIMU, we lack even the first-order constraint that would derive from $^3He/^4He$ analyses of St. Helena or Tubuaii lavas. Even so, our preferred modes of production of HIMU, involving either magmatism and degassing or loss of a metasomatic fluid within the mantle ("intramantle degassing"), are expected to lead to enrichments of U over He in HIMU source regions. Thus, we propose, following Allegre & Turcotte (1985), that HIMU will have $^3He/^4He$ that is close to or less than the atmospheric value (see Figure 16 caption).

He concentrations in HIMU, as a function of U concentrations, can be gleaned from Figure 16. Based on a present-day $U/^4He$ ratio of ~ 2000 and an "age" of 2×10^9 yr, He will range between 7.5×10^{-6} and 7.5×10^{-5} std cm^3 g^{-1} for U concentrations of 15 and 150 ppb, respectively. These U concentrations are appropriate for metasomatically depleted peridotite and degassed basalt, respectively. The mixing lines from DMM and BSE to HIMU (Figures 10–12) are based on the lower of these U concentrations; taking the higher one, the BSE-HIMU mixing line will be nearly straight, and the DMM-HIMU mixing line will be slightly convex downward.

Because of its affinity with upper continental crust and/or sediment, EM II is presumed to have $^3He/^4He$ in the range of HIMU. EM I, on the other hand, which may represent ancient metasomatized mantle, is likely to be at least moderately enriched in ^3He (Rison & Craig 1982). He concentrations in EM I will be strongly dependent on the age of the material. He concentrations, if produced as suggested by the "metasomatism" arrow in Figure 16, will be on the order of 2.5×10^{-4} std cm^3 g^{-1} (assuming 20–50 ppb U in metasomatized peridotite).

PREMA is shown near the top of the Loihi field in Figures 10–12; this is because of the coincidence of high $^3He/^4He$ Hawaiian and Icelandic localities with the overall PREMA isotopic character. The high $^3He/^4He$ ratio for PREMA is by no means certain; in fact, PREMA-like intraoceanic arcs with $^3He/^4He$ ratios of ~ 6 Ra (Craig & Rison 1983) argue against such a hypothesis. The He isotopic character of PREMA is, then, somewhat problematic, as is the existence of PREMA itself.

Having placed the various components on the He variation diagrams (Figures 10–12), we see that the possibilities for generating individual island compositions are essentially endless, particularly in conjunction with possible recent accumulation of radiogenic ^4He. While it is tempting to call on mixing between BSE and either HIMU or DMM, perhaps in conjunction with late-stage radiogenic He accumulation, to produce

Hawaiian and Icelandic arrays, mixing between PREMA, HIMU, and the EMs will serve as well. EM II islands (e.g. Samoa, Societies, Reunion, and Tahiti), identified on the basis of Sr, Nd, and Pb systematics, may represent mixing between the Hawaii-Iceland array out toward EM II.

We propose the mixing relationships in Figures 10–12 as an interim working hypothesis. Our best guess is that these relationships are significantly obscured by recent accumulation of radiogenic ^{4}He in some or all of the OIB localities, perhaps in conjunction with the paucity of data for many localities. A more quantitative understanding of He isotope systematics as they relate to Pb, Nd, and Sr will become possible as more He data are obtained in conjunction with U and Th determinations, and as more quantitative models for degassing time scales and magnitudes at specific localities are developed.

4. THE CHEMICAL AND PHYSICAL STRUCTURE OF THE MANTLE

Cosmochemical Constraints on the Bulk Composition of the Earth

A precise knowledge of the composition of the bulk silicate earth (BSE) can be used to constrain the dynamics and evolution of the crust-mantle system. For example, knowing the U content of BSE can be used to accurately estimate a value for the Urey ratio (ratio of total heat flow from the Earth to the total internal radioactive heat production), which in turn may provide constraints on the nature of mantle convection (Richter 1984). In addition, the determination of how much mantle has been depleted in large-ion lithophile (LIL) elements by continental crust extraction (e.g. Jacobsen & Wasserburg 1979, DePaolo 1980, Goldstein et al 1982, Allegre et al 1983c) depends heavily on knowledge of BSE Sr and Nd contents. In fact, our inability to specify BSE Sr and Nd contents is presently the "weak link" in deciding whether the whole mantle or just the upper mantle ($\sim$ 670 km) has been depleted. Obviously these considerations also impact the question of whole-mantle versus layered-mantle convection.

Jagoutz et al (1979) presented a novel and very important approach to determining BSE chemistry by noting that terrestrial ultramafic rocks and meteorites formed arrays of opposite slope on plots of Mg/Si and Al/Si, and proposed that the BSE composition could be established from the intersection of these arrays. They concluded that the BSE composition was about 2.5 times that of the C1 chondrites for refractory incompatible elements such as Ca, Al, and the rare-earth elements (REE). This approach (Jagoutz et al 1979) appears to be very promising (see discussion in Hart & Zindler 1986), and we have pursued it further to see if BSE refractory

element concentrations could be determined to better than 10%, which is the level required for providing useful constraints on mantle models such as those mentioned above.

First, let us set down the assumptions involved in this approach:

1. The ultramafic samples accessible to geochemists cannot be proven to sample more than the upper ~ 150–200 km of the mantle, and thus the Jagoutz et al (1979) approach will define only the uppermost mantle chemistry. Extrapolation of this to BSE will involve additional assumptions regarding the mode of accretion of the Earth and subsequent intramantle chemical fractionations.
2. The Earth is presumed to have some chemical "kinship" with meteorites. In particular, the BSE is assumed to have similar ratios of those refractory (nonvolatile) elements that can be shown to be constant throughout all classes of meteorites and the Sun.
3. Various upper-mantle ultramafic rocks are presumed to be "related" to each other by simple petrogenetic processes. In particular, since all known ultramafic samples appear to have undergone at least some modification in the light REE (LREE), and none have present-day $^{143}Nd/^{144}Nd$ isotope ratios consistent with closed-system growth for 4.55 b.y., some extrapolation will be required to project observed residual chemistries back to predepletion values. The usual model that is adopted, and which we develop below, is that depletion of a "primitive" lherzolite occurs by extraction of a partial melt, which leads to residual lherzolites with lower Ca, Al, and REE, and higher Mg.

PRIMITIVE UPPER MANTLE (PUM) ESTIMATES We have assembled a data set comprising averages of 7 classes of meteorites (E, H, L, LL, Cl, CM2, and CV-CO chondrites) and 33 individual lherzolites, including both nodules and orogenic lherzolite samples [see Hart & Zindler (1986) for details of data selection].

Figure 21*A* is a plot of our data on the Mg/Si-Al/Si plot used by Jagoutz et al (1979). The appearance of the plot is very similar to theirs, though only eight samples are common to both diagrams. We have plotted the position of Jagoutz et al's (1979) preferred composition of primitive upper mantle (JPUM) and have drawn the terrestrial and meteorite (exclusive of CM2 and CV-CO classes) arrays to intersect at this point. Note that the CM2 and CV-CO chondrites appear to have been fractionated away from C1 and ordinary chondrites by a process that did not affect these latter chondrite classes (Larimer 1979). As discussed in Hart & Zindler (1986), an "earth" composition estimated from the intersection of the terrestrial and carbonaceous chondrite arrays is clearly inappropriate and thus, the CM2 and CV-CO chondrite classes are not considered further here. Two immediate

conclusions are obvious from Figure 21*A*: (*a*) the primitive upper mantle (PUM hereafter) is chemically distinct from known meteorite classes, and (*b*) Mg/Si and Al/Si of PUM may be defined to better than $\pm 5\%$ in the context of the assumptions outlined earlier. This is indeed a major step forward, thanks to Jagoutz et al (1979)! It was our hope that similar plots involving Ca and the REE would equally well define Ca/Si and REE/Si for PUM. Figure 21*B* shows a Mg/Si-Ca/Si plot, and again the terrestrial and meteorite arrays are well defined—however, a number of samples, including JPUM, fall to the right of the intersection, which indicates the failure of one of the assumptions stated above.

Let us digress briefly here to discuss chemical fractionation in chondrites. Concentrating on the meteorite classes exclusive of CM2 and CV-CO, we find that ratios involving Nd, Sm, Ca, and Al are constant to better than 6%, and part or all of this may be analytical. Ratios involving Yb show variations of 9–13%, clearly beyond analytical error. This is probably related to the relatively low condensation temperature (T_c) of Yb compared with those of the other REE (Boynton 1975). Ratios involving Mg show variations of 23–39% except for Yb/Mg, which is only 13%. Mg also has a comparatively low T_c, relative to Ca and Al (Grossman & Larimer 1974), and apparently follows Yb to some extent. Ratios involving Si are highly fractionated (factors of 1.6–1.7); again, T_c for Si is less than that for Mg (Grossman & Larimer 1974). Thus, four ratios are of particular importance in estimating terrestrial chemistry from meteorite analogues: Sm/Nd and Ca/Al (which are constant in *all* meteorite classes), and Nd/Ca and Nd/Al (which are constant for meteorite classes exclusive of CM2 and CV-CO).

Returning now to the lherzolite data, we note that the Ca/Al ratio ranges from 0.556–1.60 versus the constant value of 1.09 for meteorites (Ahrens & Von Michaelis 1969). Furthermore, all but one of the lherzolites lying to the right of the meteorite-terrestrial array intersection in Figure 21*B* have Ca/Al ratios > 1.20. The terrestrial array is commonly viewed as a "melt-depletion" array (Loubet et al 1975, Suen 1978, Frey & Suen 1985, O'Hara et al 1975). However, recognizing that all common mantle melts have approximately chondritic Ca/Al ratios [average MORB = 1.02; oceanic alkali basalts = 0.91; all basalt types (worldwide) = 0.88 (Manson 1967, Melson et al 1976)], we can easily show that these high Ca/Al ratios cannot be produced by melt extraction.

The simplest explanation of the high Ca/Al ratios is to postulate that these samples have high and unrepresentative clinopyroxene (cpx) contents, not related to any petrogenetic process but simply a function of local heterogeneity in mineral abundances, compounded by the fact that in the field, geologists and geochemists will go for the "pretty green" cpx-rich rocks more often than the barren harzburgites. We have therefore "corrected" the lherzolite data set for excess cpx by subtracting cpx until all

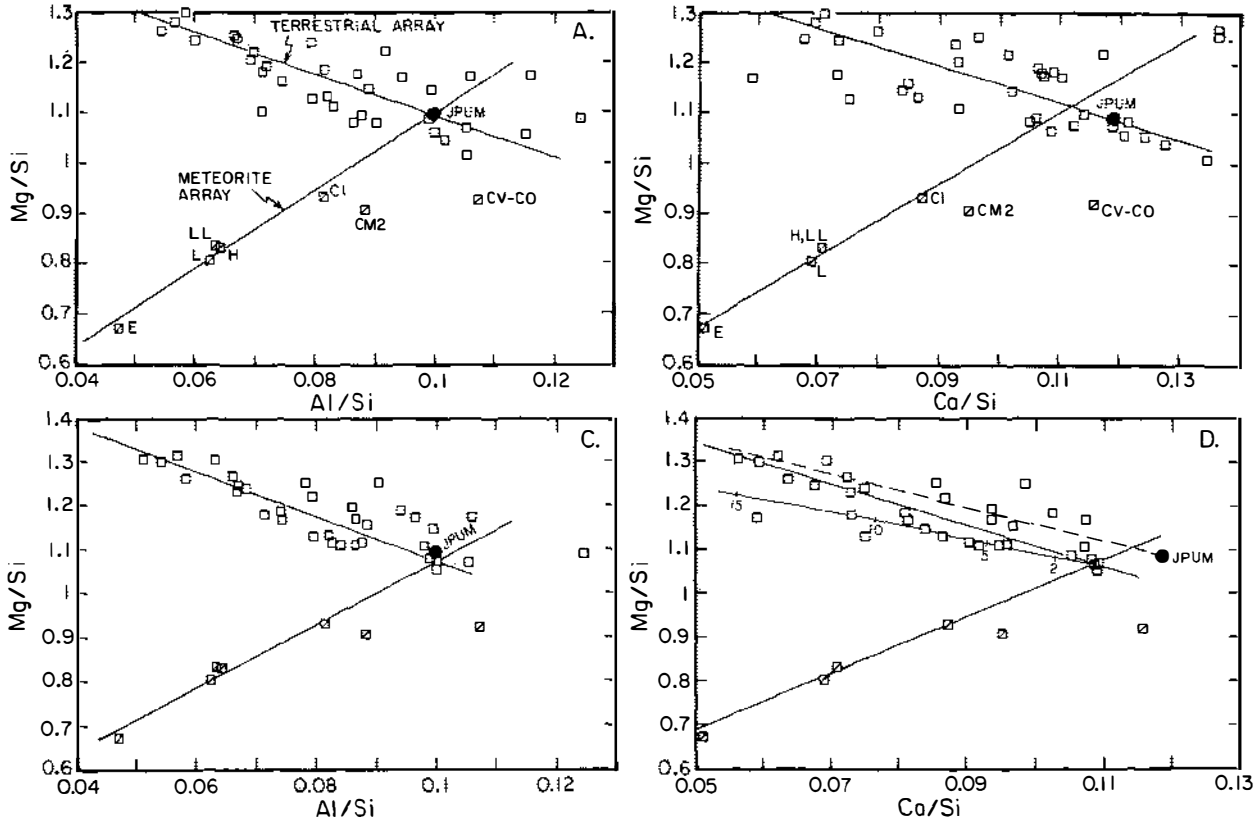

Figure 21 Mg/Si-Al/Si-Ca/Si relationships of meteorites and lherzolites. Panels *A* and *B* display data as published; panels *C* and *D* show lherzolites after subtraction of clinopyroxene (cpx) to force Ca/Al = 1.09 [= chondrites; see Hart & Zindler (1986) for complete discussion]. Solid circle labeled "JPUM" is the estimate of primitive mantle composition from Jagoutz et al (1979). Solid lines are eyeball fits to the data (forced to go through "JPUM" in *A* and *B*). Dashed line in *D* is the best-fit terrestrial line from *B* (included for reference). Solid line with the tick marks in *D* is trajectory of residual compositions resulting from melt removal; the percentage of melt removed is indicated by the numbers [see Hart and Zindler (1986) for description of this model]. CM2 and CV-CO chondrite data have been ignored in drawing the best-fit line to the meteorite array. Note that all concentration ratios are given as metal weight ratios.

Ca/Al ratios are ≤ 1.09 [see Hart & Zindler (1986) for details of this correction]. Comparisons of corrected and uncorrected data are shown in Figures 21*A* and 21*C*, and in Figures 21*B* and 21*D*. For the corrected data, only one sample (a serpentinized, recrystallized lherzolite from the Lizard peridotite) is anomalously high in Al/Si (Figure 21*C*), and all of the anomalously high Ca/Si samples have moved to lower Ca/Si ratios (Figure 21*D*), so they are now at or to the left of the meteorite-terrestrial array intersection. Based on *subjective* consideration of the data, we have placed the intersection (and its uncertainty) at Mg/Si = 1.06 ± 0.06, Al/Si = 0.100 ± 0.003, and Ca/Si = 0.109 ± 0.003. A similar plot, of Mg/Si versus Nd/Si (not shown), yields an estimate for Nd/Si $\sim 0.054 \pm 0.003$. (Note that we will give REE/major element ratios in ppm/wt% throughout this discussion; true weight ratios can be derived simply by dividing by 10^4.) Only our Ca/Si value differs significantly from that of Jagoutz et al (1979).

Since most of the lherzolites in the data set have Sm/Nd > chondrites (> 0.325), it is clear that some depletion of LREE is typical. In order to understand how the REE and major elements are coupled during the

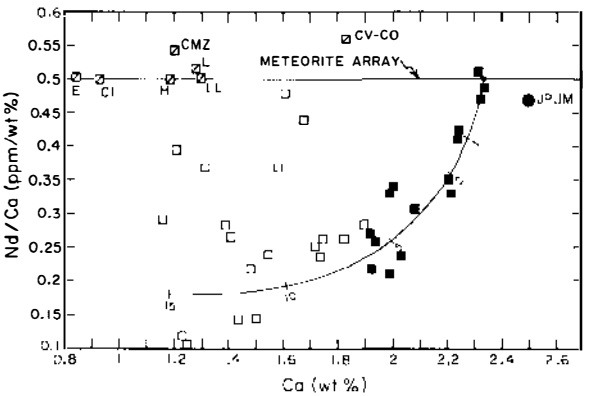

Figure 22 Nd/Ca versus Ca relationships for meteorites and lherzolites (cpx corrected). Discrepancy between our estimate for PUM (small solid circle) and that of Jagoutz et al (1979) (solid circle marked JPUM) reflects the cpx correction we have applied to the lherzolite data. The 15 most primitive lherzolites (Ca > 1.9%, Mg/Al < 14) are shown as solid squares; many of the low-Ca lherzolites (mostly xenoliths) have anomalously high Nd/Ca, perhaps due to metasomatic LREE enrichment (Frey & Green 1974). Note that many of the most metasomatized refractory xenoliths of Frey & Green (1974), not included in this data set, have Nd/Ca > chondrite. The intersection of the lherzolite array and the meteorite array at Nd/Ca (ppm/wt%) = 0.500 is taken to define Ca and Nd in PUM (= 2.34 ± 0.02 wt% Ca and 1.17 ± 0.02 ppm Nd). Al in PUM then equals 2.15%, since the chondrite Ca/Al ratio is 1.09. Solid curve is trajectory for residual lherzolite compositions derived from partial melt extraction model; the model predicts 20 ppm Nd and Sm/Nd = 0.24 for the 2% melt, and 13.7 ppm Nd and Sm/Nd = 0.26 for the 5% melt.

depletion process, we have formulated a simple depletion model to gain at least a first-order understanding of what depletion trajectories will look like on various compositional plots. Model depletion trajectories are shown in Figures 21–23, where it can be seen that the lherzolites that are least depleted (closest to PUM) have suffered $< 0.5\%$ melt extraction; typically, the average level of melt extraction for the more primitive lherzolites (black squares) is on the order of 2–3%. While this produces relatively insignificant depletions in major elements, it does significantly change REE concentrations.

We can now use all of the above considerations in concert to develop a best estimate for PUM. From a large variety of compositional plots (Hart & Zindler 1986), Figures 21–23 were selected to illustrate the approach. A summary of our estimate for PUM is given in Table 1, along with our admittedly subjective estimates of the uncertainties (which reflect only the application of the chosen data set, not the various assumptions concerning the development of the data set or its applicability to the actual upper mantle). Other refractory element abundances in PUM may be estimated

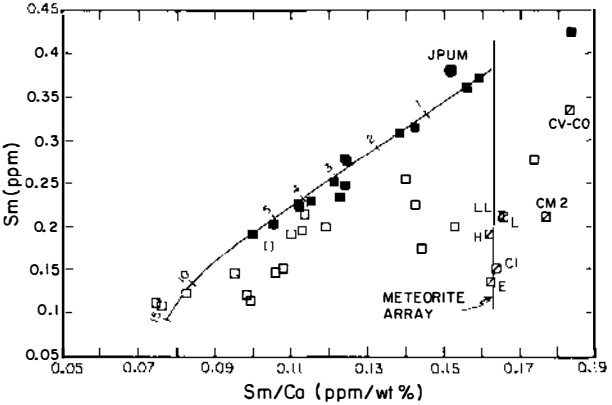

Figure 23 Sm versus Sm/Ca relationships for meteorites and lherzolites (cpx corrected). Best-fit array, as defined by the 15 most primitive lherzolites (see Figure 22 caption), intersects the meteorite array (Sm/Ca = 0.162) at Sm = 0.380 ± 0.006 ppm (small solid circle). Note that the Jagoutz et al (1979) estimate for (JPUM) falls neither on the terrestrial nor on the meteorite arrays because of the cpx correction problem; note also that sample SC-1, the most primitive of Jagoutz et al., falls above and to the right of the intersection point and is therefore quite anomalous in Sm content. The Sm value derived from the intersection, coupled with the Nd value from Figure 22, leads to Sm/Nd = 0.325 (exactly chondritic), which provides an independent verification of these Sm and Nd estimates for PUM. The solid curve is the trajectory of residual compositions resulting from melt extraction and is seen to be an excellent fit to the most primitive lherzolites. As in the Nd/Ca-Ca plot (Figure 22), many of the more residual lherzolites (open squares; mostly xenoliths) have been apparently enriched in Sm relative to Ca, probably by metasomatic processes.

based on C1 abundances relative to Ca (Anders & Ebihara 1982). Also given in Table 1 is the JPUM estimate derived by Jagoutz et al (1979). The agreement for the REE is absurdly good. [We did not expect this, nor were we predisposed to the Jagoutz et al (1979) values.] The differences in major elements arise largely from our insistence that PUM must be chondritic in Ca/Al, which thereby forces a downward revision in the Jagoutz et al (1979) Ca estimate.

THE EARTH AS A C1 CHONDRITE In addition to the above approach, we have derived a C1 chondrite–based Earth model (LOSIMAG C1) using average C1 values from Anders & Ebihara (1982) (Hart & Zindler 1986). We have assumed the following: (*a*) a near total loss or noncondensation of the

Table 1 Primitive upper mantle (PUM) composition

	This paper	Jagoutz et al (1979)
Si	21.5±0.6 wt%	21.1%
Al	2.15±0.02%	2.10%
Mg	22.8±0.6%	23.1%
Ca	2.34±0.02%	2.50%
Nd	1.17±0.02 ppm	1.17 ppm[a]
Sm	0.380±0.006 ppm	0.38 ppm
Yb	0.420±0.02 ppm	0.42 ppm
SiO_2	46.0%	45.2
Al_2O_3	4.06%	3.97
MgO	37.8%	38.3
CaO	3.27%	3.50
Sr	19.6 ppm[b]	28 ppm
U	20.8 ppb[c]	26 ppb

[a] Derived using the Sm data and Sm/Nd chondrite = 0.325.

[b] Derived using Sr data for meteorite classes E, H, L, LL, and C1 (from Allegre et al 1983c). These Sr data were coupled with the Nd and Ca data for these meteorite classes to generate an average value for these five classes of meteorites of Sr/Nd = 16.7 and Sr/Ca = 8.40 (ppm/wt%) (see Hart & Zindler 1986).

[c] Derived using U concentration data for E, H, L, LL, and C1 chondrites, (from Chen & Tilton 1976, Tilton 1973, Manhes & Allegre 1978, Tatsumoto et al 1973, 1976). These data were coupled, where possible, with Nd from the same meteorite; otherwise the data are from the same meteorite class [see Hart & Zindler (1986) for details and data sources]. The average U/Nd value for the five meteorite classes so derived is 0.01780, with a maximum range between classes of 13%. The use of the average of all five classes was felt to be preferable to using only C1 data, as only one isotope dilution analysis exists for C1's. There is no obvious trend of U/Nd with fractionation indicators such as Al/Si for the five classes; inclusion of CM2 and CV-CO meteorites, however, suggests a trend of decreasing U/Nd with increasing Al/Si. Use of the average U/Nd of 0.0178, coupled with Nd = 0.463 ppm in C1, gives U = 8.2 ppb, a value that compares well with that of 8.1 ppb for C1 from Anders & Ebihara (1982). Using U/Nd = 0.01 78 and Nd in PUM = 1.17 ppm gives U in PUM = 0.0208 ppm.

highly volatile gaseous elements and Na, K, and P, and significant loss or noncondensation of Cr and Mn (column *B*, Table 2); (*b*) a partial loss or noncondensation of Si and Mg, elements that are moderately "volatile" in a solar nebula context (e.g. Grossman & Larimer 1974; see column *B*, Table 2); and (*c*) formation of an iron core that also incorporates Ni and Co, leaving enough Fe in the mantle to yield a MgO/(MgO + FeO) molar ratio of 0.90 (column *C*, Table 2). The core generated in this calculation falls slightly short of an earth core mass (30.47% vs 31.50%, column *D*, Table 2). If sufficient oxygen (or other volatile elements) is left in the core to bring it up to mass (column *E*, Table 2), the final core is composed of 90% Fe, 5.4% Ni, 4.7% O, and a trace of Co. The fraction of O is significantly lower than the light-element abundances usually predicted for the core (10–15%) on the basis of geophysical constraints (e.g. Ringwood 1979), but in line with the recent estimates of Jeanloz (1986). When the silicate component of C1 is recalculated to 100% after core removal (column *G*, Table 2), the abundances and ratios of refractory lithophile elements are in precise agreement with the PUM model developed earlier (Table 1), as they should be since Fe is the only element not preadjusted to be compatible with PUM in this calculation. Note that if Si and Mg were treated as strictly refractory elements in this calculation, it would require 17% light elements in the core to bring it up to mass, and many of the element abundances and ratios would be at variance with the PUM composition.

Thus, by starting with a basic C1 composition, removing all or most of the highly volatile elements (H_2O, C, S, Na, K, P, etc), and allowing for small but significant deficiencies in Si (19%) and Mg (8%), we can construct an Earth that not only has a proper size core with an appropriate composition, but also has absolute abundances of the refractory lithophile elements (2.47 times the average C1 value, as given by Anders & Ebihara 1982), which agree with our PUM estimate. We call this the LOSIMAG C1 Earth model.

The apparent success in estimating a primitive mantle composition based on upper-mantle lherzolites and associated depletion trends casts considerable doubt on models that call on gross chemical differences between the upper and lower mantle in order to accommodate inferred elastic properties for candidate mantle phases (e.g. Anderson & Bass 1985).

Is There a Pb Paradox?

The so-called "Pb paradox" refers to the observation that Pb in ocean islands and MORBs is, almost without exception, more radiogenic than a 4.55-b.y. bulk Earth "geochron" (Figure 9). If the age of the Earth is 4.55 b.y. (= chondrite age), the bulk Earth must lie somewhere on this geochron. Because Pb in oceanic basalts comprises most of what is known of the

Table 2 LOSIMAG C1 Earth model

	B[b]	C	D	E	F	G
SiO_2	18.58	18.58	31.96	18.58	31.48	45.96
Al_2O_3	1.640	1.64	2.82	1.64	2.78	4.06
FeO	24.49	3.05	5.25	3.05	5.17	7.55
MgO	15.27	15.27	26.26	15.27	25.87	37.77
CaO	1.298	1.298	2.23	1.298	2.20	3.21
Na_2O	0.134	0.134	0.230	0.134	0.227	0.331
K_2O	0.013	0.013	0.022	0.013	0.022	0.032
Cr_2O_3	0.189	0.189	0.325	0.189	0.320	0.467
MnO	0.053	0.053	0.091	0.053	0.090	0.131
TiO_2	0.073	0.073	0.126	0.073	0.124	0.181
NiO	1.39	0.112	0.193	0.112	0.190	0.277
CoO	0.064	0.0052	0.009	0.0052	0.009	0.013
P_2O_5	0.008	0.008	0.014	0.008	0.014	0.020
Silicate sum	63.202	40.425	69.530	40.425	68.50	100
HVE[a]	30.21	30.21	—	30.21	—	
MVE[a]	1.258	1.258		1.258	—	
SVE[a]	5.33	5.33		5.33	—	
Oxygen[a]		5.06		4.185	—	
	36.798	41.858	—	40.983	-	
Fe	—	16.665	28.664	16.116	28.239	89.648
Ni		1.004	1.727	1.004	1.700	5.397
Co		0.046	0.079	0.046	0.078	0.248
Oxygen[a]	—		—	0.875	1.483	4.708
Core sum		17.715	30.470	18.590	31.50	100
Sum all	100	100	100	100	100	

[a] HVE = highly volatile elements (H_2O, S, C, organics); MVE = moderately volatile elements (Na, K, P, Cr, Mn); SVE = slightly volatile elements (Mg, Si); oxygen is that obtained from FeO, NiO, CoO reduction.

[b] Column headings are as follows:

B—Major components of C1 chondrites from Anders & Ebihara (1982) all HVE separated from silicate components; partial separation of MVE, to leave MVE/Al ratios in silicate similar to those of Jagoutz et al (1979) mantle; partial separation of SVE, to leave SVE/Al ratios as in PUM, Table 1.

C—Separation of metallic core, leaving enough FeO to provide MgO/(MgO + FeO) = 0.90 (molar) and enough NiO and CoO to provide ratios to Al similar to those of Jagoutz et al (1979) in mantle.

D—Removal of HVE, MVE, and SVE and oxygen from C; remainder renormalized to 100%.

E—Column C, with partial oxygen budget left in core.

F—Removal of HVE, MVE, SVE and part of oxygen from E, remainder renormalized to 100%.

G—Silicate mantle and oxide core renormalized separately to 100%.

interactive portions of the mantle, we must look to some less obvious reservoir of unradiogenic Pb (which lies to the left of the geochron) to balance the oceanic mantle. The paradox arises from the fact that no such reservoir can be unambiguously identified, although several suggestions, including the lower continental crust (e.g. O'Nions et al 1979), DMM (Anderson 1982b), the core (Vidal & Dosso 1978, Oversby & Ringwood 1971, Allegre et al 1980, Vollmer 1977, Allegre 1982), and the lower mantle (Anderson 1983), have appeared in the recent literature. Before going on to evaluate these various suggestions, we summarize pertinent constraints on U and Pb budgets in the crust and mantle.

U AND Pb BUDGETS A variety of Pb data for various average crustal rock types and composites has been compiled and is given in Table 3. There is a small but significant difference in Pb between upper and lower crustal rock types; this is largely related to the more basic character of lower crustal rocks and not to Pb depletion during granulite facies metamorphism. Relative to a PUM silicate Earth, the crust appears to contain an unusually large fraction of the silicate Earth's Pb inventory (37–70%; Table 3). This Pb enrichment is in contrast to values derived for crustal Sr and Nd inventories of 10% and 18%, respectively (Table 3), and appears inescapable.

Extreme variations of U in lower crustal (granulite facies) rocks hinder an accurate assessment of the U contents of, and the distribution within, the continental crust. Our estimates are given in Table 3 and are in reasonably good agreement with Taylor's (1982) estimates, though they have been compiled largely from independent data sources. Relative to a PUM silicate Earth, $\sim$ 22–52% of Earth's U is in the continental crust.

Our estimates for U and Pb in the continental crust lead to rather low μ values ($\mu = {}^{238}U/{}^{204}Pb$), in terms of conventional wisdom, particularly for the upper crust (mean $\mu = 8.7$, range = 6–14; Table 3). In contrast, most data that exist for upper crustal materials strongly indicate the radiogenic nature of the upper crust. [$^{206}Pb/^{204}Pb$ ratios for pelagic and terrigenous sediments range from 18.5 to 19.1 and from 18.8 to 19.8, respectively (Sun 1980, White et al 1985).] For crust with a mean age of 2.0 b.y. (Goldstein et al 1984, Allegre & Rousseau 1984), a range of μ from 10 to 14 is required to generate $^{206}Pb/^{204}Pb$ ranging from 18.5 to 19.8. While the estimated uncertainties in upper crustal U and Pb encompass μ values as high as 14, this is barely sufficient to generate the most radiogenic Pb observed in oceanic terrigenous sediments. In terms of the total crust estimate, the uncertainty in μ is large enough to tolerate a crustal reservoir lying either to the left or the right of the bulk earth geochron, though the best estimate will be well to the left of the geochron.

Insofar as U appears to be slightly more incompatible than Pb in most

Table 3 U-Pb budget for various terrestrial reservoirs

	U (ppm)	Pb (ppm)	μ	Nd (ppm)	Sr (ppm)	Sr/Nd	U/Nd	Pb/Nd
C1[a]	0.0200	6.12	0.146	1.13	19.5	17.3	0.0177	5.42
PUM[b]	0.0208	0.155	8.4	1.17	19.6	16.8	0.0178	0.132
MORB[c]	0.081	0.541	9.4	7.7	128	16.6	.0105	0.070
MORB mantle	0.0084	0.056	—	0.8	13.3	—	—	—
Upper crust[d]	2.4 ± 0.5	18 ± 4	8.7 (6–14)	32.5	300	9.2	.073	0.55
Lower crust[e]	0.7 ± 0.5	11 ± 3	3.8 (1–9)	32.5	300	9.2	.022	0.34
Total crust[f]	1.2 ± 0.5	13.1 ± 4	5.7 (3–12)	32.5 ± 1.5	300 ± 30	9.2	.037	0.40
$\frac{\text{Mass in crust}}{\text{Mass in PUM}}$	37%	54%	—	18%	10%	—	—	—

[a] Element ratios are for C1 chondrites (Anders & Ebihara 1982); abundances from C1 chondrites multipled by factor of 2.47 (see Hart & Zindler 1986) as in the LOSIMAG C1 Earth model.

[b] From Table 1; Pb calculated for $\mu = 8.4$ (see text).

[c] Average of 17 fresh MORB glasses and 4 leached whole rocks (Cohen & O'Nions 1982a,b, Cohen et al 1980, Vidal & Clauer 1981); average K for this suite is 1027 ppm. Twenty-two glasses from Jochum et al (1983) average 0.075 ppm U.

[d,e] Data sources: Allegre & Rousseau (1984), Dupuy et al (1979), Fahrig & Eade (1968), Goldstein et al (1984), Gray (1977), Gray & Oversby (1972), Heinrichs et al (1980), McLennan & Taylor (1980), Michard et al (1985), Montgomery (1977), Reilly & Shaw (1967), Shaw (1967), Shawet al (1976), Taylor & McLennan (1981), Taylor et al (1983), Tilton & Barreiro (1980), White et al (1985).

[f] Calculated as 30% upper crust–70% lower crust.

igneous processes (Watson et al 1986), it might appear contradictory to speak of a crustal μ that is lower than that of the BSE, as the crust is the end result of a series of melting and crystallization processes. However, we must consider that arc processes are complex and appear to produce numerous other element fractionation patterns that contravene conventional wisdom (see, for example, Morris & Hart 1983), and thus they may also produce enrichments of Pb over U. This contention is supported by the relatively low μ values measured in many arc volcanics (e.g. Tatsumoto & Knight 1969, Oversby & Ewart 1972, Tatsumoto 1978).

Also shown in Table 3 is the average Pb content (and U, Sr, and Nd contents) of 17 fresh MORB glasses, compiled from the literature. While the various element ratios may approximate those of the MORB source mantle itself, the concentrations have obviously been raised by partial melting and fractional crystallization processes. Approximations to the contents of U and Pb in the MORB mantle have been derived by comparison to Nd estimates of 0.6–1.0 ppm (Hart & Zindler 1986). Using the U/Nd and Pb/Nd ratios in MORB (Table 3) would place the composition of MORB mantle (for 0.8 ppm Nd) at 13.3 ppm Sr, 0.0084 ppm U, and 0.056 ppm Pb. Thus, relative to PUM, the MORB mantle is depleted in Nd, Sr, U, and Pb by factors of 0.68, 0.68, 0.40, and 0.36, respectively (i.e. U and Pb behave more incompatibly than Sr and Nd).

DISCUSSION The silicate portion of the Earth is clearly depleted in Pb relative to the LOSIMAG C1 chondrite model. This is an old observation and has been attributed to removal of Pb to the core or to volatilization or noncondensation of Pb during Earth accretion (e.g. Murthy 1975, Oversby & Ringwood 1971). In the event that any of these processes were synchronous with accretion, and provided that accretion took place rapidly at an age given by chondrites ($\sim$ 4.55 b.y.), then the 4.55-b.y. geochron accurately specifies the locus of possible BSE Pb isotope compositions. The Earth is also depleted in a variety of other volatile elements, many of which are not expected to be chalcophilic [that is, potentially core compatible (e.g., Sun 1982)], and thus there is no compelling reason, except for the Pb paradox itself, to assert that the depletion of Pb in the silicate Earth is due to "core pumping." However, it is clearly possible that the Pb depletion is a result of *both* nonaccretion and core pumping. In the event that some of the "missing" Pb was coprecipitated with the Fe-Ni core, and that core formation took a finite time to run to completion ($>$ 100 m.y.), then the bulk silicate earth is not required to lie on a 4.55-b.y. geochron. Various two-stage isochrons are shown in Figure 24 to illustrate this process.

While the $^{206}Pb/^{204}Pb$ ratio of PREMA is not well constrained, it is probably $\sim$18.2–18.5 (Figure 9); insofar as the continental crust is the

total complement to PREMA, and insofar as the crust contains ~ 50% of the silicate Earth Pb budget (Table 3), then relative to PREMA, the crust must lie on the opposite side (and equidistant from) the relevant BSE isochron. If the average crustal μ is indeed as low as 5.7, as suggested earlier (Table 3), PREMA plus crust will lie on a 4.55-b.y. geochron, and little core pumping of Pb is required. If the crustal μ is the upper limit allowed (~ 12), then about 150 m.y. of core pumping is required. At this point, the most that can be said is that the missing Pb needed to explain the Pb paradox may be accommodated in either the crust or the core, or both.

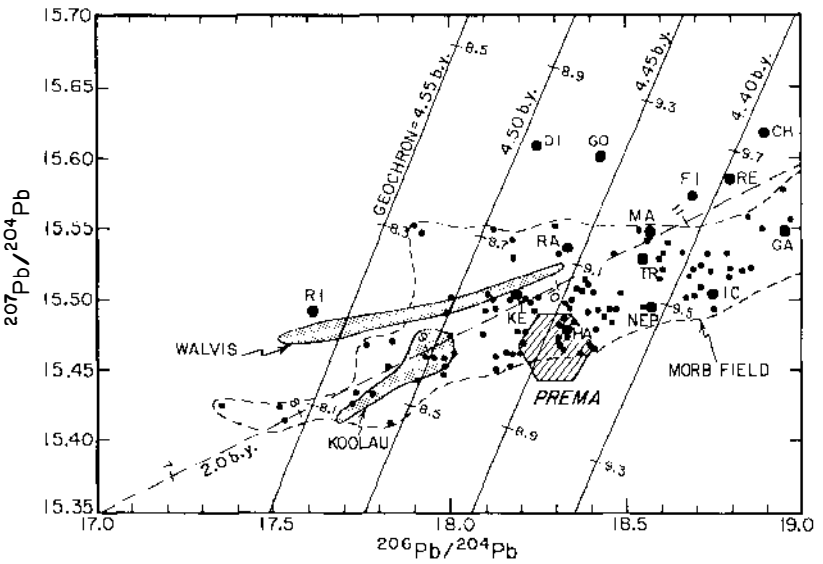

Figure 24 $^{207}Pb/^{204}Pb$-$^{206}PB/^{204}Pb$ plot, showing MORB data (small dots), selected averaged oceanic islands (large dots), and the field for Koolau (Oahu) and Walvis Ridge basalts, in comparison with various terrestrial isochrons. The true age (t_0) of the Earth (geochron) is taken to be 4.55 b.y.; the other isochrons represent possible core-mantle differentiation "ages." These isochrons are calculated for a first-stage $\mu = 0.21$ from t_0 to t, and second stage from t to present. Various closed-system μ values for the second stage are indicated as tick marks on the isochrons. Also shown for reference is a 2-b.y. secondary isochron (dashed), calculated with a first-stage $\mu = 8.1$ (t_0 to 2 b.y.)—second-stage μ values are shown as tick marks. This isochron may be used to estimate positions of various crust and mantle reservoirs having a ~ 2.0-b.y. mean age as a function of second-stage-reservoir μ value. Cross-hatched field indicates possible position for PREMA. Data references are given in Zindler et al (1982), Hart (1984b), and Hamelin & Allegre (1985b), Koolau data are from Stille et al (1983) and S. R. Hart (unpublished), and primordial Pb parameters are from Tatsumoto et al (1973). Oceanic islands: CH (Christmas), DI (Discovery), FI (Fiji), GA (Galapagos), GO (Gough), HA (Hawaii), IC (Iceland), KE (Kerguelen), MA (Marion), RA (Raratonga), RE (Reunion), RI (Rio Grande Rise), NEP (NE Pacific seamounts), TR (Tristan da Cunha).

We may also examine the other solutions to the Pb paradox introduced earlier. Can the depleted MORB mantle be the reservoir that "balances" the other oceanic Pb components? Certainly some MORBs have Pb isotope compositions lying to the left of the geochron (see Figure 24), although the great majority lie to the right. Relative to PUM, the MORB mantle only contains $\sim$ 11% of the silicate Earth Pb budget (if we assume that the MORB reservoir is 30% of the mantle mass), and DMM likely contains much less. Clearly the continental crust dominates the Pb budget of the Earth, and it is unlikely that an unradiogenic DMM component can be effective in balancing the mantle segment represented by the oceanic Pb array. (Here, we presume that much or all of the mantle, exclusive of the MORB reservoir, is characterized by radiogenic Pb similar to that observed in oceanic islands.) Obviously one can postulate that the lower mantle is unradiogenic (and also never sampled in erupted volcanics). For example, Anderson's (1983) model derives a lower-mantle μ value that is 25% lower than the μ of the upper mantle; however, his bulk silicate Earth also has a very high μ (10.5), which would demand more than 150 m.y. of core pumping of Pb.

We conclude that the Pb paradox is at least a "pink" herring, although we feel it is an important issue insofar as it may be one of the few ways available to constrain the time interval of core formation if, in fact, Pb did partition into the core. In this context, however, it seems that a modern Pb budget is not a promising approach, and that much better constraints are available by working with Pb isotope data from Archean rocks. Various works of this kind have been reported (Manhes et al 1979, Gancarz & Wasserburg 1977, Tera 1980); generally these give ages for the BSE (= core formation?) of 4.4–4.5 b.y., but with uncertainties that include the probable accretion age of 4.55 b.y.

Geochemical Mass Balance

The derivation of constraints on the relative volumes of geochemically distinct mantle components has received considerable attention in the recent literature (e.g. Jacobsen & Wasserburg 1979, DePaolo 1980, O'Nions et al 1979, Allegre et al 1980, Turcotte 1985). Most of these models are based only on Sr and Nd systematics and have assumed that the depleted MORB mantle is the sole complement of the enriched continental crust (the remainder of the mantle being BSE); thus, they have not dealt with much of the geochemical complexity known to characterize the mantle. In addition, many modelers have chosen to utilize input parameters without considering the effects of the substantial uncertainties known to be associated with them. Consequently, the conclusions based on these models (e.g. 32–45% of the mantle is depleted) are difficult to interpret at best.

Goldstein et al (1982) considered a more complex model, via inclusion of a HIMU component and U-Th-Pb systematics, and investigated the effects of input parameter uncertainties using a Monte Carlo approach. They concluded that the mass fraction of the depleted mantle is ill constrained by the present-day geochemical data base and could conceivably range from $< 20\%$ to $> 90\%$ of the mantle. Allegre et al (1983c) used an inversion method to investigate the effects of input uncertainties; even without the inclusion of a HIMU component, they concluded that the error bounds on the estimate of depleted mantle mass were large and could encompass values ranging from 30–90% of the entire mantle. Even with clearly oversimplified models, it has not been possible to delineate definitive constraints on the mass fraction of depleted mantle.

In this section, we derive constraints on the nature of mantle reservoirs by making simplifying assumptions that are consistent with the degree of chemical complexity known to characterize the mantle. It is appropriate here that we clarify our usage of the terms "reservoir" and "component." We have used component, in the preceding discussion, to refer to a geochemically distinct mantle segment that is homogeneous on scales sampled by the smallest effective melting volume. Obviously it may also be homogeneous on smaller or larger scales. Thus, a component may compose the entire upper mantle or be dispersed as meter- or even centimeter-scale veins or blobs. In contrast, we use the term reservoir to denote a portion of the mantle that is under discussion; it need not be chemically homogeneous nor physically contiguous. That is, we can speak of the MORB source reservoir, which is thought to be physically contiguous but chemically heterogeneous, as comprising HIMU and EM components in a DMM matrix, or we can refer to a relatively enriched reservoir that includes the sum of HIMU and EM components and is thus neither contiguous nor homogeneous.

As a starting point, we consider the simplest form of crust-mantle mass balance where the mantle and crust constitute complementary reservoirs. In addition, we consider only the Sm-Nd system, since (geochemically speaking) it constitutes the best-behaved parent-daughter pair. This approach does not deny that the mantle is very heterogeneous; it simply asks what the mean composition of this heterogeneous mantle is. The mass balance equation for this model may be rewritten (from Allegre et al 1983c) as

$$\mu_m = (0.0064\,\mathrm{Nd_c}\mu_c - \mu_t\mathrm{Nd_t})/(0.0064\,\mathrm{Nd_c} - \mathrm{Nd_t}),$$

where the subscripted μ is $^{147}Sm/^{144}Nd$, subscripts c, m, and t refer to crust, depleted mantle, and bulk Earth, respectively, and Nd is the concentration

in ppm. The factor 0.0064 is simply the mass ratio of continental crust to total mantle plus crust (Turcotte & Schubert 1982).

The selection of input parameters is given in the caption to Figure 25, with uncertainties that represent a subjective estimate of the maximum allowable range. The value for Nd_t is taken as that in PUM (see above). The calculated value for μ_m is $0.215 \pm 1.1\%$; the error in this value was propagated by allowing the errors in the individual parameters to combine in the worst possible way, and thus the error bounds are fairly conservative. Figure 25 also shows how μ_m varies as a function of Nd_c only. From simple mass balance, using the chosen parameters, we find that $\sim 18\%$ of the Earth's Nd budget is stored in the crust (Table 3), and thus the Nd

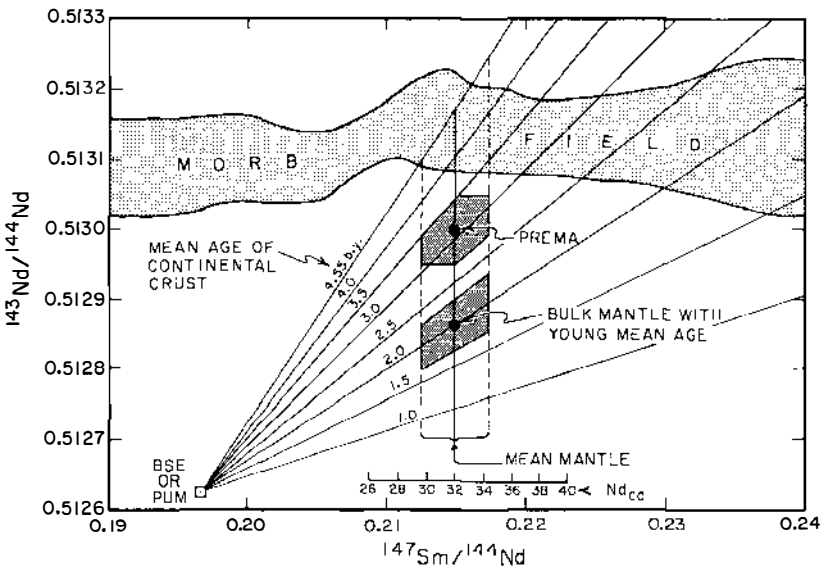

Figure 25 Sm/Nd isochron diagram showing various mean age isochrons and the value for $^{147}Sm/^{144}Nd$ of the mean depleted mantle (0.2148 ± 0.0024) calculated from a bulk Earth–continental crust depletion model. MORB field taken from literature values. Parameters and uncertainties chosen for model as follows: primitive mantle (bulk Earth) Nd = 1.17 ± 0.02 ppm (PUM value; see text), $^{147}Sm/^{144}Nd = 0.1967 \pm 0.0003$ (PUM value taken from Jacobsen & Wasserburg 1984); continental crust Nd = 32.5 ± 1.5 ppm, $^{147}Sm/^{144}Nd = 0.113 \pm 0.003$ (Goldstein et al 1984, Taylor et al 1983, Allegre & Rousseau 1984, Michard et al 1985, Allegre et al 1983c). The effect of other choices for crustal Nd concentration may be judged from the scale labeled Nd_{cc}. Shaded polygons delimit solutions for two choices of mean age = 2.0 ± 0.3 b.y. and $3.1. \pm 0.4$ b.y. The lack of significant overlap between the mean depleted mantle field and that of MORB mantle simply means that the whole mantle is, on average, unlikely to be of MORB isotopic composition unless the mean age of depletion is significantly greater than 3.5 b.y. See text for discussion of error propagation.

concentration of mean depleted mantle is 0.96 ppm (18% depleted from 1.17 ppm).

This model value of μ_m can be used to derive the $^{143}Nd/^{144}Nd$ ratio of mean depleted mantle if we can estimate the mean age of the total crust-mantle system. If continental crust extraction has occurred at a constant rate over the age of the Earth, the mean age of the system will be $\sim$ 2.28 b.y.; if crust extraction was more rapid during the Archean, when there was more heat available for differentiation (as argued for by Allegre & Rousseau 1984), then the mean age will be older. However, for either of these scenarios, significant recycling of average crustal material into the mantle, which is consistent with Sm-Nd systematics in modern and ancient sediments (Goldstein et al 1984, Allegre & Rousseau 1984), will tend to push the crust toward younger mean ages (perhaps as young as 1.7. b.y.). If all or a significant fraction of the continental crust was extracted early, as in continental big-bang models (e.g. Patterson & Tatsumoto 1964, Armstrong 1981), the mean age might be as old as 3.8 b.y. All things considered, there is an extremely large range of mean ages that have been proposed as characterizing the continental crust.

We have chosen to consider the consequences of two "end-member" mean-age ranges for the continental crust: 2.0 ± 0.3 b.y., corresponding to mean mantle $^{143}Nd/^{144}Nd$ of $0.51286 \pm \frac{8}{6}$; and 3.1 ± 0.4 b.y., with mean mantle $^{143}Nd/^{144}Nd$ of 0.51300 ± 5 (Figure 25). The latter estimate has the additional significance that it corresponds to the composition of PREMA. Based on the concentration of Nd and the $^{143}Nd/^{144}Nd$ ratio in the MORB reservoir (0.5–0.9 ppm, 0.51315; see Figure 14), we can now investigate mass and compositional relationships between the MORB reservoir and the remainder of the mantle, which we refer to as the "complementary reservoir." This complementary reservoir is enriched relative to the MORB reservoir, though it may be depleted or enriched relative to BSE or PUM. Figure 26 shows the relationship between the relative masses of the MORB and complementary reservoirs and the $^{143}Nd/^{144}Nd$ ratio of the complementary reservoir for the two mean mantle $^{143}Nd/^{144}Nd$ ratios estimated above. Contours for Nd concentration in the complementary reservoir are also shown in Figure 26 and document a positive correlation between this parameter and the mass of the MORB mantle.

If the complementary reservoir is primitive (BSE or PUM), as has been assumed in most geochemical models, then the relationships in Figure 26 can be used to constrain the mass fraction of this reservoir. This is done by ascertaining the mass of the complementary reservoir, which corresponds to the intersection of the PUM $^{143}Nd/^{144}Nd$ value with the PUM (1.17 ppm) Nd contour. The resulting mass fractions for a PUM reservoir are $\sim$ 30 and 48 wt%, respectively, for the models shown in Figures 26*A*

and 26*B*. Taken at face value, this result suggests that if any primitive mantle volume survives today, it must constitute significantly less than the ~ 70% of the mantle that lies below the 670-km seismic discontinuity. This result lies within the permissible ranges calculated by Goldstein et al (1982) and Allegre et al (1983c); the higher precision and, therefore, enhanced significance of the current result are largely due to our improved understanding of Nd in PUM.

This result implies a material flux into and/or out of the lower mantle at some time during Earth history and, thus, is not compatible with the oft-proposed persistent, unbreachable chemical boundary layer at 670 km;

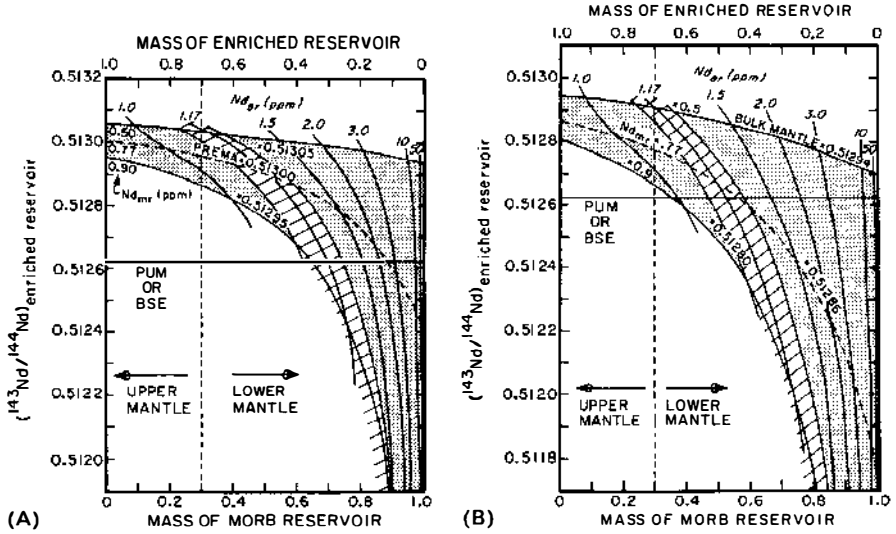

Figure 26 $^{143}Nd/^{144}Nd$ for the complementary enriched reservoir as a function of the mass of the MORB source reservoir (expressed as a mass fraction of the whole mantle). Panels *A* and *B* are for different mean mantle compositions corresponding to "old" and "young" mean ages for the continental crust, respectively (see Figure 25). In Panel *A*, the mean mantle has the composition of PREMA. "Upper" and "lower" mantle volumes are defined by the position of the 670-km seismic discontinuity. The shaded areas correspond to the uncertainties indicated in Figure 25 for the two mean mantle compositions in conjunction with Nd concentrations in the MORB reservoir (Nd_{mr}) ranging from 0.5–0.9 ppm. Nd concentrations in the complementary enriched reservoir (Nd_{er}) are shown as contours across the shaded areas. $^{143}Nd/^{144}Nd$ in PUM or BSE is shown as a horizontal line across each diagram. Approximate error bounds are shown for the Nd_{er} = 1.17 (= PUM) contour. The intersection of this error band with the PUM $^{143}Nd/^{144}Nd$ value defines the mass fraction of the complementary reservoir, if it comprises primitive, undifferentiated mantle. Resulting estimates for such a PUM reservoir are 26–38% and 42–53% of the mantle for models in Panels *A* and *B*, respectively. This suggests that if a primitive, undifferentiated mantle reservoir exists, it cannot constitute the entire lower mantle.

such a boundary may exist today, but it cannot have existed continuously since the earliest Archean. Furthermore, it seems likely that there is no convectively isolated reservoir for PUM today, and if PUM survives, it must exist as a dispersed component within a convecting medium. Hence, arguments citing the need for convective isolation of a PUM or BSE component (e.g. O'Nions & Oxburgh 1983) need to be reevaluated.

Earlier, we suggested that PREMA may be a physically distinct mantle component. If we now consider that the complementary reservoir is PREMA, then it must be volumetrically dominant, with the MORB reservoir constituting less than $\sim 10\%$ of the mass of the mantle (Figure 26*A*). Alternatively, if the complementary reservoir comprises PREMA + HIMU + EM I + EM II $\pm$ PUM (or BSE), then the relative masses of the MORB and complementary reservoirs are ill constrained.

These mass-balance considerations, together with component characterizations, suggest a mantle that is composed of DMM, HIMU, EM I, and EM II components and may also include PREMA and/or PUM. The MORB reservoir is volumetrically dominated by DMM (as a result of its highly depleted character) but contains various amounts of the enriched components, so that its mean composition is essentially that of average MORB. This heterogeneous MORB reservoir may be underlain by, or may grade downward into, mantle with an overall more enriched isotopic character. If the mean $^{143}Nd/^{144}Nd$ of this complementary reservoir is taken to be no lower than the most enriched OIB (~ 0.5123—Kerguelen), then the relationships in Figure 26 allow this reservoir to account for as little as 20% or (based on a mean isotopic character similar to the mean mantle composition) as much as $\sim 90\%$ of the mantle. The geochemical character of this relatively enriched reservoir may be satisfied by any number of scenarios involving variable fractions of HIMU, EM I, EM II, PREMA, PUM, and DMM. This relatively enriched reservoir could contain dispersed enriched components in the DMM matrix, differing from the MORB reservoir only in the relative abundance or representation of the enriched components, or it could represent a convectively isolated mantle domain.

Three factors tend to preclude derivation of definitive geochemical constraints on the placement of and physical relationships of the various geochemical components within the mantle: (*a*) Most observed isotopic compositions represent mixtures between two or more components; (*b*) studies of small seamounts, orogenic lherzolites, and ultramafic nodule suites document small-scale heterogeneities within the upper mantle; and (*c*) the number of components identified here (considered to be a minimum) makes it impossible to define uniquely mixing scenarios to explain isotope ratios observed in specific tectonic settings.

As geochemical philosophers, unaware of the various and sundry geophysical constraints on the structure of the mantle, we can objectively make and defend the following statements:

1. The MORB source reservoir, which is situated in the upper mantle, contains small-scale heterogeneities.
2. The MORB reservoir cannot constitute the whole mantle unless the mean age of the continental crust is on the order of 4.0 b.y.
3. The MORB source reservoir may either grade downward into mantle that is (on average) less depleted or abruptly contact such mantle across a midmantle chemical boundary layer. The possible existence of an enriched layer in the uppermost mantle, which overlies the MORB reservoir (Anderson 1982c), cannot be excluded.
4. Mantle of PUM composition cannot constitute more than half of the mantle. Some depleted mantle must be present below the 670-km discontinuity.
5. The mantle below the MORB reservoir may represent a mixture similar in style to the MORB reservoir, but with less DMM component, or it may be highly stratified with homogeneous or heterogeneous layers.
6. The Southern Hemisphere Dupal anomaly documents megascale lateral heterogeneity within the mantle.
7. Basalts with PREMA isotopic characteristics are found in a wide variety of oceanic, arc, and continental tectonic settings. These basalts must represent either the melting of a PREMA reservoir or a highly reproducible mixing between other components.
8. The constancy of $^{3}He/^{4}He$ ratios in MORBs likely results from a mixing between He in the various components that compose the MORB reservoir. High $^{3}He/^{4}He$ components may include PUM, EM I, and/or PREMA; low $^{3}He/^{4}He$ components may include DMM, EM II, and HIMU. The small range of $^{3}He/^{4}He$ ratios in MORB relative to the other isotope ratios of interest documents an enhanced mobility of He in the upper mantle, due either to high diffusion rates in the presence of melt or to migration of volatile-rich phases in the uppermost mantle.
9. Thc association of excess ^{129}Xe and high $^{40}Ar/^{36}Ar$ in some of the most depleted MORBS reflects the early ($\geq$ 4.4 b.y.) and continuing degasssing of at least some portions of the MORB reservoir.
10. Mechanisms that account for the production of EM I, EM II, and HIMU components operate in conjunction with magmatism or metasomatism and associated tectonic activity within the mantle. Some or all of the proposed mechanisms may be operative in subduction environments, and thus some enriched mantle components (e.g. EM II) may incorporate or represent recycled crustal materials.

Together, these statements constitute a geochemist's view of the mantle, and without the benefit of geophysical contraints, they say disappointingly little regarding the physical structure of the mantle. We offer them as hopefully objective constraints that can be used to build mantle models in the context of the various geophysical constraints that are being developed. In the next section, we consider the interplay of these geochemical constraints with the geophysical constraints, as seen through the eyes of a geochemist.

The Nature of Mantle Convection

Perhaps the most fundamental question in solid-earth geophysics today pertains to the nature of the ~670-km seismic discontinuity (e.g. Dziewonski et al 1975, Dziewonski & Anderson 1981). Early workers (e.g. Anderson 1967, 1976, Ringwood 1975) attributed the discontinuity to a phase change in a homogeneous mantle. Recently, compelling arguments have been (re)made in support of a compositional boundary at 670 km. The existence of a chemical boundary at 670 km (with higher SiO_2 in the lower mantle) is expected to act as a barrier to convection and to limit mixing between upper- and lower-mantle reservoirs (e.g. Richter & McKenzie 1981, Olson & Yuen 1982), whereas convection across a phase boundary is likely permissible (e.g. Schubert & Turcotte 1971). Thus, resolution of this question is critical to the development of realistic models for the chemical and thermal evolution of the Earth.

Both whole-mantle and layered-mantle camps have argued persuasively for their respective mantle models. Unfortunately, individual authors have not always addressed apparently conflicting arguments made on the basis of similar observations by other authors. The current state of the art is, therefore, difficult to assess, particularly for the naive but well-intentioned geochemist. Hence, in the following paragraphs, we summarize the present state of geophysical arguments pertaining to the nature of the 670-km discontinuity.

UNDERSIDE REFLECTIONS The high reflection coefficient inferred for the 670-km discontinuity on the basis of *P'670P'* underside reflections (Richards 1972) suggests that the transition in physical properties at this boundary occurs over 5 km or less. Through comparison with calculated reflection coefficients, Lees et al (1983) have shown that observed reflectivities cannot be produced by phase transitions alone and require an associated discontinuous change in chemical composition. However, Muirhead (1985) has summarized arguments, largely from the works of J. R. Cleary, that permit an alternative interpretation for some of the *P'670P'* data; this interpretation involves a core-mantle scattering phase. P. G. Richards (personal communication) acknowledges the viability of the

Muirhead-Cleary hypothesis for some of the "low quality" *P'670P'* reflections, but he asserts that in other cases, the evidence for a midmantle reflector is incontrovertible.

The possibly discontinuous nature of the 670-km discontinuity is suggested by a comparison of two recent investigations of different subduction zones. Jordan (1977) and Creager & Jordan (1984) have compiled evidence for a high-velocity path extending to depths of at least 1000 km along an extension of the subducting slab in the Kuriles. These authors believe that this documents an aseismic portion of the slab itself that is extending into the lower mantle and contend that their initial results receive further support from their ongoing investigations (T. H. Jordan, personal communication). In contrast, Giardini & Woodhouse (1984) have shown that seismicity at Tonga documents the "en echelon" stacking of broken slab fragments, suggesting the impenetrable character of the 670-km discontinuity at this locality.

CONVECTIVE DESTRUCTION OF HETEROGENEITIES The need to preserve chemical heterogeneities within the mantle has led a number of convection dynamicists to investigate the fate of such heterogeneities in a convecting mantle (e.g. Richter & Ribe 1979, Richter et al 1982, Olson et al 1984, Hoffman & McKenzie 1985). The results of these studies are in general accord (when heterogeneity and sampling scales are considered) and can be summarized as follows: (*a*) Large heterogeneities (similar in scale to the depth of the convecting layer) require very long time scales for dispersal and will likely persist for the age of the Earth; (*b*) small-scale heterogeneities will be mixed over "regional" volumes on time scales significantly shorter than the age of the Earth; and (*c*) total destruction of even the smallest scale heterogeneities depends on chemical diffusion. It is important to note that in all models, heterogeneities were considered to be passive (that is, indistinguishable from the ambient mantle matrix with regard to rheology and density). It is, therefore, difficult to generalize these results to a more realistic situation involving contrasting rheologies (such as subducted eclogite in a peridotite matrix). In such cases, the survival of heterogeneities may be fostered by the distinct rheologies, and in fact, density differences may produce a heterogeneity gradient with depth (e.g. Davies 1983). A further consequence of distinct chemical properties is a difference in solidus temperatures, which may facilitate sampling of even the smallest scale heterogeneities during melting (Zindler et al 1984, Sleep 1984). All in all, we see nothing in the modeling that precludes the long-term survival of heterogeneities within a convecting mantle domain, at least when very small-scale lengths are considered to be important. We therefore contend

that convective isolation is not necessary to preserve ancient mantle heterogeneity.

PHYSICAL PROPERTIES OF MANTLE MINERALS The elastic properties of mantle phases are being used to test the suitability of candidate bulk compositions to explain observed seismic velocities and inferred densities at various mantle levels (Lees et al 1983, Bass & Anderson 1984). Results from both of these studies agree that above 400 km, both olivine- and pyroxene-rich assemblages ("pyrolite" and "piclogite," respectively) can satisfy seismic constraints. While this may also be true for the lower mantle below 670 km, as recently pointed out by Wolf & Bukowinski (1985), D. L. Anderson (personal communication) and Knittle et al (1985) consider, respectively, that the relatively low *velocity* and low *density* of olivine in the lower mantle (perovskite plus magnesiowustite) may preclude an olivine-rich (e.g. pyrolite) lower mantle. Within the transition region, there are a number of problems: (*a*) The phases investigated by Lees et al (1983; olivine, orthopyroxene, and garnet) are too fast to satisfy PREM or PEM earth models (Dziewonski et al 1975, Dziewonski & Anderson 1981); and (*b*) the deeper phase transitions summarized by Jeanloz & Thompson (1983) and studied by Lees et al (1983) occur at substantially shallower depths than can be made consistent with a 670-km seismic discontinuity. Bass & Anderson (1984) and D. L. Anderson (personal communication) have suggested that these apparent enigmas may be explained if Ca-rich pyroxene persists in its low-pressure manifestation through much of the transition region and if increased alumina in the garnet and pyroxene component pushes the perovskite transition to higher pressures (via the ilmenite transition). The contentions of Bass & Anderson (1984), taken at face value, suggest that the transition region is rich in clinopyroxene, and therefore that piclogite is more appropriate than pyrolite as a bulk composition and that eclogite cannot penetrate the 670-km discontinuity because of its retarded transformation to perovskite (Bass & Anderson 1984, Anderson & Bass 1985). In contrast, Weidner (1985) has argued that a classic pyrolite composition is consistent with seismic data in and above the transition region.

Because cosmochemical constraints are seriously violated by a piclogite transition region *and* lower mantle, Anderson & Bass (1985) propose that the 670-km discontinuity represents a fundamental chemical boundary across which the piclogite transition region is in contact with an orthopyroxene-rich lower mantle. They suggest that this chemical discontinuity was formed as a result of extensive melting of the Earth during accretion, and that the enstatite-rich lower mantle is essentially devoid of

incompatible trace elements. This leads, however, to absolute abundance levels of these elements in the upper mantle that are 2.5–3 times higher than the PUM value derived earlier. No upper-mantle materials are as yet known that both are this enriched in refractory lithophile elements and preserve chondritic abundance ratios. At present, the uncertainties associated with the basic physical properties data are significant and (as suggested by the transition region problems mentioned above) may be more important than is indicated by the experiments. Although a chemically layered mantle appears favored in current interpretations of the physical properties data, the data cannot preclude a more-or-less homogeneous composition (e.g. pyrolite or PUM) extending from the upper mantle, through the transition region, and into the lower mantle.

An interesting consequence of Anderson's hypothesized sub-670-km transformation of eclogite to perovskite, in conjunction with the density relationships shown by Lees et al (1983) and Bass & Anderson (1984), is that the transition region would act as a "density trap" for subducted eclogite. Having undergone the eclogite transformation, subducted oceanic crust will drop through the upper mantle into the transition region, where it becomes neutrally buoyant. Penetration into the lower mantle will be retarded by the alumina-induced late transformation to the perovskite structure (D. L. Anderson, personal communication). The production of eclogite through the generation and subduction of oceanic crust over the age of the Earth can account for as much as 12% of the mantle if the average rate of crust production has been about twice the present rate. The trapping of this eclogite in the transition region can satisfy the velocity constraints of the Bass & Anderson (1984) model without invoking fractional crystallization of an early magma ocean.

THERMAL STRUCTURE AND VISCOSITY OF THE MANTLE Observations pertaining to postglacial rebound, nontidal acceleration, true polar wander, and changes in the degree-two component of the Earth's gravitational potential field all suggest that the viscosity of the mantle is constant (within about a factor of 5) across its entire thickness (Peltier & Andrews 1976, Peltier 1981, 1983). This condition is most easily met in the context of whole-mantle convection models. If viscosity is proportional to homologous temperature (T_m/T; e.g. Schubert & Spohn 1981, Spohn & Schubert 1982), constant viscosity across a midmantle thermal boundary layer implies that the melting temperatures (T_m) of the lower- and upper-mantle materials would have to fortuitously differ by an amount comparable to the temperature increase across the boundary layer ($\sim$ 500–700°C; Jeanloz & Richter 1979). However, if we accept only a mantle with nearly constant viscosity, only *one* of the following conditions need hold: (*a*) There is no

thermal boundary layer at 670 km; (*b*) the change in chemical properties associated with a chemical discontinuity at 670 km fortuitously results in a nearly constant homologous temperature across the boundary; or (*c*) the relationship between the homologous temperature and viscosity is not as simple as has been supposed. Although the contention that the mantle is isoviscous has been taken as support for whole-mantle convection (e.g. Peltier 1981, Spohn & Schubert 1982), this requirement is not absolute, since there are clearly other alternatives.

Assuming a constant homologous temperature throughout the mantle, Spohn & Schubert (1982) have further argued that the temperature increase across a midmantle thermal boundary layer predicts core-mantle temperatures significantly in excess of the 3200–3500 K estimated by Jeanloz & Richter (1979). R. Jeanloz (pesonal communication) has made preliminary measurements of the melting temperature of perovskite as a function of pressure that suggest little or no pressure dependence of T_m. In their calculation, Spohn & Schubert (1982) assumed a melting temperature gradient of 0.64°C km^{-1} for the lower mantle, and thus the new data of Jeanloz may be qualitatively consistent with an isoviscous lower mantle and reasonable core-mantle temperatures, even in the presence of a thermal boundary layer at 670 km. Essentially, this result predicts that the geotherm proposed by Jeanloz & Richter (1979) may be reconcilable with an isoviscous lower mantle.

MANTLE HEAT FLOW AND THE UREY RATIO The ratio of heat flow to heat production in the Earth (the so-called Urey ratio) can potentially constrain the nature of mantle convection by offering a measure of the efficiency of heat removal from the mantle (Richter 1984). Using heat flow data from Sclater et al (1980) and estimates for PUM U (20.8 ppb; Table 1), with Th/U = 3.8 and K/U = 1.27×10^4, we obtain a Urey ratio of approximately 2.1. Furthermore, if we eliminate that fraction of the total Earth heat flow ($\sim 15\%$) and heat production ($\sim 37\%$) thought to originate in the continental crust, where thermal steady state is closely approached, a "reduced" Urey ratio for mantle heat flow to heat production is obtained of about 2.8. This suggests that mantle heat flow requires a significant component ($\sim 64\%$) of secular cooling. As discussed by Richter (1984), predictions from whole-mantle convection calculations suggest $< 20\%$ secular cooling (given no significant heat source within, or cooling of, the core) due to the efficiency of heat removal in these models. Layered models, on the other hand, are capable of accounting for much larger percentages of secular cooling ($\sim 50\%$). Typical convection calculations, however, ignore the insulating effects of continental lithosphere, a consideration that will tend to increase the secular component available in whole- and layered-

mantle models. Even so, taken at face value, these arguments suggest either a layered mantle or a significant heat source in the core, given that no more than about 5–10% of the present-day heat flow can result from cooling of the core (Stacey 1969). Speculation regarding the nature and magnitude of possible core heat sources is not fruitful at this time other than to say that K has long been considered a possibility (Hall & Murthy 1971, Lewis 1971), and that more than about one silicate Earth budget of K in the core would violate cosmochemical constraints related to K depletion during accretion of the Earth (Sun 1982). One silicate Earth budget of K in the core would account for 15% of the present total Earth heat flow (at steady state), or up to 60% of the total heat flow if the core heat is fossil production from a few billion years ago. The above analysis assumes that the heat flow estimates of Sclater et al (1980) are representative of time-integrated values. If the rate of present-day volcanic activity at midocean ridges, and associated heat flow, is higher than the time-integrated average, then the appropriate mantle Urey ratio would be smaller than that calculated here. Further, F. M. Richter, W. R. Peltier & D. L. Turcotte (personal communication) all concur that when realistic uncertainties in the convection calculations are considered, the possibility of an extensive secular component in whole-mantle convection models cannot be excluded.

O'Nions & Oxburgh (1983) have argued that the relationship between the oceanic ^{4}He flux (Craig et al 1975) and heat flow supports the contention of a depleted upper mantle that is convectively isolated from a primitive lower mantle. Implicit in their reasoning are the assumptions that ^{4}He and heat are removed from the upper mantle with the same efficiency (i.e. that the entire oceanic crustal section, including both extrusive and intrusive components, is outgassed completely) and that radiogenic ^{4}He has a very short residence time in the upper mantle. This is in marked contrast to their contention that heat is transported across the 670-km boundary layer much more efficiently than is He. In principle, the He flux and heat flow data could be used to calculate a "fractionation factor" for heat and He at the ridge.

He arguments aside, the conclusions of O'Nions & Oxburgh (1983) are essentially based on the inferred depletion of U in the MORB source reservoir (a fact easily documented by examination of U in fresh MORBs) in conjunction with convection arguments similar to those summarized by Richter (1984). In this context, we note that the U budget of O'Nions & Oxburgh (1983) ($\sim$ 1.5 ppm U in the crust and 20 ppb U in the BSE) has about 47% of the Earth's U concentrated in the continental crust, and thus it precludes total convective isolation of a primitive lower mantle (since the mantle above 670 km constitutes only $\sim$ 30% of the total mantle).

DISCUSSION The geophysical arguments summarized above do not clearly support either the whole-mantle or layered-mantle convection hypotheses; at some level, all observations could be reconciled with either hypothesis, although some special begging would be required. Based on the geochemical arguments presented in the preceding section, we contend that if the lower mantle is chemically distinct and convectively isolated from the upper mantle, it does not have a primitive or undifferentiated PUM (or BSE) composition. Thus, if there is an unbreachable chemical boundary layer at 670 km at present, it could not have existed for all of Earth history. At some time, this boundary must have been permeable in order to permit differentiation (depletion) of the lower mantle. We also know that the MORB source reservoir, which probably composes some portion of the upper mantle, cannot represent the mean composition of the mantle (see Figure 26), and therefore the present-day mantle must contain large-scale chemical gradients or discontinuities (though, as discussed earlier, these heterogeneities are largely documented by trace elements and isotopic ratios and need not imply significant major-element variations).

A compromise model that is compatible with many geochemical and geophysical observations might involve a chemical boundary layer at 670 km that is subject to periodic instability in time and/or space [similar to the model proposed by Herzberg (1983) and Herzberg & Forsythe (1983)]. Such a model offers a means to achieve some differentiation of the lower mantle, while at the same time providing for the current existence of a chemical boundary or gradient at 670 km. In fact, material exchange across the 670-km discontinuity may be necessary in order to effect the chemical differentiation between the upper and lower mantle that is necessary to stabilize a convective boundary layer. Heat and material flux across the boundary will serve to "buffer" the mean mantle temperature distribution near an adiabat and thus satisfy the viscosity predictions of Peltier (1981) and the thermal constraints discussed by Spohn & Schubert (1982). The high reflectivity of some of the $P'670P'$ reflections would then document stable portions of the boundary at a given time and place. We stress that with regard to geochemical budgets and mass balances, this compromise model has many of the same ramifications as whole-mantle convection.

5. SUMMARY AND CONCLUSIONS

Chemical geodynamics, the study of the physical and chemical evolution of the Earth (Allegre 1982), is a field of inquiry that is clearly still in its infancy. However, great strides have been made over the past decade as solid-earth geochemists and geophysicists have begun more and more to work together

in this quest. Although the present state of the art does not permit the absolute definition of broad and sweeping constraints on the physical and chemical structure of the Earth, we believe that the outlook for the near future is indeed rosy. We are currently on the steep part of a learning curve, and answers to many of the most intriguing problems in the geosciences appear to be almost within grasp.

The synthesis presented here explores three principal boundary conditions relating to the nature and development of chemical structure in the Earth's mantle: (*a*) inferred scale lengths for mantle chemical heterogeneities, (*b*) interrelationships of the various isotopic tracers, and (*c*) the bulk composition of the Earth. These boundary conditions are integrated with geophysical constraints in an attempt to evaluate models for the development of the physical and chemical structure of the mantle. The major points of the synthesis are the following:

1. Kilometer-size heterogeneities can survive diffusive equilibration for billions of years, even in the presence of a melt phase. The situation for the rare gases is not drastically different than that for other elements of interest.
2. The mantle is chemically heterogeneous on both very small (10 m) and very large ($>$ 1000 km) scales. There is a clear positive correlation between the amplitudes of isotopic variations and the maximum scale lengths of observation.
3. Isotopic heterogeneities in the mantle require the existence of four "end-member" components (DMM, HIMU, EM I, and EM II) and are consistent with the existence of at least two additional components (BSE, PREMA).
4. Primitive undepleted mantle (BSE or PUM) can make up no more than about 55% of the total mantle, and convective isolation of such material is therefore precluded.
5. He isotope data cannot be simply interpreted in terms of the mantle components delineated by Sr, Nd, and Pb. Preeruptive degassing of He may explain high observed U/He ratios; consequent ingrowth of radiogenic ^{4}He may significantly perturb mantle He signals.
6. The composition of the primitive upper mantle (PUM) can be ascertained via comparison of mantle-derived lherzolites and chondrites using a procedure modified after Jagoutz et al (1979). Resulting abundances of lithophile refractory elements in PUM are constrained to better than $\pm 5\%$, and are equal to $2.51 \times$ C1 chondrites (Anders & Ebihara 1982).
7. The Pb paradox is shown to be essentially nonparadoxical. Numerous

low-μ reservoirs are available to balance the ubiquitous high-μ oceanic basalt data.

8. The U content of the BSE is tightly constrained to be $\sim$ 21 ppb. The fraction of this that now resides in the continental crust is less well constrained, but it lies between 22–52%. The reduced mantle Urey ratio (crustal heat flow and heat production subtracted) derived from these values is $\sim$ 2.8; this high value suggests either a poor thermal efficiency for mantle convection or a significant component of heat deriving from the core.

ACKNOWLEDGMENTS

This work contains a myriad of old and new ideas that we have attempted to weave into a coherent self-consistent view of the Earth's mantle. We have endeavored to accurately cite appropriate references for old ideas, and we apologize in advance for where we have failed. The development of our new ideas has been immeasurably aided by conversations with many friends and colleagues. While we cannot hope to name them all, there are those whom we cannot fail to mention: Dave Graham, Don Anderson, Claude Allegre, Bill White, John Ludden, Jim Rubenstone, Charlie Langmuir, Ed Stolper, Jill Pasteris, Hubert Staudigel, Gerd Worner, Emil Jagoutz, Steve Goldstein, Laurie Reisberg, Ray Jeanloz, Frank Richter, Don Turcotte, and Dick Peltier. We would also like to thank Mark Kurz, Don Anderson, Ray Jeanloz, Claude Allegre, Fred Frey, Roger Hart, Dave Graham, and Gerd Worner for furnishing helpful preprints and unpublished data; Claude Allegre for his early role as a silent partner; and Emil Jagoutz for inspiring "PUM." AZ would like to thank the participants in his recent mantle geochemistry seminar for acting as a sounding board for earlier manifestations of much of this material, and to assure them that the learning process was always a two-way street. SRH acknowledges the denizens of the eleventh floor for abiding his absence during the writing of this manuscript, and MIT for paying him to stay home for a year. This manuscript was skillfully produced by Michelle Lezie, who suffered through untold versions while thoroughly crash-testing Proofwriter version 2.09, and Joan Totton, who provided timely help with the final staging. As usual, Patty Catanzaro did a superb job with the graphics, under no small amount of pressure from us. And finally, the work we present would not have been possible without the generous support of the National Science Foundation (grants EAR 82-11461, EAR 83-20066, and OCE 84-10615 to AZ, and EAR 83-08809 to SRH). This work represents Lamont-Doherty Geological Observatory Contribution No. 3941.

Literature Cited

Ahrens, L. H., Von Michaelis, H. 1969. The composition of stony meteorites. III. Some inter-element relationships. *Earth Planet. Sci. Lett.* 5: 395–400

Allegre, C. J. 1982. Chemical geodynamics. *Tectonophysics* 81: 109–32

Allegre, C. J., Rousseau, D. 1984. The growth of the continents through geological time studied by Nd isotope analysis of shales. *Earth Planet. Sci. Lett.* 67: 19–34

Allegre, C. J., Turcotte, D. L. 1985. Geodynamic mixing in the mesosphere boundary layer and the origin of oceanic islands. *Geophys. Res. Lett.* 12: 207–10

Allegre, C. J., Othman, D. B., Polve, M., Richard, P. 1979. The Nd-Sr isotopic correlation in mantle materials and geodynamic consequences. *Phys. Earth Planet. Inter.* 19: 293–306

Allegre, C. J., Brevart, O., Dupre, B., Minster, J.-F. 1980. Isotopic and chemical effects produced in a continuously differentiating convecting Earth mantle. *Philos. Trans. R. Soc. London Ser. A* 297: 447–77

Allegre, C. J., Staudacher, T., Sarda, P., Kurz, M. 1983a. Constraints on evolution of Earth's mantle from rare gas systematics. *Nature* 303: 762–66

Allegre, C. J., Dupre, B., Hamelin, B. 1983b. Geochemistry of oceanic ridge basalts explained by blob–upper mantle mixing, *Eos, Trans. Am. Geophys. Union* 64: 324

Allegre, C. J., Hart, S. R., Minster, J.-F. 1983c. Chemical structure and evolution of the mantle and continents determined by inversion of Nd and Sr isotopic data. II. Numerical experiments and discussion. *Earth Planet. Sci. Lett.* 66: 191–213

Allegre, C. J., Hamelin, B., Dupre, B. 1984. Statistical analysis of isotopic ratios in MORB: the mantle blob cluster model and the convective regime of the mantle. *Earth Planet. Sci. Lett.* 71: 71–84

Allegre, C. J., Staudacher, T., Sarda, P. 1986. Rare gas systematics: formation of the atmosphere, evolution and structure of the Earth's mantle. *Earth Planet. Sci. Lett.* In press

Anders, E., Ebihara, M. 1982. Solar system abundances of the elements. *Geochim. Cosmochim. Acta* 46: 2363–80

Anderson, D. L. 1967. Phase changes in the upper mantle. *Geophys. J. R. Astron. Soc.* 14: 135–64

Anderson, D. L. 1976. The 650-km mantle discontinuity. *Geophys. Res. Lett.* 5: 347–49

Anderson, D. L. 1979. Chemical stratification of the mantle. *J. Geophys. Res.* 84: 6297–98

Anderson, D. L. 1982a. Hotspots, polar wander, Mesozoic convection and the geoid. *Nature* 297: 391–93

Anderson, D. L. 1982b. Isotopic evolution of the mantle: the role of magma mixing. *Earth Planet. Sci. Lett.* 57: 1–12

Anderson, D. L. 1982c. Isotopic evolution of the mantle: a model. *Earth Planet. Sci. Lett.* 57: 13–24

Anderson, D. L. 1983. Chemical composition of the mantle. *J. Geophys. Res.* 88: B41–B52 (*Proc. Lunar Planet. Conf., 14th*)

Anderson, D. L. 1985. Hotspot magmas can form by fractionation and contamination of MORB. *Nature.* In press

Anderson, D. L., Bass, J. D. 1985. The transition region of the Earth's upper mantle. *Nature.* In press

Armstrong, R. L. 1981. Radiogenic isotopes: the case for crustal recycling on a near-steady-state no-continental growth Earth. *Philos. Trans. R. Soc. London Ser A* 301: 443–72

Bass, J. D., Anderson, D. L. 1984. Composition of the upper mantle: geophysical tests of two petrological models. *Geophys. Res. Lett.* 11: 237–40

Basu, A. R., Tatsumoto, M. 1979. Samarium-neodymium systematics in kimberlites and in the minerals of garnet lherzolite inclusions. *Science* 205: 398–401

Basu, A. R., Tatsumoto, M. 1980. Nd-isotopes in selected mantle-derived rocks and minerals and their implications for mantle evolution. *Contrib. Mineral. Petrol.* 75: 43–54

Batiza, R., Vanko, D. 1984. Petrology of young Pacific seamounts. *J. Geophys. Res.* 89: 11235–60

Birch, F., Schairer, J. F., Spicer, H. C. 1942. Handbook of physical constants. *Geol. Soc. Am. Spec. Pap.* 36. 325 pp.

Boynton, W. V. 1975. Fractionation in the solar nebula: condensation of yttrium and the rare earth elements. *Geochim. Cosmochim. Acta* 39: 569–84

Brueckner, H., Zindler, A., Petrini, R., Otonello, G., Bonatti, E. 1986. Nd and Sr isotope systematics of Zabargad Island, Red Sea. Submitted for publication

Carlson, R. W. 1984. Isotopic constraints on Columbia River flood basalt genesis and the nature of the subcontinental mantle. *Geochim. Cosmochim. Acta* 48: 2357–72

Carter, S. R., Evensen, N. M., Hamilton, P. J., O'Nions, R. K. 1978. Continental volcanics derived from enriched and depleted source regions: Nd and Sr isotope evidence. *Earth Planet. Sci. Lett.* 37: 401–8

Chase, C. G. 1981. Ocean island Pb: two-stage histories and mantle evolution. *Earth Planet. Sci. Lett.* 52: 277–84

Chen, J. H., Tilton, G. R. 1976. Isotopic lead

investigations on the Allende carbonaceous chondrite. *Geochim. Cosmochim. Acta* 40: 635–43

Cohen, R. S., O'Nions, R. K. 1982a. The lead, neodymium and strontium isotopic structure of ocean ridge basalts. *J. Petrol.* 23: 299–324

Cohen, R. S., O'Nions, R. K. 1982b. Identification of recycled continental material in the mantle from Sr, Nd and Pb isotope investigations. *Earth Planet. Sci. Lett.* 61: 73–84

Cohen, R. S., Evensen, N. M., Hamilton, P. J., O'Nions, R. K. 1980. U-Pb, Sm-Nd and Rb-Sr systematics of mid-ocean ridge basalt glasses. *Nature* 283: 149–53

Cohen, R. S., O'Nions, R. K., Dawson, J. B. 1984. Isotope geochemistry of xenoliths from East Africa: implications for development of mantle reservoirs and their interaction. *Earth Planet. Sci. Lett.* 68: 209–20.

Condomines, M., Gronvold, K., Hooker, P. J., Muehlenbachs, K., O'Nions, R. K., et al. 1983. Helium, oxygen, strontium and neodymium isotopic relationships in Icelandic volcanics. *Earth Planet. Sci. Lett.* 66: 125–36

Craig, H., Lupton, J. E. 1978. Helium isotope variations: evidence for mantle plumes at Yellowstone, Kilauea and the Ethiopian Rift Valley. *Eos, Trans. Am. Geophys. Union* 59: 1194 (Abstr.)

Craig, H., Rison, W. 1982. Helium 3: Indian Ocean hotspots and the East African Rift. *Eos, Trans. Am. Geophys. Union* 63: 1144 (Abstr.)

Craig, H., Rison, W. 1983. Helium isotopes and mantle heterogeneity. *Eos, Trans. Am. Geophys. Union* 64: 348

Craig, H., Clarke, W. B., Beg, M. S. 1975. Excess ^{3}He in deep water on the East Pacific Rise. *Earth Planet Sci. Lett.* 26: 125–32

Creager, K. C., Jordan, T. H. 1984. Slab penetration into the lower mantle. *J. Geophys. Res.* 89: 3031–50

Dasch, E. J., Green, D. H. 1975. Strontium isotope geochemistry of lherzolite inclusions and host basaltic rocks, Victoria, Australia. *Am. J. Sci.* 275: 461–69

Davidson, J. P. 1983. Lesser Antilles isotopic evidence of the role of subducted sediment in island arc magma genesis. *Nature* 306: 253–56

Davies, G. F. 1983. Viscosity structure of layered convecting mantle. *Nature* 301: 592–94

Delaney, J. R., Muenow, D. W., Graham, D. G. 1978. Abundance and distribution of water, carbon and sulfur in the glassy rims of submarine pillow basalts. *Geochim. Cosmochim. Acta* 42: 581–94

DePaolo, D. J. 1980. Crustal growth and mantle evolution: inferences from models of element transport and Nd and Sr isotopes. *Geochim. Cosmochim. Acta* 44: 1185–96

DePaolo, D. J. 1981. Nd isotopic studies: some new perspectives on Earth structure and evolution. *Eos, Trans. Am. Geophys. Union* 62: 137–140

DePaolo, D. J., Wasserburg, G. J. 1976a. Inferences about magma sources and mantle structure from variations of $^{143}Nd/^{144}Nd$. *Geophys. Res. Lett.* 3: 743–46

DePaolo, D. J., Wasserburg, G. J. 1976b. Nd isotopic variations and petrogenetic models. *Geophys. Res. Lett.* 3: 249–52

DePaolo, D. J., Wasserburg, G. J. 1977. The sources of island arcs as indicated by Nd and Sr isotopic studies. *Geophys. Res. Lett.* 4: 465–68

Dupre, B., Allegre, C. J. 1983. Pb-Sr isotope variation in Indian Ocean basalts and mixing phenomena. *Nature* 303: 142–46

Dupuy, C., Leyreloup, A., Vernierest, J. 1979. The lower continental crust of the massif central (Bournac, France)—with special references to REE, U and Th composition, evolution, heat-flow production. In *Origin and Distribution of the Elements, Physics and Chemistry of the Earth*, Vol. II, ed. L. H. Aherns, New York: Pergamon

Dziewonski, A., Anderson, D. L. 1981. Preliminary reference Earth models. *Phys. Earth Planet. Inter.* 25: 297–356

Dziewonski, A. M., Hales, A. L., Lapwood, E. R. 1975. Parametrically simple earth models consistent with geophysical data. *Phys. Earth Planet. Inter.* 10: 12–48

Fahrig, W. F. Eade, K. E. 1968. The chemical evolution of the Canadian shield, *Can. J. Earth Sci.* 5: 1247–52

Flemings, M. C. 1974. *Solidification Processing*. New York: McGraw-Hill.

Frey, F. A., Green, D. H. 1974. The mineralogy, geochemistry and origin of lherzolite inclusions in Victorian basanites. *Geochim. Cosmochim. Acta* 38: 1023–59

Frey, F. A., Suen, C.-Y. J. 1985. The Ronda high temperature peridotite: geochemistry and petrogenesis. *Geochim. Cosmochim. Acta* 49: 2469–91

Gancarz, A. J., Wasserburg, G. J. 1977. Initial Pb of the Amitsoq gneiss, West Greenland, and implications for the age of the Earth. *Geochim. Cosmochim. Acta* 41: 1283–1301.

Giardini, D., Woodhouse, J. H. 1984. Deep seismicity and modes of deformation in Tonga subduction zone. *Nature* 307: 505–9

Goldstein, S., Zindler, A., Jagoutz, E. 1982. Evolution of the mantle-crust system: quantitative geochemical modelling of

Pb, Sr, and Nd isotopic systematics. *Eos, Trans. Am. Geophys. Union* 63: 460 (Abstr.)
Goldstein, S. L., O'Nions, R. K., Hamilton, P. J. 1984. A Sm-Nd isotopic study of atmospheric dusts and particulates from major river systems. *Earth Planet. Sci. Lett.* 70: 221–36
Graham, D., Zindler, A., Reisberg, L., Kurz, M. D., Jenkins, W. J., Batiza, R. 1984. He, Sr and Nd isotopes in basaltic glasses from young Pacific seamounts. *Eos, Trans. Am. Geophys. Union* 65: 1079 (Abstr.)
Graham, D., Zindler, A., Reisberg, L., Kurz, M., Jenkins, W., Batiza, R. 1986. He, Sr, and Nd isotope geochemistry of young Pacific seamounts. Submitted for publication.
Gray, C. M. 1977. The geochemistry of central Australian granulites in relation to the chemical and isotopic effects of granulite facies metamorphism, *Contrib. Mineral. Petrol.* 65: 79–89
Gray, C. M., Oversby, V. M. 1972. The behaviour of lead isotopes during granulite facies metamorphism. *Geochim. Cosmochim. Acta* 36: 939–52
Greenland, L. P., Rose, W. I., Stokes, J. B. 1985. An estimate of gas emissions and magmatic gas content from Kilauea volcano. *Geochim. Cosmochim. Acta* 49: 125–29
Grossman, L., Larimer, J. W. 1974. Early chemical history of the solar system. *Rev. Geophys. Space Phys.* 12: 71–101
Hall, H. T., Murthy, V. R. 1971. The early thermal history of the Earth. *Phys. Earth Planet. Inter.* 2: 19–29
Hamelin, B., Allegre, C. J. 1985a. Lead isotopic composition of high-temperature peridotites from Lherz, Lanzo, Beni-Bousera and the genesis of isotopic heterogeneities in the earth's mantle. *Eos, Trans. Am. Geophys. Union* 46: 1114
Hamelin, B., Allegre, C. J. 1985b. Large scale regional units within the depleted upper mantle: Pb-Sr-Nd study of the south-west Indian ridge. *Earth Planet. Sci. Lett.* In press
Hamilton, P. J., Evensen, N. M., O'Nions, R. K., Tarney, J. 1979. Sm-Nd systematics of Lewisian gneisses: implications for the origin of granulites. *Nature* 277: 25–28
Hart, R., Hogan, L., Dymond, J. 1985. The closed system approximation for evolution of argon and helium in the mantle, crust, and atmosphere. *Isotope Geoscience* 52: 45–73
Hart, R., Hogan, L., Dymond, J. 1986. Archaean degassing of the upper mantle and formation of the atmosphere. *Earth Planet. Sci. Lett.* In press
Hart, S. R. 1980. Diffusion compensation in natural silicates. *Geochim. Cosmochim. Acta* 45: 279–91
Hart, S. R. 1984a. He diffusion in olivine. *Earth Planet. Sci. Lett.* 70: 297–302
Hart, S. R. 1984b. A large-scale isotope anomaly in the Southern Hemisphere mantle. *Nature* 309: 753–57
Hart, S. R., Zindler, A. 1986. In search of a bulk Earth composition. *Chem. Geol.* In press
Hawkesworth, C. J., Vollmer, R. 1979. Crustal contamination versus enriched mantle: $^{143}Nd/^{144}Nd$ and $^{87}Sr/^{86}Sr$ evidence from the Italian volcanics. *Contrib. Mineral. Petrol.* 69: 151–69
Hawkesworth, C. J., Erlank, A. J., Marsh, J. S., Menzies, M. A., Van Calsteren, P. 1983. Evolution of the continental lithosphere: evidence from volcanics and xenoliths in southern Africa. In *Continental Basalts and Mantle Xenoliths*, ed. C. J. Hawkesworth, M. J. Norry, pp. 111–38. Cheshire, Engl: Shiva
Hawkesworth, C. J., Rogers, N. W., van Calsteren, P. W. C., Menzies, M. A. 1984. Mantle enrichment processes. *Nature* 311: 331–35
Heinrichs, H., Schulz-Dobrick, B., Wedepohl, K. H. 1980. Terrestrial geochemistry of Cd, Bi, Tl, Pb, Zn and Rb. *Geochim. Cosmochim. Acta* 44: 1519–33
Herzberg, C. T. 1983. Chemical stratification in the silicate Earth. *Earth Planet. Sci. Lett.* 67: 249–60
Herzberg, C. T., Forsythe, R. D. 1983. Destabilization of a 650-km chemical boundary layer and its bearing on the evolution of the continental crust. *Phys. Earth Planet. Inter.* 32: 352–60
Hoffman, N. R. A., McKenzie, D. P. 1985. The destruction of geochemical heterogeneities by differential fluid motions during mantle convection. *Geophys. J. R. Astron. Soc.* 82: 163–206
Hofmann, A. W., Hart, S. R. 1978. An assessment of local and regional isotopic equilibrium in the mantle. *Earth Planet. Sci. Lett.* 38: 44–62
Hofmann, A. W., Magaritz, M. 1977. Equilibrium and mixing in a partially molten mantle. In *Magma Genesis, Bull. 96*, ed. H. J. B. Dick, pp. 37–42. Portland: Oreg. Dep. Geol. Miner. Ind.
Hofmann, A. W., White, W. M. 1982. Mantle plumes from ancient oceanic crust. *Earth Planet. Sci. Lett.* 57: 421–36
Jacobsen, S. B., Wasserburg, G. J. 1979. The mean age of mantle and crustal reservoirs. *J. Geophys. Res.* 84: 7411–27
Jacobsen, S. B., Wasserburg, G. J. 1984. Sm-Nd isotopic evolution of chondrites and achondrites, II. *Earth Planet. Sci. Lett.* 67: 137–50
Jagoutz, E., Palme, H., Badenhausen, H., Blum, K., Cendales, M., et al. 1979. The

abundances of major, minor and trace elements in the Earth's mantle as derived from primitive ultramafic nodules. *Proc. Lunar Planet. Sci. Conf., 10th*, pp. 2031–50

Jagoutz, E., Carlson, R. W., Lugmair, G. W. 1980. Equilibrated Nd–unequilibrated Sr isotopes in mantle xenoliths. *Nature* 286: 708–10

Jeanloz, R. 1986. High pressure chemistry of the Earth's mantle and core. In *Mantle Convection*, ed. W. R. Peltier. New York: Gordon & Breach. In press

Jeanloz, R., Richter, F. M. 1979. Convection, composition, and the thermal state of the lower mantle. *J. Geophys. Res.* 84: 5497–5504

Jeanloz, R., Thompson, A. B. 1983. Phase transitions and mantle discontinuities. *Rev. Geophys. Space Phys.* 21: 51–74

Jeffrey, P. M., Anders, E. 1970. Primordial noble gases in separated meteoritic minerals—I. *Geochim. Cosmochim. Acta* 34: 1175–98

Jochum, K. P., Hofmann, A. W., Ito, E., Seufert, H. M., White, W. M. 1983. K, U, and Th in mid-ocean ridge basalt glasses. The terrestrial K/U and K/Rb ratios and heat production in the depleted mantle. *Nature* 306: 431–36

Jordan, T. H. 1977. Lithospheric slab penetration into the lower mantle beneath the Sea of Okhotsk, *J. Geophys.* 43: 473–96

Khitarov, N. I., Kadik, A. A. 1973. Water and carbon dioxide in magmatic melts and peculiarities of the melting process. *Contrib. Mineral. Petrol.* 41: 205–15

Knittle, E., Jeanloz, R., Smith, G. L. 1985. The thermal expansion of silicate perovskite and stratification of the Earth's mantle. *Nature* 319: 214–16

Kramers, J. D., Smith, C. B., Lock, N. P., Harmon, R. S., Boyd, F. R. 1981. Can kimberlites be generated from an ordinary mantle? *Nature* 291: 53–56

Kramers, J. D., Roddick, J. C. M., Dawson, J. B. 1983. Trace element and isotope studies on veined, metasomatic and "MARID" xenoliths from Bultfontein, South Africa. *Earth Planet. Sci. Lett.* 65: 90–106

Kurz, M. D. 1982. *Helium isotope geochemistry of oceanic volcanic rocks: implications for mantle heterogeneity and degassing.* PhD thesis. Mass. Inst. Technol./ Woods Hole Oceanogr. Inst., Cambridge/ Woods Hole, Mass. 281 pp.

Kurz, M. D., Jenkins, W. J. 1981. The distribution of helium in oceanic basalt glasses. *Earth Planet. Sci. Lett.* 53: 41–54

Kurz, M. D., Jenkins, W. J., Schilling, J. G., Hart, S. R. 1982. Helium isotopic systematics of ocean islands and mantle heterogeneity. *Nature* 297: 43–47

Kurz, M. D., Jenkins, W. J., Hart, S. R., Clague, D. 1983. Helium isotopic variations in volcanic rocks from Loihi Seamount and the Island of Hawaii. *Earth Planet. Sci. Lett.* 66: 388–406

Kurz, M. D., Meyer, P. S., Sigurdsson, H. 1985. Helium isotopic systematics within the neovolcanic zones of Iceland. *Earth Planet. Sci. Lett.* 74: 291–305

Langmuir, C. H., Vocke, R. D., Hanson, G. N. 1978. A general mixing equation with applications to Icelandic basalts. *Earth Planet. Sci. Lett.* 37: 380–92

Larimer, J. W. 1979. The condensation and fractionation of refractory lithophile elements. *Icarus* 40: 446–54

Lees, A. C., Bukowinski, M. S. T., Jeanloz, R. 1983. Reflection properties of phase transition and compositional change models of the 670-km discontinuity. *J. Geophys. Res.* 88: 8145–59

leRoex, A. P., Dick, H. J. B., Erlank, A. J., Reid, A. M., Frey, F. A., Hart, S. R. 1983. Geochemistry, mineralogy and petrogenesis of lavas erupted along the Southwest Indian Ridge between the Bouvet Triple Junction and 11 degrees east. *J. Petrol.* 24: 267–318

Lewis, J. S. 1971. Consequences of the presence of sulfur in the core of the Earth. *Earth Planet. Sci. Lett.* 11: 130–34

Loubet, M., Shimizu, N., Allegre, C. J. 1975. Rare earth elements in Alpine peridotites. *Contrib. Mineral. Petrol.* 53: 1–12

Lupton, J. E., Craig, H. 1975. Excess ^{3}He in oceanic basalts: evidence for terrestrial primordial helium. *Earth Planet. Sci. Lett.* 26: 133–39

Manhes, G., Allegre, C. J. 1978. Time differences as determined from the ratio of lead 207–206 in concordant meteorites. *Meteoritics* 13: 543–48

Manhes, G., Allegre, C. J., Dupre, B., Hamelin, B. 1979. Lead-lead systematics, the "age of the Earth" and the chemical evolution of our planet in a new representation space. *Earth Planet. Sci. Lett.* 44: 91–104

Manson, V. 1967. Geochemistry of basaltic rock: major elements. In *Basalts*, ed. H. H. Hess, A. Poldervaart, pp. 215–69. New York: Interscience

McKenzie, D., O'Nions, R. K. 1983. Mantle reservoirs and ocean island basalts. *Nature* 301: 229–31.

McLennan, S. M., Taylor, S. R. 1980. Th and U in sedimentary rocks: crustal evolution and sedimentary recycling. *Nature* 285: 621–24

Melson, W. G., Vallier, T. L., Wright, T. L., Byerly, G., Nelen, J. 1976. Chemical diversity of abyssal volcanic glass erupted along Pacific, Atlantic, and Indian ocean seafloor spreading centers. In *The Geophysics*

of the Pacific Ocean Basin and its Margin, Geophys. Monogr., ed. G. H. Sutton, M. H. Manghnani, R. Moberly, pp. 351–68. Washington DC: Am. Geophys. Union

Menzies, M. 1983. Mantle ultramafic xenoliths in alkaline magmas: evidence for mantle heterogeneity modified by magmatic activity. In *Continental Basalts and Mantle Xenoliths*, ed. C. J. Hawkesworth, M. J. Norry, pp. 92–110. Cheshire, Engl: Shiva. 272 pp.

Menzies, M., Murthy, V. R. 1980a. Enriched mantle: Nd and Sr isotopes in diopsides from kimberlite nodules. *Nature* 283: 634–36

Menzies, M., Murthy, V. R. 1980b. Nd and Sr isotope geochemistry of hydrous mantle nodules and their host alkali basalts: implications for local heterogeneities in metasomatically veined mantle. *Earth Planet. Sci. Lett.* 46: 323–34

Menzies, M. A., Wass, S. Y. 1983. CO_2- and LREE-rich mantle below eastern Australia: a REE and isotopic study of alkaline magmas and apatite-rich mantle xenoliths from the Southern Highlands Province, Australia. *Earth Planet. Sci. Lett.* 65: 287–302

Michard, A., Gurriet, P., Soudant, M., Albarede, F. 1985. Nd isotopes in French Phanerozoic shales: external vs. internal aspects of crustal evolution. *Geochim. Cosmochim. Acta* 49: 601–10

Montgomery, C. P. W. 1977. *Uranium-lead isotopic investigation of the Archean Imataca complex, Guayana shield, Venezuela.* PhD thesis, Mass. Inst. Technol. 261 pp.

Morgan, W. J. 1971. Convection plumes in the lower mantle. *Nature* 230: 42–43

Morris, J. D. 1984. *Enriched geochemical signatures in Aleutian and Indonesian arc lavas: an isotopic and trace element investigation.* PhD thesis. Mass. Inst. Technol., Cambridge. 320 pp.

Morris, J. D., Hart, S. R. 1983. Isotopic and incompatible element constraints on the genesis of island arc volcanics from Cold Bay and Amak Island, Aleutians, and implications for mantle structure. *Geochim. Cosmochim. Acta* 47: 2015–30

Muirhead, K. 1985. Comments on "Reflection properties of phase transition and compositional change models of the 670-km discontinuity" by Alison C. Lees, M. S. T. Bukowinski, and Raymond Jeanloz. *J. Geophys. Res.* 90: 2057–59

Murthy, V. R. 1975. Composition of the core and the early chemical history of the Earth. In *The Early History of the Earth*, ed. B. F. Windley, pp. 21–31. London: Wiley. 619 pp.

Mysen, B. O., Arculus, R. J., Eggler, D. H. 1975. Solubility of carbon dioxide in melts of andesite, tholeiite and olivine nephelenite composition to 3 kbar pressure. *Contrib. Mineral. Petrol.* 53: 227–39

O'Hara, M. J., Saunders, M. J., Mercey, E. L. P. 1975. Garnet peridotite, primary ultrabasic magma and eclogite: interpretation of upper mantle processes in kimberlite. In *Physics and Chemistry of the Earth*, 9: 571–604. New York: Pergamon

Olson, P., Yuen, D. A. 1982. Thermochemical plumes and mantle phase transitions. *J. Geophys. Res.* 87: 3993–4002

Olson, P., Yuen, D. A., Balsiger, D. 1984. Mixing of passive heterogeneities by mantle convection. *J. Geophys. Res.* 89: 425–36

O'Nions, R. K., Oxburgh, E. R. 1983. Heat and helium in the Earth. *Nature* 306: 429–31

O'Nions, R. K., Evensen, N. M., Hamilton, P. J. 1979. Geochemical modeling of mantle differentiation and crustal growth. *J. Geophys. Res.* 84: 6091–6101

O'Nions, R. K., Hamilton, P. J., Evensen, N. M. 1977. Variations in $^{143}Nd/^{144}Nd$ and $^{87}Sr/^{86}Sr$ ratios in oceanic basalts. *Earth Planet. Sci. Lett.* 34: 13–22

Oversby, V. M., Ewart, A. 1972. Lead isotopic compositions of Tonga Kermadec volcanics and their petrogenetic significance. *Contrib. Mineral. Petrol.* 37: 181–210

Oversby, V. M., Ringwood, A. E. 1971. Time of formation of the Earth's core. *Nature* 234: 463–65

Ozima, M., Podosek, F. A. 1983. *Noble Gas Geochemistry.* New York: Cambridge Univ. Press. 367 pp.

Ozima, M., Zashu, S. 1983. Noble gases in submarine pillow volcanic glasses. *Earth Planet. Sci. Lett.* 62: 24–40

Patchett, P. J., Tatsumoto, M. 1980. Hafnium isotope variations in oceanic basalts. *Geophys. Res. Lett.* 7: 1077–80

Patterson, C. C., Tatsumoto, M. 1964. The significance of lead isotopes in detrital feldspar with respect to chemical differentiation within the Earth's mantle. *Geochim. Cosmochim. Acta* 28: 1–28

Peltier, W. R. 1981. Ice age geodynamics. *Ann. Rev. Earth Planet. Sci.* 9: 199–225

Peltier, W. R. 1983. Constraint on deep mantle viscosity from Lageos acceleration data. *Nature* 304: 434–36

Peltier, W. R., Andrews, J. T. 1976. Glacial isostatic adjustment. I. The forward problem. *Geophys. J. R. Astron. Soc.* 46: 605–46

Polve, M., Allegre, C. J. 1980. Orogenic lherzolite complexes studied by ^{87}Rb-^{87}Sr: a clue to understand the mantle convection processes? *Earth Planet. Sci. Lett.* 51: 71–93

Poreda, R., Craig, H., Schilling, J.-G. 1980.

$^{3}He/^{4}He$ variations along the Reykjanes Ridge. *Eos, Trans. Am. Geophys. Union* 61: 1158 (Abstr.)

Reilly, G. A., Shaw, D. M. 1967. An estimate of the composition of part of the Canadian shield in Northwestern Ontario. *Can. J. Earth Sci.* 4: 725–39

Reisberg, L., Zindler, A. 1985. The scale of mantle heterogeneity: isotopic evidence from Ronda. *Eos, Trans. Am. Geophys. Union* 66: 413 (Abstr.)

Reisberg, L., Zindler, A. 1986. Extreme isotopic variability in the upper mantle: evidence from Ronda. *Earth Planet. Sci. Lett.* In press

Richard, P., Allegre, C. J. 1980. Neodynium and strontium isotope study of ophiolite and orogenic lherzolite petrogenesis. *Earth Planet. Sci. Lett.* 47: 327–42

Richard, P., Shimizu, N., Allegre, C. J. 1976. $^{143}Nd/^{144}Nd$, a natural tracer: an application to oceanic basalt. *Earth Planet Sci. Lett.* 31: 269–78

Richards, P. G. 1972. Seismic waves reflected from velocity gradient anomalies within the Earth's upper mantle. *J. Geophys.* 38: 517–27

Richardson, S. H., Erlank, A. J., Duncan, A. R., Reid, D. L. 1982. Correlated Nd, Sr and Pb isotope variation in Walvis Ridge basalts and implications for the evolution of their mantle source. *Earth Planet. Sci. Lett.* 59: 327–42

Richardson, S. H., Gurney, J. J., Erlank, A. J., Harris, J. W. 1984. Origin of diamonds in old enriched mantle. *Nature* 310: 198–202

Richardson, S. H., Erlank, A. J., Hart, S. R. 1985. Kimberlite-borne garnet peridotite xenoliths from old enriched subcontinental lithosphere. *Earth Planet. Sci. Lett.* 75: 116–28

Richter, F. M. 1984. Regionalized models for the thermal evolution of the Earth. *Earth Planet. Sci. Lett.* 68: 471–84

Richter, F. M., McKenzie, D. P. 1981. On some consequences and possible causes of layered mantle convection. *J. Geophys. Res.* 86: 6133–42

Richter, F. M., Ribe, N. M. 1979. On the importance of advection in determining the local isotopic composition of the mantle. *Earth Planet. Sci. Lett.* 43: 212–22

Richter, F. M., Daly, S. F., Nataf, H. C. 1982. A parameterized model for the evolution of isotopic heterogeneities in a convecting system. *Earth Planet. Sci. Lett.* 60: 178–94

Ringwood, A. E. 1975. *Composition and Petrology of the Earth's Mantle.* New York: McGraw-Hill. 618 pp.

Ringwood, A. E. 1979. *Origin of the Earth and Moon.* New York: Springer-Verlag. 295 pp.

Rison, W. 1981. Loihi seamount: mantle volatiles in the basalts. *Eos, Trans. Am. Geophys. Union* 62: 1083 (Abstr.)

Rison, W., Craig, H. 1982. Helium-3: coming of age in Samoa. *Eos, Trans. Am. Geophys. Union* 63: 114 (Abstr.)

Roden, M. K., Hart, S. R., Frey, F. A., Melson, W. G. 1984. Sr, Nd and Pb isotopic and REE geochemistry of St. Paul's Rocks: the metamorphic and metasomatic development of an alkali basalt mantle source. *Contrib. Mineral. Petrol.* 85: 376–90

Sarda, P., Staudacher, T., Allegre, C. J. 1985. $^{40}Ar/^{36}Ar$ in MORB glasses: constraints on atmosphere and mantle evolution. *Earth Planet. Sci. Lett.* 72: 357–75

Schilling, J.-G. 1973. Icelandic mantle plume: geochemical evidence along the Reykjanes Ridge. *Nature* 242: 565–71

Schubert, G., Spohn, T. 1981. Two-layer mantle convection and the depletion of radioactive elements in the lower mantle. *Geophys. Res. Lett.* 8: 951–54

Schubert, G. D., Turcotte, D. L. 1971. Phase changes and mantle convection. *J. Geophys. Res.* 76: 1424–32

Sclater, J. G., Jaupart, C., Galson, D. 1980. The heat flow through oceanic and continental crust and the heat loss of the earth. *Rev. Geophys. Space Phys.* 18: 269–311

Shaw, D. M. 1967. U, Th, and K in the Canadian Precambrian shield and possible mantle compositions. *Geochim. Cosmochim. Acta* 31: 1111–13

Shaw, D. M., Dostal, J., Keays, R. R. 1976. Additional estimates of continental surface Precambrian shield composition in Canada. *Geochim. Cosmochim. Acta* 40: 73–83

Sleep, N. H. 1984. Tapping of magmas from ubiquitous mantle heterogeneities: an alternative to mantle plumes? *J. Geophys. Res.* 89: 10,029–41

Sneeringer, M., Hart, S. R., Shimizu, N. 1984. Strontium and samarium diffusion in diopside. *Geochim. Cosmochim. Acta* 48: 1589–1608

Spohn, T., Schubert, G. 1982. Modes of mantle convection and the removal of heat from the Earth's interior. *J. Geophys. Res.* 87: 4682–96

Stacey, F. D. 1969. *Physics of the Earth.* New York: Wiley. 414 pp.

Staudacher, T., Allegre, C. J. 1982. Terrestrial xenology. *Earth Planet. Sci. Lett.* 60: 389–406

Staudigel, H., Zindler, A., Hart, S. R., Leslie, T., Chen, C. Y., Clague, D. 1984. The isotope systematics of a juvenile intraplate volcano: Pb, Nd and Sr isotope ratios of basalts from Loihi Seamount, Hawaii. *Earth Planet. Sci. Lett.* 69: 13–29

Stille, P., Unruh, D. M., Tatsumoto, M. 1983. Pb, Sr, Nd and Hf isotopic evidence of

multiple sources for Oahu, Hawaii basalts. *Nature* 304: 25–29

Stosch, H. G., Lugmair, G. W. 1984. Evolution of lower continental crust as recorded by granulite facies xenoliths from the Eifel/Germany. *Eos, Trans. Am. Geophys. Union* 65: 230 (Abstr.)

Stosch, H. G., Carlson, R. W., Lugmair, G. W. 1980. Episodic mantle differentiation: Nd and Sr isotopic evidence. *Earth Planet. Sci. Lett.* 47: 263–71

Stueber, A. M., Ikramuddin, M. 1974. Rubidium, strontium and the isotopic composition of strontium in ultramafic nodule minerals and host basalts. *Geochim. Cosmochim. Acta* 38: 207–16

Suen, C. J. 1978. *Geochemistry of peridotites and associated mafic rocks, Ronda Ultramafic Complex, Spain.* PhD thesis. Mass. Inst. Technol., Cambridge. 305 pp.

Sun, S.-S. 1980. Lead isotopic study of young volcanic rocks from mid-ocean ridges, ocean islands and island arcs. *Philos. Trans. R. Soc. London Ser. A* 297: 409–45

Sun, S.-S. 1982. Chemical composition and origin of the Earth's primitive mantle. *Geochim. Cosmochim. Acta* 46: 179–92

Sun, S.-S., Hanson, G. N. 1975. Evolution of the mantle: geochemical evidence from alkali basalts. *Geology* 3: 297–302

Tatsumoto, M. 1978. Isotopic composition of lead in oceanic basalt and its implication to mantle evolution. *Earth Planet. Sci. Lett.* 38: 63–87

Tatsumoto, M., Knight, R. J. 1969. Isotopic composition of lead in volcanic rocks from central Honshu—with regard to basalt genesis. *Geochem. J.* 3: 53–86

Tatsumoto, M., Knight, R. J., Allegre, C. 1973. Time difference in the formation of meteorites as determined from the ratio of lead-207 to lead-206. *Science* 180: 1278–83

Tatsumoto, M., Unruh, D. M., Desborough, G. A. 1976. U-Th-Pb and Rb-Sr systematics of Allende and U-Th-Pb systematics of Orgueil. *Geochim. Cosmochim. Acta* 40: 617–34

Taylor, S. R. 1982. Lunar and terrestrial crusts: a contrast in origin and evolution. *Phys. Earth Planet. Inter.* 29: 233–41

Taylor, S. R., McLennan, S. M. 1981. The composition and evolution of the continental crust: rare earth element evidence from sedimentary rocks. *Philos. Trans. R. Soc. London Ser. A* 301: 381–99

Taylor, S. R., McLennan, S. M., McCulloch, M. T. 1983. Geochemistry of loess, continental crustal composition and crustal model ages. *Geochim. Cosmochim. Acta* 47: 1897–1905

Tilton, G. R. 1973. Isotopic lead ages of chondritic meteorites. *Earth Planet. Sci. Lett.* 19: 321–29

Tilton, G. R., Barreiro, B. A. 1980. Origin of lead in Andean calcalkaline lavas, Southern Peru. *Science* 210: 2145–47

Turcotte, D. L. 1985. Chemical geodynamic models. In preparation

Turcotte, D. L., Schubert, G. 1982. *Geodynamics.* New York: Wiley. 435 pp.

Vidal, P., Clauer, N. 1981. Pb and Sr isotopic systematics of some basalts and sulfides from the East Pacific Rise at 21°N (project RITA). *Earth Planet. Sci. Lett.* 55: 237–46

Vidal, P., Dosso, L. 1978. Core formation: catastrophic or continuous? Sr and Pb isotope geochemistry constraints. *Geophys. Res Lett.* 5: 169–72

Vollmer, R. 1977. Terrestrial lead evolution and formation time of the Earth's core. *Nature* 270: 144–47

Wasserburg, G. J., DePaolo, D. J. 1979. Models of Earth structure inferred from neodymium and strontium isotopic abundances. *Proc. Natl. Acad. Sci. USA* 76: 3594–98

Watson, E. B., Othman, D. B., Luck, J. M., Hofmann, A. W. 1986. Partitioning of U, Pb, Cs, Yb, Hf, Re and Os between chromian diopsidic pyroxene and haplobasaltic liquid. *Geochim. Cosmochim. Acta* In press

Weidner, D. J. 1985. A mineral physics test of a pyrolite mantle. *Geophys. Res. Lett.* 12: 417–20

White, W. M. 1985. Sources of oceanic basalts: radiogenic isotopic evidence. *Geology* 13: 115–18

White, W. M., Hofmann, A. W. 1982. Sr and Nd isotope geochemistry of oceanic basalts and mantle evolution. *Nature* 296: 821–25

White, W. M., Patchett, J. 1984. Hf-Nd-Sr isotopes and element abundances in island arcs: implications for magma origins and crust mantle evolution. *Earth Planet. Sci. Lett.* 67: 167–85

White, W. M., Dupre, B., Vidal, P. 1985. Isotope and trace element geochemistry of sediments from the Barbados Ridge–Demerara Plain region, Atlantic Ocean. *Geochim. Cosmochim. Acta* 49: 1875–86

Wolf, G. H., Bukowinski, M. S. T. 1985. Ab initio structural and thermoelastic properties of orthorhombic $MgSiO_3$ perovskite. *Geophys. Res. Lett.* 12: 809–12

Worner, G., Zindler, A., Staudigel, H. 1986. Sr, Nd, and Pb isotope geochemistry of Tertiary and Quaternary volcanics from W. Germany. Submitted for publication

Yoder, H. S. Jr. 1976. *Generation of Basaltic Magma.* Washington, DC: Natl. Acad. Sci. 265 pp.

Zindler, A., Hart, S. R. 1986. Helium: problematic primordial signals. *Earth Planet. Sci. Lett.* In press

Zindler, A., Jagoutz, E. 1986. Mantle cryptology. *Geochim. Cosmochim. Acta* In press
Zindler, A., Hart, S. R., Frey, F. A., Jakobsson, S. P. 1979. Nd and Sr isotope ratios and rare earth elements abundances in Reykjanes Peninsula basalts: evidence for mantle heterogeneity beneath Iceland. *Earth Planet. Sci. Lett.* 45: 249–62
Zindler, A., Jagoutz, E., Goldstein, S. 1982. Nd, Sr and Pb isotopic systematics in a three-component mantle: a new perspective. *Nature* 58: 519–23
Zindler, A., Staudigel, H., Batiza, R. 1984. Isotope and trace element geochemistry of young Pacific seamounts: implications for the scale of upper mantle heterogeneity. *Earth Planet. Sci. Lett.* 70: 175–95
Zindler, A., Staudigel, H., Hart, S. R., Endres, R., Goldstein, S. 1983. Nd and Sr isotopic study of a mafic layer from Ronda ultramafic complex. *Nature* 304: 226–30